

Natural Desert and Human Controlled Landscapes:
Remote Sensing of LULC Response to Drought

by

Shai Kaplan

A Dissertation Presented in Partial Fulfillment
of the Requirements for the Degree
Doctor of Philosophy

Approved December 2013 by the
Graduate Supervisory Committee:

Soe W. Myint, Chair
Anthony J. Brazel
Matei Georgescu

ARIZONA STATE UNIVERSITY

May 2014

ABSTRACT

Droughts are a common phenomenon of the arid South-west USA climate. Despite water limitations, the region has been substantially transformed by agriculture and urbanization. The water requirements to support these human activities along with the projected increase in droughts intensity and frequency challenge long term sustainability and water security, thus the need to spatially and temporally characterize land use/land cover response to drought and quantify water consumption is crucial.

This dissertation evaluates changes in ‘undisturbed’ desert vegetation in response to water availability to characterize climate-driven variability. A new model coupling phenology and spectral unmixing was applied to Landsat time series (1987-2010) in order to derive fractional cover (FC) maps of annuals, perennials, and evergreen vegetation. Results show that annuals FC is controlled by short term water availability and antecedent soil moisture. Perennials FC follow wet-dry multi-year regime shifts, while evergreen is completely decoupled from short term changes in water availability. Trend analysis suggests that different processes operate at the local scale. Regionally, evergreen cover increased while perennials and annuals cover decreased.

Subsequently, urban land cover was compared with its surrounding desert. A distinct signal of rain use efficiency and aridity index was documented from remote sensing and a soil-water-balance model. It was estimated that a total of 295 mm of water input is needed to sustain current greenness.

Finally, an energy balance model was developed to spatio-temporally estimate evapotranspiration (ET) as a proxy for water consumption, and evaluate land use/land cover types in response to drought. Agricultural fields show an average ET of 9.3

mm/day with no significant difference between drought and wet conditions, implying similar level of water usage regardless of climatic conditions. Xeric neighborhoods show significant variability between dry and wet conditions, while mesic neighborhoods retain high ET of 400-500 mm during drought due to irrigation. Considering the potentially limited water availability, land use/land cover changes due to population increases, and the threat of a warming and drying climate, maintaining large water-consuming, irrigated landscapes challenges sustainable practices of water conservation and the need to provide amenities of this desert area for enhancing quality of life.

To Talli, Saar and Lahav – my true PhD in life,

To my grandfather – Zvi

ACKNOWLEDGMENTS

I am particularly grateful for the guidance and support of my committee chair, Professor Soe W. Myint. His depth of knowledge, immense wisdom, and advice greatly aided my scholarly development. He provided a patient and critical eye on my ideas, analyses, and writing throughout the past 5 years – I am very thankful for that, and more. Many thanks are also due for the members of my committee, Professor Anthony J. Brazel and Dr. Matei Georgescu, for their comments and suggestions throughout the process of planning, executing, and writing up my research for this dissertation.

I wish to acknowledge Talli Ilani for providing endless advice, graphical aid and field support; The Environmental Remote Sensing and Informatics lab for providing field equipment; and Mike and Lauren Kuby for editing.

During my time here, I received support, encouragements and assistance of various kinds from very many friends and colleagues in graduate school. Naming all of you is an impossible task; but do know that I would have never been able to complete this demanding and time-consuming endeavor without your help. I have to specifically mention Laura Grosso, Kathleen Tucker, and Marcie and Barton Lee, who made me, and my family, feel at home away from home.

Financial aid for this research was provided by Professor Soe W. Myint, the School of Geographical Sciences and Urban Planning, and the Central Arizona-Phoenix Long-term Ecological Research project (CAP-LTER).

The final words of gratitude are for my family, who has stuck with me throughout my academic endeavors in a foreign land. Dad, Mom, Ziva, and Dani – thank you for all the help despite being 7,450 miles away. Lastly, to my wife and daughters – thank you

for encouraging and believing in me, giving me a reason to pursue my dreams, and always being there for me with a smile at the end of the day.

TABLE OF CONTENTS

	Page
LIST OF TABLES	xi
LIST OF FIGURES	xii
CHAPTER	
1 INTRODUCTION	1
1.1: Dissertation Format	5
2 MONITORING LONG-TERM ECOSYSTEM RESPONSE TO DROUGHT: A CASE STUDY FROM THE MOJAVE DESERT	8
2.1: Abstract	8
2.2: Introduction	9
2.3: Study area	13
2.4: Data and methods	16
2.4.1: Climate	16
2.4.2: Imagery and spectral data	16
2.4.3: Multiple end-member spectral mixture analysis	20
2.4.4: Delineating functional types	21
2.4.5: Trend analysis	22
2.5: Results and Discussion	23
2.5.1: Climate change	23
2.5.2: Model validation	24
2.5.3: Annuals	25
2.5.3.1: Annuals trend analysis	29

CHAPTER	Page
2.5.4: Perennials	32
2.5.4.1: Perennials trend analysis.....	33
2.5.5: Evergreens.....	37
2.5.5.1: Evergreens trend analysis	38
2.6: Remaining uncertainties	41
2.7: Summary and conclusions.....	42
2.8: Acknowledgment.....	43
2.9: References	44
 3 RESPONSE OF URBAN AND NON-URBAN LAND-COVER IN SEMI-ARID ECOSYSTEM TO SUMMER PRECIPITATION VARIABILITY	 48
3.1: Abstract	48
3.2: Introduction.....	49
3.3: Study area.....	52
3.4: Data and methodology.....	53
3.4.1: Remote sensing data	53
3.4.2: Precipitation data	55
3.4.3: Horton index	56
3.5: Results and Discussion.....	58
3.5.1: Precipitation analysis	58
3.5.2: Response of different land-cover types to seasonal – precipitation	 61
3.5.3: Rain use efficiency and irrigation.....	63

CHAPTER	Page
3.5.4: Implications for vegetation RUE.....	65
3.6: Conclusions.....	66
3.7: References.....	68
4 ESTIMATING IRRIGATED AGRICULTURE WATER USE THROUGH LANDSAT TM AND A SIMPLIFIED SURFACE ENERGY BALANCE MODELING IN THE SEMI-ARID ENVIRONMENTS OF ARIZONA	70
4.1: Abstract.....	70
4.2: Introduction.....	70
4.3: Data and study area.....	75
4.3.1: Study area.....	75
4.3.2: Data	76
4.4: Methodology.....	78
4.4.1: Land use/land cover mapping.....	78
4.4.2: The S-ReSET model.....	81
4.5: Results and discussion	86
4.5.1: Model validation	86
4.5.2: Water consumption and drought effect.....	90
4.6: Conclusions.....	95
4.7: Acknowledgments	97
4.8: References.....	98

CHAPTER	Page
5 QUANTIFYING OUTDOOR WATER CONSUMPTION OF URBAN LAND USE/LAND COVER: SENSITIVITY TO DROUGHT	102
5.1: Abstract	102
5.2: Introduction	103
5.3: Study area	107
5.4: Data and methods	109
5.4.1: Satellite and weather data	109
5.4.2: Evapotranspiration and water use	111
5.4.3: Land use/land cover data	114
5.5: Results and Discussion	115
5.5.1: Model validation	115
5.5.2: Seasonal ET estimations	118
5.5.3: ET coefficient of variance for wet and drought years	120
5.5.4: Water consumption for major urban land covers	121
5.6: Conclusions	123
5.7: Acknowledgments	124
5.8: References	125
6 CONCLUSIONS	129
6.1: Summary of dissertation results	129
6.2: Contribution to academic knowledge	131
REFERENCES	133

	Page
APPENDIX A: STATEMENT OF PERMISSION.....	145
APPENDIX B: PRECIPITATION AND TEMPERATURE TREND MAPS.....	147

LIST OF TABLES

Table	Page
1. Acquisition dates for Landsat 5 TM images used (day/month).....	18
2. Monthly mean storm depth (α) and mean arrival time (λ) for the years of study	57
3. Input parameters for the Soil Water Balance model for two vegetation types representing desert and urban ecosystems.....	58
4. Precipitation and Horton index for urban and desert land-cover.....	66
5. Median, standard error and Mann-Whitney P-value for comparison of model and weather station ET estimations.....	88
6. Comparison between the seasonal ET estimated by S-ReSET and the AZmet report by Brown (2005).....	88
7. Area of the main irrigated crops and seasonal actual ET in 2008 for the Roosevelt irrigation district.....	92
8. Dates (Day/Month) of Landsat 5 TM used to estimate ET. Final time span considered only overlapping dates – April 1 to May 19.....	110
9. Land Use/Land Cover classes distribution within the study area after excluding areas that have undergone change (Modified from Buyantuyev, 2007)....	115

LIST OF FIGURES

Figure	Page
1. Location of selected study areas. The Mojave National Preserve represents natural desert environment, and Phoenix represents human-controlled landscapes, i.e., urban and agriculture).....	3
2. The MNP study area within the Mojave Desert ecosystem, field sample locations and the three weather stations used to characterize the climate.....	14
3. Annual water-year precipitation at three weather stations around the MNP. Note the high temporal variability (Data source: Western Regional Climate Center, http://www.wrcc.dri.edu/).....	15
4. The percentage of precipitation falling during autumn and winter (October - March).....	15
5. A false color composite of Landsat-TM 30m resolution data over the MNP (March 2003) by displaying channel 4 (0.750-0.900 μm), channel 3 (0.630-0.690 μm), and channel 2 (0.525-0.605 μm) in red, green, and blue, respectively.....	19
6. The endmember spectra used for the MESMA.....	19
7. The conceptual model of plant competition for resources. Each curve represents the response of plant carbon gain to increased environmental stress during the growing season (decrease in precipitation and increased temperature). Adapted from Ehleringer 1985).....	22
8. Relationship between 2003 and 2005 field estimated annuals cover and the annuals cover derived from our algorithm (n=42).....	24

Figure	Page
9. Relationship between 1997 evergreen field measurements and the evergreen cover derived from our algorithm (n=32).....	25
10. Yearly fractional cover of annuals.	28
11. Fractional cover of annuals in wet and dry conditions.....	29
12. Fractional cover histogram for wet (2005, 1992) and dry (1994, 2007) years.....	29
13. Left – 1987-2010 Monotonic trend for annuals fractional cover in the MNP. Green indicates upward trend; red indicate downward trend. Right – Areas of statistically significant change (active washes and piedmonts).....	30
14. Yearly perennials fractional cover. Arrows point to areas characterized by high fractional cover during favorable conditions. Dynamics follows long term decadal climate and regime shifts identified by Hereford et al. 2006).....	35
15. Up – 1987-2010 MK trend for perennial vegetation; down – areas with statistically significant changes at the 0.05 level.....	36
16. Yearly evergreens fractional cover.....	39
17. Top - 1987-2010 monotonic (MK) trend for evergreen fractional cover; bottom – areas of statistically significant change (in red).....	40
18. Map of the study area land cover (Buyantuyev and Wu, 2009). Black arrows point the locations selected for comparison. Gray arrow indicates the meteorological station location.....	52

Figure	Page
19. a) Grayscale image of the 2005 growing season ANPP. Black arrows point selected pixels; Gray marks Greenway meteorological station; b) Zoom of the desert pixel; c) Zoom of the urban pixel. Whiter and darker pixels represent higher and lower ANPP, respectively.....	55
20. The Soil Water Balance model. P – precipitation; ET - evapotranspiration; Q - runoff; L - leakage (assumed to be zero); R= stream flow. Letters in parenthesis are the corresponding representation of Troch et al. 2009.....	56
21. Yearly precipitation. Red line is the multi-year average, and dashed lines are 1 standard deviation from that mean.....	59
22. Yearly summer/growing season (May – October) precipitation. Red line is the multi-year average, and dashed lines are 1 standard deviation from that mean.....	60
23. Average monthly precipitation for the Greenway meteorological station (2000 – 2009).....	61
24. Vegetation dynamics in response to precipitation for the year 2000.....	62
25. ANPP as a function of Precipitation for three land cover types.....	63
26. RUE for urban and desert land cover.....	64
27. Vegetation rain-use efficiency vs. the Horton index variability for urban and dessert land cover in the Phoenix metropolitan area.....	65
28. The CAP-LTER study area as seen by Landsat 5. Flags represent location of the meteorological stations. Arrows indicate the stations used for validation.....	76
29. Land use/land cover classification of the study area for 2000 (top) and 2008 (bottom).....	80

Figure	Page
30. Changes in land cover area between 2000 and 2008. Labels indicate change in class cover percentage.....	81
31. Comparison between S-ReSET predicted ET _{actual} and weather stations reference ET.....	86
32. S-ReSET seasonal ET estimations compared to ground water wells data at four different irrigation and water districts across the region.....	90
33. Daily ET for the Central Arizona Phoenix Long Term Ecological Research area, and a subset depicting agricultural areas (active and fallow).....	91
34. Seasonal ET for drought year (top) and wet year (bottom).....	93
35. Location map for the Central Arizona Phoenix Long Term Ecological Research study area. Map on the right indicates the location of Arizona within the continental USA.....	108
36. Monthly Precipitation and maximum average Temperature for 2000 and 2008.....	111
37. Correlation between the S-ReSET predicted ET and actual water usage from parks, golf courses and sports and recreation facilities across the metropolitan area (n=49).....	117
38. Seasonal ET for a dry year (2000) and a wet year (2008); the effect of drought.....	119
39. ET coefficient of variance of wet (2008) and dry (2000) years for different land Use/land cover types.....	120
40. Mean ET (water consumption) of main urban land covers (Apr 1 – May 19).....	121

CHAPTER 1: INTRODUCTION

“Drought is a condition of moisture deficit sufficient to have an adverse effect on vegetation, animals, and man over a sizeable area” (Warwick, 1975).

Droughts are common phenomena of the highly variable climate of drylands. The impacts of climate variability on the dynamics of physical and biological systems and their socioeconomic implications are critical for decision makers and society in general (Vitousek and Mooney 1997). Due to its various causes, wide geographical extent, and multidimensional impacts, drought is considered one of the most complex and least understood climate-related hazards.

Drylands ecosystems, including arid, semi-arid, and dry sub-humid regions, are the largest terrestrial biomes, composing about 41% of the Earth’s landmass and containing 38% of the global population (Reynolds et al. 2003). Characterized by low (<250mm for arid and 250–500mm for semi-arid) and highly variable precipitation, arid ecosystems are susceptible to structural changes due to the sensitive balance among vegetation structure, soils, and climates (Rodriguez-Iturbe et al.1999). Even small perturbations in water availability can impact vegetation distribution and landscape functionality over the long term (Whilhite 2000; Newman et al. 2006). Changes in vegetation may lead to a positive feedback with the climate system by impacting on both the surface energy- and moisture- balance. For example, land degradation in the form of reduced vegetation cover will result in less evapotranspiration and higher sensible heat flux. These changes may result in higher temperature and reduced precipitation that, in turn, could result in further vegetation degradation and accelerate the rate of change.

In addition to climate-driven changes, human activities such as herding practices, agriculture, deforestation, and more recently urbanization, have transformed many of the world drylands (Vitousek and Mooney 1997; Grimm et al, 2008; Imhoff et al. 2004). These land transformations are all associated with changes in vegetation and have been identified as first-order human climate forcing (Mahmood et al. 2010). Thus, vegetation is an indicator of ecosystem condition and can indicate magnitude of change. Identifying vegetation changes and understanding the dynamics of human-controlled and natural landscape vegetation patterns in response to climate variability (specifically drought) and their relationships with ecosystem functions need to be based upon detailed spatiotemporal data analysis over wide regions. An examination of detailed spatiotemporal data can help us distinguish between human-induced and natural climatic impacts on vegetation.

This dissertation focuses upon the arid and semi-arid deserts of the Southwest: the Mojave and Sonora. The Intergovernmental Panel on Climate Change (IPCC 2007) concluded that, for most arid regions, new climate conditions are evolving. Based on these new conditions, most scenarios for the Southwest predict drier, warmer, and more extreme climate (Archer and Predick 2008; CLIMAS 2012). With predictions of increased drought intensity and frequency, it is important to quantify the responses of different landscapes to drought.

In addition, changes in drought intensity and frequency have societal implications. Human activities, specifically agricultural practices and, more recently, rapid urbanization, have greatly modified the Southwest. Agriculture and cities add vegetation to an already water-stressed environment. Because water supplies are limited and

vulnerable, population growth and intensification of human activities, coupled with a drier climate, will result in increased competition among industrial, agricultural, and residential sectors. Regional water security (i.e., the ability of the water system to meet environmental and societal needs) will invariably decline. Furthermore, Barnett et al. (2008) showed that over 60% of climate-related trends in the Southwest are human-induced, amplifying the need for better understanding of the interactions between land-use/land-cover changes (LULCC) and climate as well as the implications of drought on both natural and human-controlled landscapes.

Using remote sensing methodologies, this dissertation characterizes LULC response to drought, exploring the three main landscapes in the Southwest: Natural desert (the Mojave Preserve), agricultural (around Phoenix), and urban (Phoenix metro-politan area) (Figure 1).

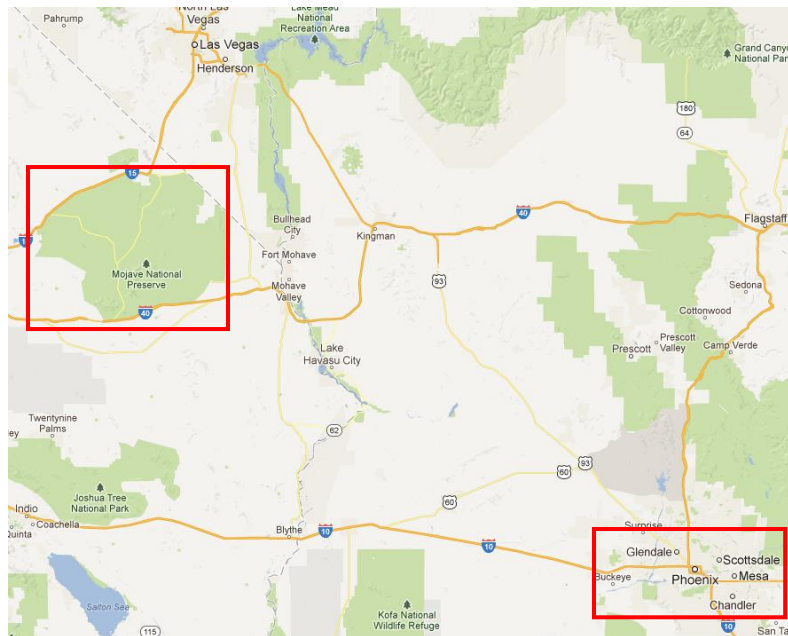


Figure 1. Location of selected study areas. The Mojave National Preserve represents natural desert environment, and Phoenix represents human-controlled landscapes, i.e., urban and agriculture.

In the natural desert (i.e., the Mojave National Preserve), human impacts on the landscape have been minimal and restricted to specific areas within the preserve, in an attempt to maintain the natural ecological balance. Thus, any observed changes in vegetation should be climate-driven. Despite a large body of literature on landscape response to climate variability (e.g., Huxman et al. 2004; Hereford et al. 2006; Pennington and Collins 2007; McAuliffe and Hamerlynck 2010), there is a paucity of spatiotemporally explicit information on changes at the level of vegetation functional types, (i.e., annuals, perennials, and evergreens). Filling the gap in the spatiotemporal pattern and dynamics of vegetation will help us understand the driving forces of change at the functional-type level and the severity of corresponding effects.

Thus, the first part of this research involved developing and evaluating new remote-sensing methods to delineate functional types and describe their spatiotemporal distribution. The monitoring of long-term changes in this distribution will reveal the natural landscape's response to climate variability, specifically drought.

Irrigation using collected surface water and groundwater sustains human activity in the arid climate of the Southwest. These water sources are limited, vulnerable and, in the long run, depend on climate as well as societal factors such as population growth, technological change, culture, and policy. Given projected climate and limited water sources, and likely continued population growth, we expect less water will be available for irrigation. Thus, this research will seek to quantify the spatiotemporal water consumption of human-controlled landscapes and their sensitivity to drought. Quantifying the evolving consumption of water is key for better water management and

long-term sustainability of urban and agriculture environments in this region (Gober et al. 2011).

Several factors strongly recommend the use of remote-sensing data to quantify land-cover response to climate variability over time and space. Remote sensing allows for fast, efficient monitoring of land-surface processes at different scales, from local to global (Anyamba and Tucker 2005; Bastiaanssen et al. 1999). Remote sensing enables researchers to monitor the large spatial extent of the Southwest over the long term. Finally, remote sensing is well-suited to detecting changes in vegetation, which is important considering the role vegetation dynamics play in both natural-desert and human-controlled environments. Comparing the response of these environments to climate variability at different scales will reveal the climate–ecosystem–hydrology feedback. This feedback mechanism influences nutrient, water, and energy allocation at the land surface (Troch et al. 2009) and thus has significant implications for land degradation, water security, and sustainability.

1.1 Dissertation Format

There are six chapters in this dissertation: an introduction, a conclusion, and four chapters that each serves as a first-authored manuscript. Three of these manuscripts have been submitted to peer-reviewed journals.

The first manuscript (Chapter 2) views the Mojave National Preserve as a window to undisturbed desert environment. The chapter’s approach combines phenology, remote sensing, and trend analysis to delineate, quantify, and monitor the spatiotemporal distribution of vegetation functional types (evergreen, perennials, annuals) in arid

environments. The main goal of this approach is to estimate the fractional cover of the different functional types and to examine long-term temporal changes related to precipitation variability.

The second manuscript (Chapter 3) examines the differences between arid urban landscapes and their surrounding natural ecosystems in terms of their phenology and response to summer water inputs. I use a remote sensing and a soil-water balance model to analyze rain-use efficiency (RUE), interannual and intraannual vegetation phenology, and above-ground net primary production (ANPP) of the two land-cover types. These results are then used to simulate the Horton index (H) as a measure of land-cover response to climate variability. This chapter was published in the Journal of the Arizona Nevada Academy of Science in 2012.

The third manuscript (Chapter 4) develops and evaluates a simplified energy balance model: S-RESET, which is used to estimate the region's agricultural water consumption. By comparing water consumption in wet versus drought years, the manuscript examines agriculture sensitivity to drought and farmers' resilience in the context of water usage. This manuscript was published in a special issue of Photogrammetric Engineering and Remote Sensing journal in August 2012.

The fourth paper (Chapter 5) uses the S-RESET model developed in Chapter 4 to model evapotranspiration (ET) over the urban area of Phoenix as a proxy for outdoor water consumption. The objectives of this chapter were to estimate outdoor water consumption for various LULC types and determine their sensitivity to drought and implications for regional water security. The chapter was submitted to Environmental Management in November 2013.

A short, concluding chapter summarizes the methods, results, and contributions of this dissertation to the debate on the roles of climate vs. humans in LULC response to drought and the implications therein.

CHAPTER 2: MONITORING LONG-TERM ECOSYSTEM RESPONSE TO DROUGHT: A CASE STUDY FROM THE MOJAVE DESERT

2.1: Abstract

Scientists typically classify arid vegetation into three main functional types: annuals, perennials, and evergreens. The aim of this study is to delineate these three types with remote sensing and evaluate their response to drought. We focus on the Mojave National Preserve as a window to the undisturbed natural desert environment where most changes can be attributed to climate. This study applies multi-date adaptive unmixing to Landsat 5 TM time-series data from 1987-2010. Using this method, we produced new maps of yearly annuals, perennials, and evergreen cover at the subpixel level. Results attribute the spatiotemporal variability of annuals to short-term winter precipitation, underlying soil and geomorphology, and preceding soil moisture. We identified no regional change in the response of annuals to drought conditions. Perennial cover was highly variable spatially, yet consistent over a period of several years, following a multi-year regime shift between wet and dry conditions. Evergreen vegetation has the highest and most spatially consistent fractional cover, with many areas showing high fractional cover (>30%) even during drought years, indicating its decoupling from the short-term climate variability. We then analyzed the linear trends in the resulting dataset to characterize the spatiotemporal dynamics of each functional type. Results indicated both upward and downward monotonic trends, suggesting different processes dominate at the local scale. Regionally, evergreen shows a positive trend, while perennials and annuals show a negative trend. Although changes in most areas are insignificant, the existence of a monotonic trend may point to the overall direction of each functional type (rehabilitation

vs. degradation). The resulting functional types and trend maps enhance ecosystem monitoring and efforts to identify where local forces operate. Furthermore, the proposed method allows us to look simultaneously at both local and regional scales and offers insights into the relationship among different functional types.

2.2: Introduction

Drylands ecosystems—including arid, semi-arid, and dry sub-humid—are the largest terrestrial biome, composing about 41% of the Earth’s landmass. These ecosystems are typically fragile and highly sensitive to any form of change, (i.e., even small perturbations may affect vegetation distribution and landscape functionality over the long term [Whilhite 2000; Newman et al. 2006]). For the arid Southwest, the 2007 Intergovernmental Panel on Climate Change (IPCC 2007) concluded that new climate conditions are evolving. Based upon these new conditions, most scenarios for the Southwest predict drier, warmer, and more extreme climate (Archer and Predick 2008; CLIMAS 2012).

Vegetation in arid landscapes varies in response to precipitation (Pennington and Collins 2007; Buyantuyev and Wu 2009) and across general geographic regions (McAluiffe and Hamerlynck 2010). Over the short term, vegetation can adapt to climate variations (Troch et al. 2009). Nevertheless, changes in seasonal and annual precipitation patterns can have a dramatic spatial effect that may lead to changes in ecosystem structure and functioning. Such changes in vegetation can feed back to climate and accelerate change, potentially triggering degradation. Several studies have shown the importance of precipitation pulses—their timing, depth, and duration (Beatley 1979; Ogle

and Reynolds 2004). Other studies indicated a strong relationship between precipitation variability on the one hand and vegetation cover and above-ground net primary productivity (ANPP) on the other (Hereford et al. 2006). Although these relationships are believed to hold true over long periods, most studies were carried out during periods of above-normal precipitation and have yet to be confirmed during periods of low precipitation. Monitoring long-term gradual changes in arid ecosystems is therefore important.

To better understand, predict, and simplify ecosystem processes, organisms are usually generalized into functional type groups. Functional types are groups of species that are similar in their role within the community or ecosystem processes. The concept of functional types uses structural, physiological, and/or phenological differences to group species in response to environmental conditions. Resource limitations such as water availability (i.e., precipitation and soil moisture) link, in predictable ways, adaptation and response. Gain or loss of functional types can permanently change the ecosystem characteristics through changes in resource distribution, nutrient supply, and/or disturbance regime (Chapin et al. 2002). The general functional types in arid environments are perennials, annuals, and evergreens (woody vegetation/shrubs). Bonan et al. (2002) concluded that mapping the spatially continuous distribution of functional types is critical for linking climate and ecosystem models.

Functional type estimations at the landscape scale are required to evaluate wildfire risk, endangered species, soil erosion, and ecosystem health. Quantitative approaches to monitoring functional type abundance at high resolution are few. Most studies use point data from fieldwork or low-resolution satellite data. As a result, there is

a paucity of spatiotemporally explicit information on changes at the vegetation functional-type level. In addition, many studies refer to perennials and evergreen vegetation as a single group (Wallace et al. 2008; McAuliffe and Hamerlynck, 2010; Guida et al. 2013). A gap remains between ecological theory and spatiotemporal studies of vegetation patterns and dynamics on the driving forces of change and the severity of corresponding effects. The need for long-term monitoring—as well as greater understanding of the scale of changes and the role of vegetation dynamics in the feedback mechanism—suggest that only remote sensing data can fill the gap.

In this chapter, we combine phenology, remote sensing, and trend analyses to quantify and monitor the spatiotemporal distribution of vegetation functional types in arid environments. The first objective is to develop a framework to derive and quantify the abundance of plant functional types. This framework requires three steps. First, we use multiple end-member spectral mixture analysis (MESMA) to quantify vegetation fractional cover at different times of the year. We then define functional types based on phenology and quantify annual growth. Finally, we use a non-parametric trend analysis to evaluate temporal changes.

Remote sensing offers retrospective monitoring and continuous assessment, as well as future predictions when combined with modeling. It is well suited to measuring vegetation functional types, in that Ustin and Gamon (2009) referred to functional types as “optical types” and reviewed the spectral information and methods for identifying them. They recommended using temporal images of vegetation indices to capture the landscape greenness and incorporating phenology to identify vegetation functional types. Wallace and Thomas (2008) and Wallace (2008) used phenological metrics as proxies for

growth of annuals and perennials in the Mojave Desert. Roderick et al. (1999) used NDVI time series analysis to estimate cover of different functional types. Recently, Casady et al. (2013) used time series analysis based on the MODIS Enhanced Vegetation Index (EVI) combined with field observation to estimate winter annuals in the Mojave and Sonora deserts. All these studies rely upon high temporal resolution satellites such as the MODIS or AVHRR. Yet, while capturing the entire phenological cycle, the spatial resolution of these sensors is often too coarse to detect subtle land-cover changes. Furthermore, they capture only the greenness of the landscape as a whole, which means they must infer biophysical indicators such as biomass and cover.

The Landsat system constitutes the longest time series of imagery worldwide and fulfills both spatial and temporal prerequisites combined with an adequate spectral resolution to monitor and analyze long-term changes in ecosystem processes and land-cover change. Hostert et al. (2003) and Sonnenschien et al. (2011) used Landsat time series and linear trends to model vegetation fractional cover and analyze spatio-temporal changes. Although Landsat offers a long time series, the number of observations for each location is limited, and the noise level in the data tends to be high, especially for arid environments. A non-parametric trend analysis is more robust to noise and more suitable to use with limited number of observations/images.

By incorporating vegetation fractional cover as a biophysical indicator from the Landsat time series with phenological differences, one may differentiate among these functional types (Shoshany and Svoray 2002; Ustin and Gamon 2010). Analyzing long-term changes in the pattern of each functional type may indicate subtle environmental

changes and help identify the ecohydrological implications of climate-driven, land-cover changes.

2.3: Study Area

Our test site is the Mojave National Preserve (MNP), CA (Figure 2). Established as a national preserve in 1994, the MNP covers 6475 km², most of which are designated as wilderness and critical habitat for the desert tortoise. Human activities include mining, roads/rail tracks, and grazing—all controlled to minimize impact on natural resources (Mojave National Preserve 2002).

The Mojave Desert has cold winters and hot summers, with average temperatures ranging from 11°C in winter to over 30°C in summer. Precipitation is highly variable (Figure 3), with no significant change over time. Climate variability has two main forcing processes: (1) El-Nino southern oscillation (ENSO), which controls interannual up to decadal variability, and (2) Pacific Decadal Oscillation (PDO), which modulates decadal to multi-decadal variability. At a regional scale, ENSO conditions promote wetter winters across the Southwest, with spatially homogenous precipitation events. La-Nina typically results in dry winters (Bonan 2002). Hereford et al. (2006) identified three patterns of regime shift for the Mojave Desert, corresponding to 35, 5, and 2.2 years. The 35- and 5-year shifts correspond to PDO and ENSO, respectively. The 2.2-year cycle corresponds to the quasi-biannual oscillation, a periodic change in the direction of the equatorial zonal wind between easterlies and westerlies (Baldwin et al. 2001). The analysis of Hereford et al suggested that interannual and multi-decadal climate variation affect vegetation. We thus need long-term analysis to identify trends and changes in plant

phenology and productivity that, in turn, emphasize the need to use remote-sensing data over long periods.

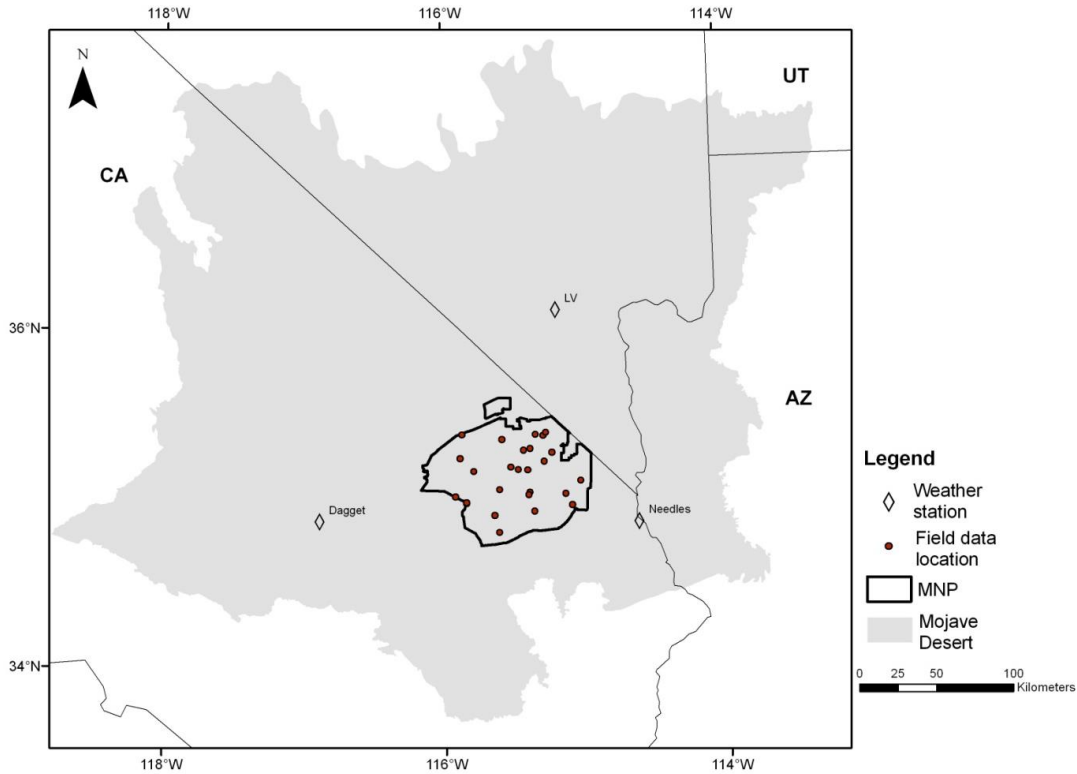


Figure 2. The MNP study area within the Mojave Desert ecosystem, field sample locations, and the three weather stations used to characterize the climate.

Beatley (1974) showed that, for the Mojave Desert, the autumn-winter precipitation is the critical pulse that triggers biological activity for the following spring and summer. Winter precipitations replenish shallow and deep soil moisture and produce a relatively uniform phenology pattern (Loik et al. 2004). Figure 4 shows a long-term analysis of the percentage of precipitation.

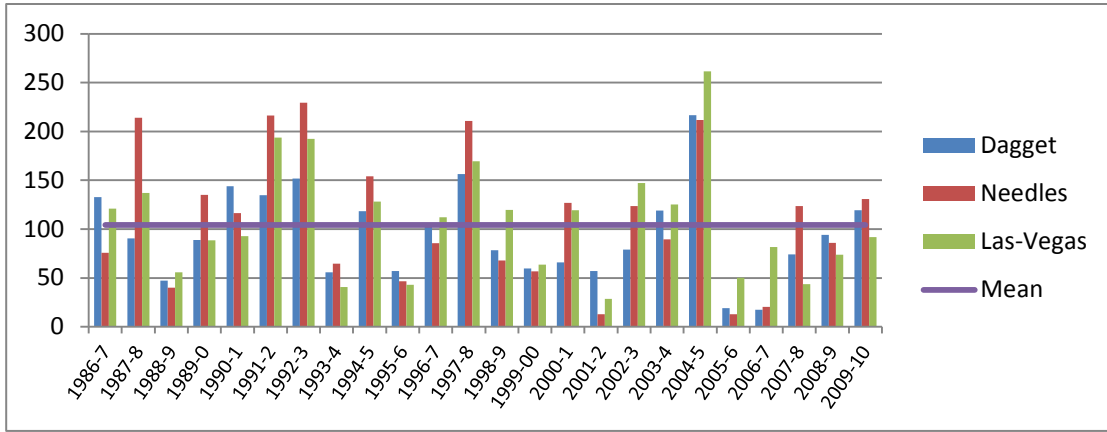


Figure 3. Annual water-year precipitation at three weather stations around the MNP. Note the high temporal variability. The 2001-2, 2005-6, and 2006-7 were extremely dry where as 1990-1 to 1992-3, and 2004-5 had high annual precipitation (Data source: Western Regional Climate Center, <http://www.wrcc.dri.edu/>).

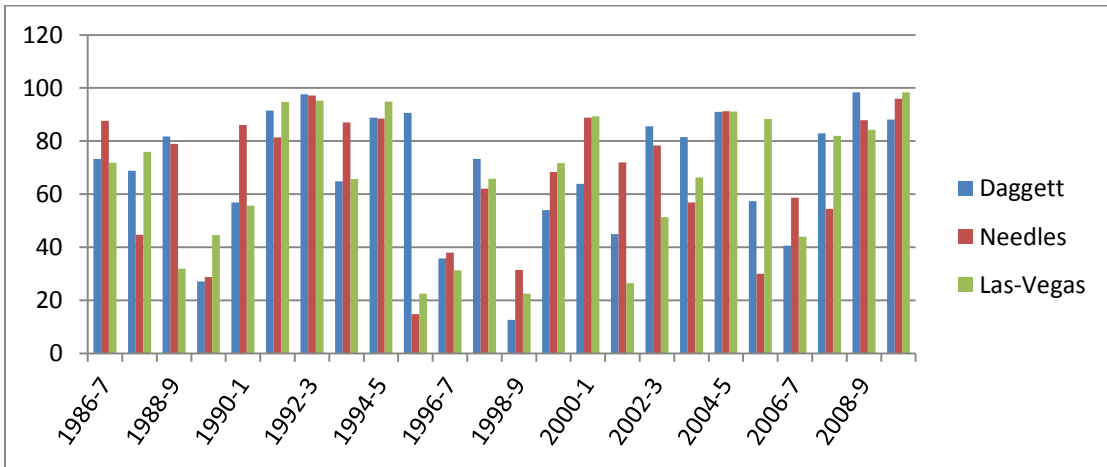


Figure 4. The percentage of precipitation falling during autumn and winter (October-March). On average, over 67% of precipitations fall during this period.

2.4: Data and Methods

2.4.1: Climate

Although meteorological stations provide accurate observations of climate variables, their spatial coverage is limited and thus may be insufficient to represent the spatial variability of climate. To examine climatic change over the study's time period in conjunction with vegetation changes, we use the Parameter-elevation Regressions on Independent Slopes Model (PRISM) data. PRISM is an interpolation method used to create continuous climate data at 4km resolution across the United States for precipitation, maximum temperature (Tmax), and minimum temperature (Tmin) (PRISM Climate Group, 2011). In addition to its continuous coverage, PRISM also accounts for elevation, slope and proximity to a coastline. Areas with large variations in terrain such as the MNP are relatively well modeled by PRISM. Furthermore, Hereford et al. (2006) highlighted the importance of long-term climatic conditions to evaluate changes in desert vegetation. Following figure 7 and Beatley (1974) we considered annual precipitation, winter precipitation (January-March), annual Tmax, and annual Tmin. For each variable we performed trend analysis as mentioned in section 2.4.5.

2.4.2: Imagery and spectral data

A long time series of Landsat-5 TM images (70) was acquired for the MNP study area, covering the period between 1987 and 2010. This period covers a wet period (1987-1998) followed by a regime shift into a current dry period (Hereford et al. 2006). For each year, we used three images: beginning of spring, end of spring and end of summer. We selected these acquisition dates based on climate analysis to reflect the optimal

conditions (i.e., minimum competition for resources) for each functional type (see next section for details). The specific dates were also a function of cloud free image availability (Table 1). Image analysis was preceded by geometric registration. Radiometric and atmospheric calibrations following the procedure elaborated by Chavez (1996) were applied to improve the image quality and accuracy. This step also insures an adequate consistency between multi-temporal data sets, a critical consideration when referring to vegetation fractional cover.

To account for the variety of land-cover types, we collected spectral signatures for dominant photosynthetic active vegetation functional types (PV), non-photosynthetic vegetation (NPV), and soils during two field trips in September 2012 and March 2013. We used a FieldSpec 4 Hi-Res Spectroradiometer, measuring reflectance from 350 to 2500 nm in 2151 bands and a Spectralon panel as spectral white reference. All samples were taken under natural illumination conditions on site. We then resampled the spectra to match the spectral resolution of the Landsat TM and create a spectral library. Figure 5 shows a Landsat scene of the study area. Figure 6 shows the spectral library developed from field measurements.

Final analysis included only areas with slope $<10^\circ$ because elevation is a significant determinant of climatic patterns in the MNP. Ranging from 270m to 2417m, elevation differences lead to significant differences in slope and aspect, affecting water and light availability and resulting in different vegetation communities and patterns. Histogram analysis indicated that 85% of the area has slope $<10^\circ$. Additionally, snow often persists at higher elevations late into spring.

Table 1. Acquisition dates for Landsat 5 TM images used (day/month)

Year	End of winter (max. vegetation)	End of spring	End of summer (min. vegetation)
1987	22/4	11/7	29/9
1988	08/4	03/6	15/9
1989	11/4	14/6	18/9
1990	09/2	03/7	23/10
1991	17/4	20/6	24/9
1992	03/4	14/6	09/8
1993	21/3	09/6	29/9
1994	08/3	12/6	16/9
1995	27/3	01/7	19/9
1996	29/3	17/6	20/8
1997	17/4	20/6	23/8
1998	19/3	07/6	25/7
1999	22/3	10/6	13/8
2000	25/4	12/6	16/9
2001	28/4	15/6	18/8
2002	30/3	18/6	21/8
2003	18/4	21/6	08/8
2005	06/3	25/5	29/8
2006	10/4	28/5	16/8
2007	12/3	16/6	03/8
2008	14/3	18/6	06/9
2009	17/3	21/6	25/9
2010	16/2	24/6	27/8

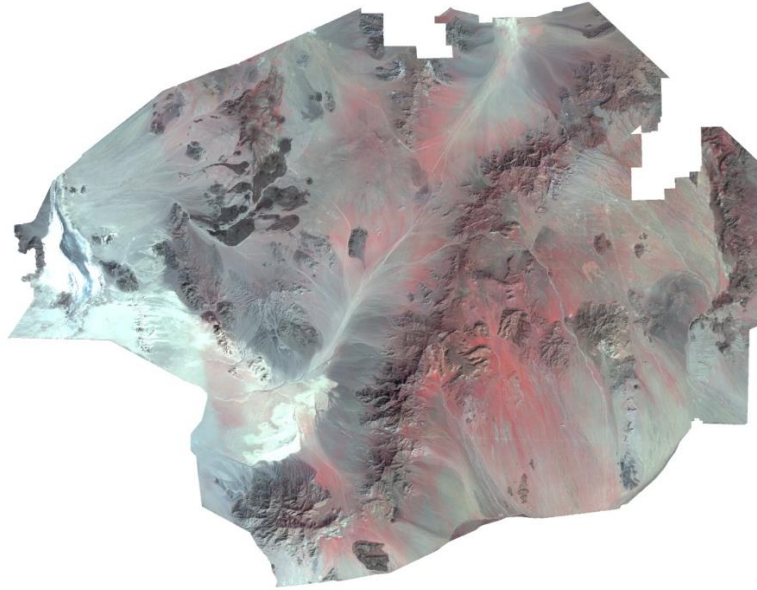


Figure 5. A false color composite of Landsat-TM 30m resolution data over the MNP (March 2003) by displaying channel 4 (0.750-0.900 μm), channel 3 (0.630-0.690 μm), and channel 2 (0.525-0.605 μm) in red, green, and blue respectively.

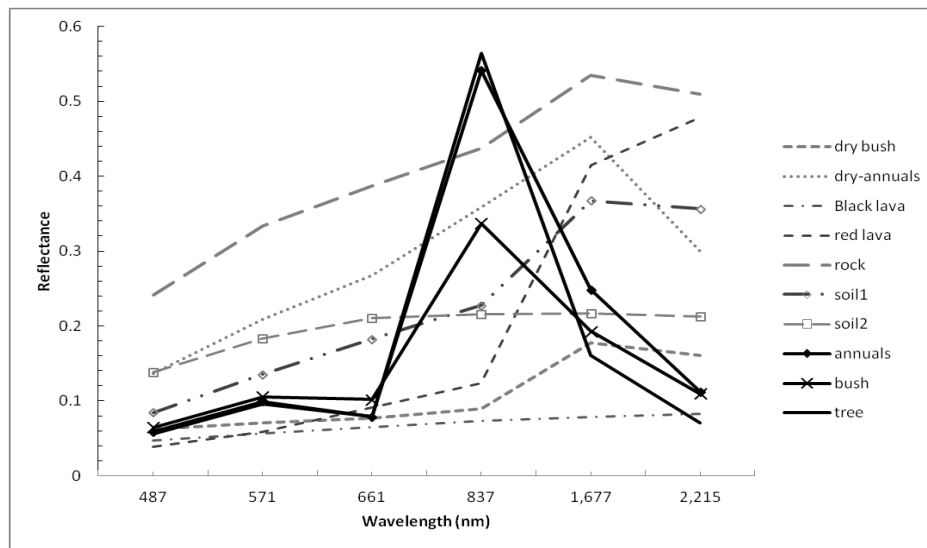


Figure 6. The endmember spectra used for the MESMA. The use of multiple endmembers allows variation of solution on a pixel basis therefore minimizes the error. The distinct signature of green vegetation is noted as well as the lower reflectance of bushes in the Near Infra-Red (837nm) band.

2.4.3: Multiple end-member spectral mixture analysis

Elmore et al. (2000) have demonstrated the superiority of a subpixel approach over vegetation indices for arid regions with sparse vegetation. To account for diversity of vegetation and soil components, we employed the Multiple Endmember Spectral Mixture Analysis algorithm using the VIPER tool extension in ENVI software. The MESMA allows the number and type of end-members to vary for each pixel within an image, thus minimizing error. It provides a quantitative measure in the form of fractional cover—a biophysical indicator for ecosystem status and land degradation at the subpixel level.

We used the spectral library derived from field measurements as end-members (EM) input to MESMA. We considered the following combinations:

2EM = soil+shade; PV+shade; NPV+shade

3EM = soil+NPV+shade; soil+PV+shade; NPV+PV+shade

4EM = soil+NPV+PV+shade

The shade end-member was included in all models to account for illumination variation (Dennison and Roberts 2003). For each pixel, we applied two constraints: fraction values between -0.1 and 1.1 and a threshold of $RMS < 0.05$. We then normalized the resulting fractional cover maps for shade following Myint and Okin (2009). The final vegetation fraction maps were produced by saving the model that minimizes both number of EM and the RMS for each pixel.

2.4.4: Delineating Functional Types

To map the different functional types, we applied an adaptive spectral mixture analysis approach (Svoray and Shoshany 2002). We developed a new algorithm, based on the differences in the vegetation fractional (Fv) cover between dates and used it to delineate the different functional types as follows:

- Evergreen = Fv (end of the summer ~ September).
- Annuals = Fv (beginning of spring ~ March) - Fv (late spring ~ May-June).
- Perennials = Fv (end of spring ~ May-June) - Fv (end of summer ~ September).

This algorithm follows a conceptual model of plant competition for resources (Figure 7), especially water. Immediately following winter water input, and when temperatures start to rise, annuals start to grow, reaching their peak biomass and greenness. As the season progress, environmental stress increases (i.e., water input decreases and temperature increases), leading to annuals wilting as topsoil dries out. Perennial vegetation growth also starts following winter water input, but reaches its peak growth later in the season. Evergreen vegetation has a deeper rooting system that uses water from deeper soil levels (Reynolds et al. 2004); thus, it can survive the dry period and maintain consistent greenness throughout the year. These growth strategies reduce competition between the different functional types and maximized use of resources.

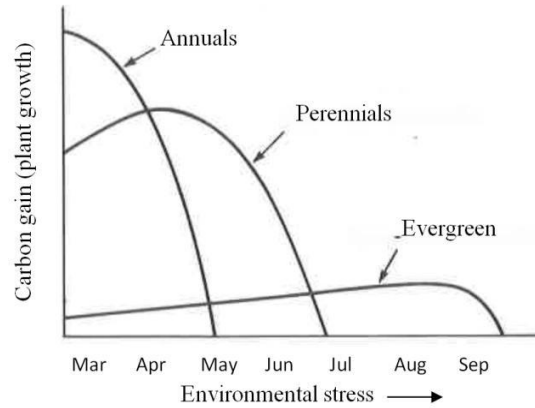


Figure 7. The conceptual model of plant competition for resources. Each curve represents the response of plant carbon gain to increased environmental stress during the growing season (decrease in precipitation and increased temperature). Adapted from Ehleringer (1985).

2.4.5: Trend analysis

To determine change over time, we used the Mann-Kendall (MK) test. The MK is a nonparametric trend analysis robust to outliers. It tests for the existence of a monotonic trend, (i.e., it measures the degree to which a trend is consistently increasing or decreasing by evaluating the slopes between all pair-wise combinations). The test values range from -1 to +1, where positive values indicate an increasing trend, and negative values indicate a decreasing trend. Values closer to +1 and -1 indicate more direct or inverse correlation, respectively, between the ranking of vegetation cover and time, while a value of 0 indicates no consistent trend. We conducted the analysis on a pixel-by-pixel basis using the IDRISI software Earth trend Modeler. To determine the magnitude of the trend, we used Theil's regression approach that estimated the slope of the trend line as the median of the slopes calculated between all pair-wise time steps. Similar to the MK test, the Theil's approach is robust to outliers (Daniel 1990).

2.5: Results and Discussion

2.5.1: Climate change

Resampling of the PRISM data and performing trend analysis show no regionally consistent significant change in climate during 1987-2010 over the MNP at the P-value=0.05. At the P-value=0.1, annual precipitation analysis show that the higher elevations experienced significant decrease. Similar results were reported by to Guida et al. (2013), who compared climate decadal averages between 1970-1979s and 1999-2008. The decrease in precipitation over the mountains may lead to changes in water availability due to reduced flow in channels, which in its turn reduces vegetation cover, specifically annuals.

Trend analysis for Tmax showed most of the MNP did not experience significant changes. For Tmin, the analysis indicate that the western parts the MNP experienced an increase in Tmin, while the areas east of the Providence mountains show a decrease of 0.1°C/yr over the 1987-2010 period. These results are within the range reported by Guida et al. (2013) for temperature difference between 1970s and 2000s. The maps of significant trend and its direction are shown in appendix B. The increase in Tmin with no change in Tmax may suggest human impact. However, given the low density of weather stations in the region from which the dataset is derived, the methodology used to create the dataset, and the high variability of temperatures between years, we conclude that regional temperatures have been fairly stable over the MNP over the last 3 decades.

2.5.2: Model evaluation

To validate our model's results, we compared annuals and evergreen vegetation to field estimations. We compared the annuals' fractional cover results to field data collected by Wallace and Thomas (2008) during April 2003 and 2005. Annuals are the most sensitive functional type of the three evaluated and the most difficult to capture from a remote-sensing perspective. Figure 8 presents the relationship between the field estimates and model values. The R^2 for this relationship was 0.72, based on 42 samples taken throughout the MNP, with root mean square error (RMSE) of 4.06% fractional cover.

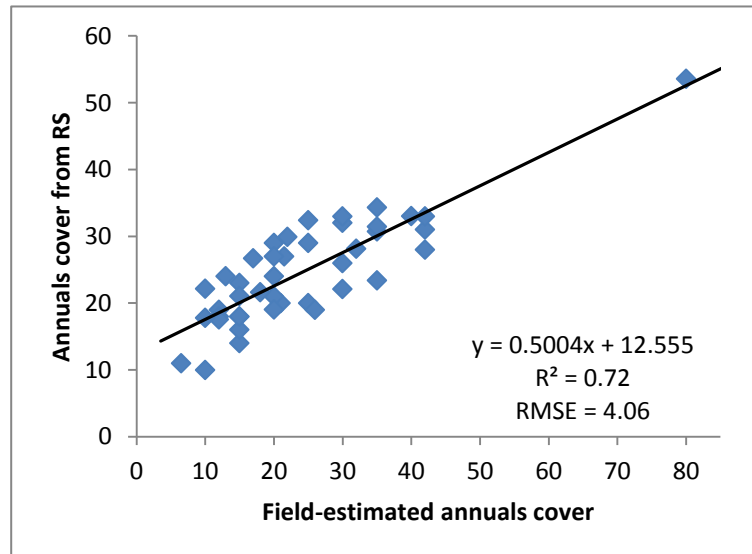


Figure 8. Relationship between 2003 and 2005 field estimated annuals cover and the annuals cover derived from our algorithm (n=42)

Evergreen fractional cover was compared to field data from 1997 provided by K.A. Thomas (USGS, unpublished data) (Figure 9). In this field dataset, evergreen vegetation included shrubs (mainly creosote bush) and trees (mainly juniper). The study

year 1997 had close to average precipitation, with less than 40% falling during autumn-winter, which means that the vegetation signal can be attributed mainly to evergreen vegetation that survived the dry period (Beatley 1974). Generally there is a good agreement between our model estimations and Thomas's field observations, with $R^2=0.8$ and $RMSE=2.59\%$ fractional cover. The high correlation for both evergreen and annuals confirms that our algorithm performs reasonably well.

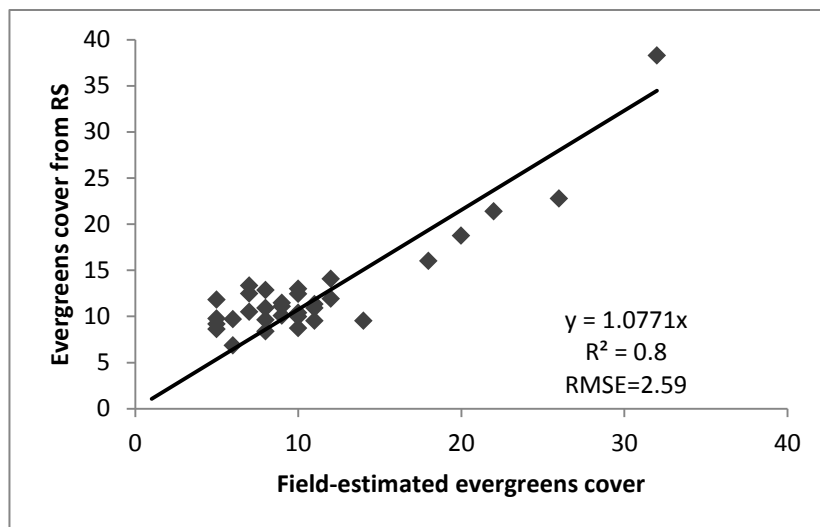


Figure 9. Relationship between 1997 evergreen field measurements and the evergreen cover derived from our algorithm (n=32)

2.5.3: Annuals

Winter annuals play an important role in Mojave ecosystem: they are a food source for livestock and native wildlife, and they impact disturbance regime (fire) and soil erosion (wind and water). Figure 10 presents fractional cover maps for annuals grouped into 11 categories with 5% intervals. As can be seen from Figure 10, annuals are highly variable spatially and temporally.

Temporal variability is controlled mainly by annual precipitation (Beatley, 1974; Reynolds 2004). Despite an overall low cover and high spatial variability, statistical analysis indicated that annuals average fractional cover is correlated to water year precipitation ($R^2=0.31$, $p\text{-value}< 0.01$), and to precipitation between January to March ($R^2=0.29$, $p\text{-value}<0.01$). Reynolds et al. (2004), Beatley (1974), and Rundel and Gibson (1996) reported similar results. They attributed intraannual spatial variability to the spatial pattern of precipitation and to the underlying soil and geomorphology. Spatially, annuals fractional cover is $<5\%$. They identified areas showing high annual cover as alluvial terraces/piedmonts, and channels, coming down from the Providence Mountains (south east of the MNP). Another area with high fractional cover during wet years is the Cinder Cone lava field, northwest of the MNP. In both cases, the high annuals cover during wet years is likely due to higher water availability at the upper soil level (Reynolds et al. 2004) and nutrient availability. Nimmo et al. (2009) supported these findings; he concluded that the water infiltration depth is smaller in Quaternary soils that characterize the upper parts of alluvial terraces typical to the MNP.

To evaluate annuals response to drought conditions, we selected one image from each decade to represent wet and dry conditions: drought years 1994 and 2007 and wet years 1992 and 2005 (Figures 11 and 12). We selected these years because they have extremely low/high annual precipitation with a high percentage falling from October to March. Drought conditions reduce spatial heterogeneity of annuals cover. During drought years, over 80% of the area has $<5\%$ annuals fractional cover, compared with less than 40% during wet years. We identified no change in histogram shape between the two decades (Figure 12), which suggests no change in the landscape response to drought. In

other words, annuals' fractional cover, though highly variable, has not changed over the last two decades. The fact that 2007 was a second consecutive year with extreme drought conditions (see Figure 2 and 3) further supports this conclusion, yet 2008 and 2009 show an increase in annuals fractional cover in response to moderate rainfall when antecedent soil water is low, consistent with Reynolds et al.'s (2004) earlier findings. We attribute the positive response to the seed bank of annuals within the soil that enables them to recover after long prevailing drought conditions when a minimum water availability threshold is met. In summary, annuals fractional cover is highly variable spatially and temporally. Similar to other arid regions (Pennington and Collins 2007), during drought conditions a more homogenous and lower fractional cover was observed. Annuals have adapted to the climate variability that characterize the MNP. Fractional cover follows the short-term (seasonal/annual) climatic conditions, and responds positively to precipitation pulses during wet years. The lack of long-term change in annuals' response to precipitation suggests the Mojave ecosystem is highly resilient to drought.

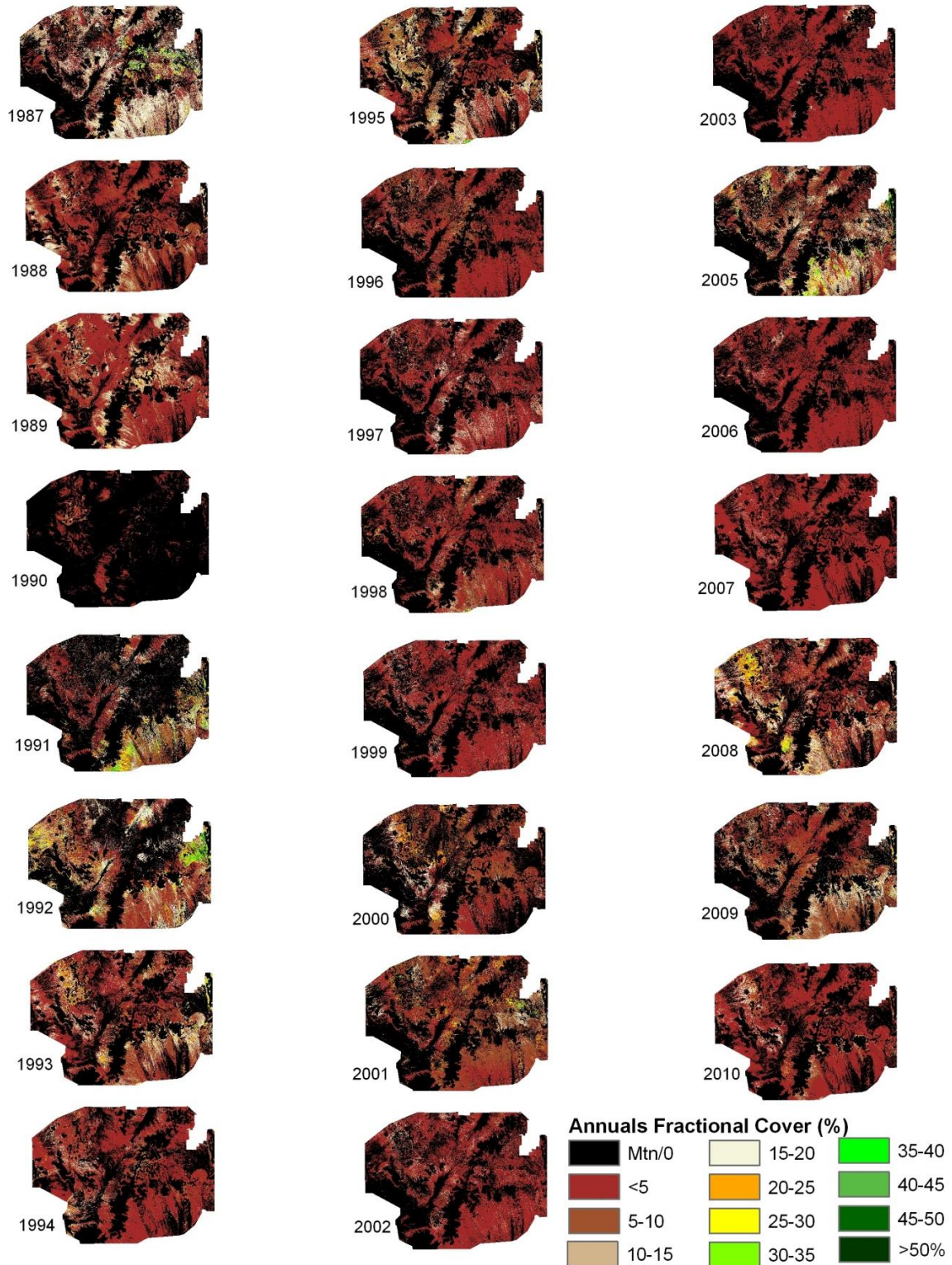


Figure 10. Yearly fractional cover of annuals. The dynamics closely follow the winter precipitation regime: wet years show high growth (e.g., 1992, 1993) and drought years show low growth (e.g. 2006, 2007).

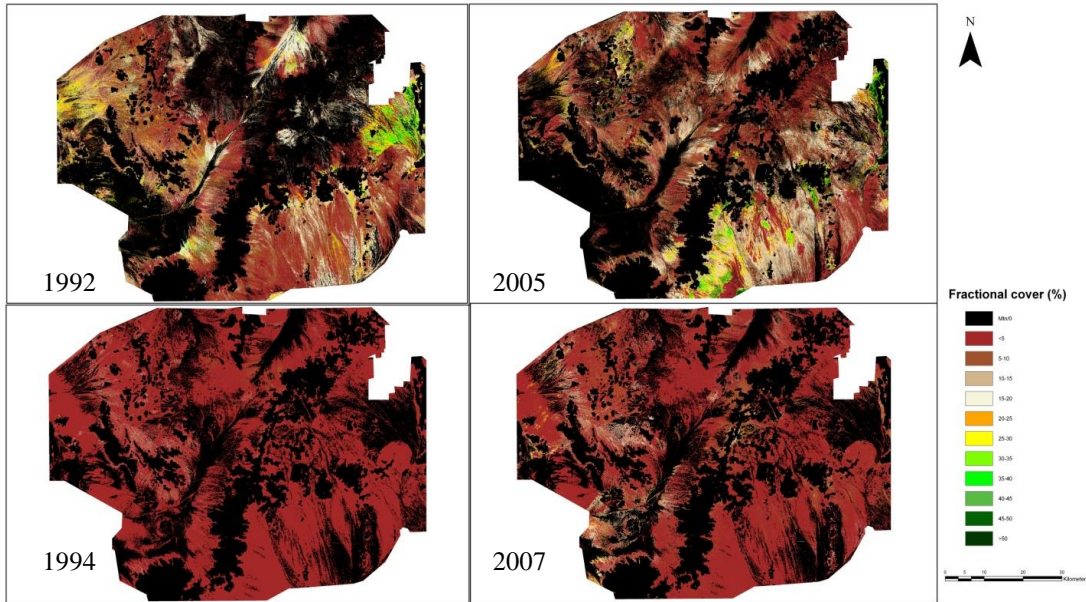


Figure 11. Fractional cover of annuals in wet and dry conditions.

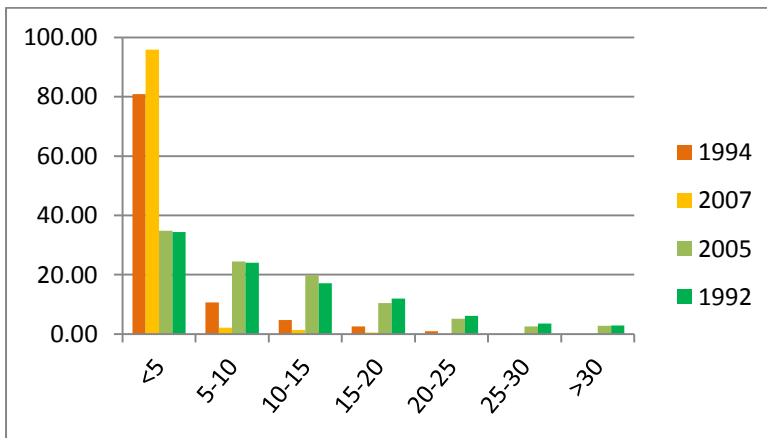


Figure 12. Fractional cover histogram for wet (2005, 1992) and dry (1994, 2007) years.

2.5.3.1: Annuals Trend Analysis:

Figure 13 shows the Mann-Kandel monotonic trend for annuals, and the cluster of statistically significant areas. Overall, 29% of the MNP area shows increase of annuals fractional cover, while 71% show a decrease. Regionally, the negative trend is dominant

in the southeast part of the MNP, while the rest of the MNP show a mix of positive and negative trends.

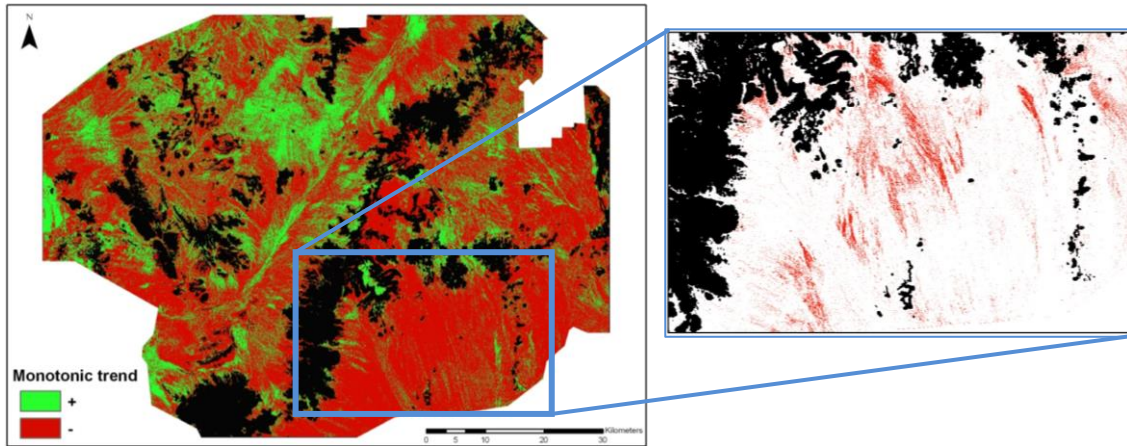


Figure 13. Left – 1987-2010 Monotonic trend for annual fractional cover in the MNP. Green indicates upward trend; red indicate downward trend. Right - Areas of statistically significant change (active washes and piedmonts).

The co-existence of both upward and downward trend suggest difference processes are dominant in different areas within the MNP. Many factors could have contributed to this trend. For example, the positive-trend linear feature in the center of the image (going SW to NE) is attributed to the road and railway crossing the MNP. Water availability is higher alongside roads as runoff diverts to roadsides. Another area showing an upward monotonic trend is the Cima Dome volcanic field, which we attribute to richer soil nutrients and the higher runoff. On the other hand, the SE corner of the MNP shows a negative trend. The negative trend may be attributed to reduced precipitation at high elevation.

The magnitude of change evaluated by Theil's regression ranges from -1.15% to 1.82%, for areas with downward and upward trends respectively. At the regional scale,

this further suggests that annuals cover has not changed dramatically over the past three decades.

Statistically, the trend for most pixels was not significant. Annuals respond to short-term water availability in the form of individual or seasonal pulses (Beatley 1974; Reynolds et al. 2004), and thus are highly variable between years. We identified several statistically significant clusters of negative trends (Figure 13 – right). Clusters correspond to active washes and parts of their alluvial piedmonts (on the edges of the washes). Precipitation analysis using the PRISM data indicated significant reduced precipitation at high elevations. The reduction of precipitation on the mountaintop reduces water flow in the channels which may lead to reduced annual growth. Other possible expansion may be changes in the runoff regime or pattern due to changes in frequency and intensity of rain events or due to emotional/fluvial processes that changes actual flow location. Another explanation may be a change in the soil properties as erosion increased over time. Nimmo et al. (2009) concluded that active washes have little ability to retain water with time, and that heterogeneity in water retention potential is likely to cause shallow rooted plants (annuals) to distribute themselves near the edges of the active wash. The spatial pattern of our results supports this and indicates reduced water availability in the upper soil horizon of these areas. As these areas show high fractional cover during wet years, the significant decrease in cover may suggest land degradation.

Geomorphology and soil play significant roles in addition to precipitation. Wallace and Thomas (2008) concluded that both Cima Dome and the SE corner of the MNP have high potential for annuals' growth. These areas experience different direction of changes presumably due to the discrepancies in geomorphology and other soil properties

such as nutrient availability. Additionally, Joshua trees dominate the Cima Dome area as the evergreen component, while creosote bush dominates the southeast region and its alluvial piedmonts and washes. Whether these plants create favorable soil characteristics for the growth of annuals or take advantage of existing soil conditions remains an open question beyond the scope of this paper.

2.5.4: Perennials

In most studies, perennial vegetation refers to a combination of short-lived deciduous plants and evergreen shrubs. In this paper, perennials are short-lived, drought-deciduous plants, mostly dwarf shrubs. Shoshany and Svorary (2002) demonstrated the importance of this functional type in other arid ecosystems and transition zones in Mediterranean climate. Visual estimation during both the March and September 2012 field visits showed that perennials comprise over 20% of total cover. Note that fractional cover as measured here refers to green canopies, whereas many perennials are dormant for 6–8 months. During dormancy, above-ground biomass dries up, increasing the fuel load and fire potential. This emphasizes the need to estimate perennial cover as a separate ecosystem component.

Figure 14 shows the dynamics of perennial fractional cover over the study period. Perennial cover is highly variable spatially. We identified two areas of high fractional cover in the southwest and center of the MNP. The southwest area is the lower part of an alluvial piedmont where runoff from the mountains is slowed, which allows infiltration to deeper soil horizons (Nimmo et al. 2009) that contain higher clay content and thus retains higher moisture content that lasts through the dry periods (McAuliffe and Hamerlynck

2010). In addition, the relatively large stones on the surface act as an evaporation barrier further keeping the relative higher soil moisture (Smith et al. 1995; McAuliffe and Hamerlynck 2010). The area in the center of the MNP is identified as the gentle slope piedmont coming down from the volcanic field, bounded by the Cima Dome geological structure. The high fractional cover during wet periods is a result of both high local precipitation and additional runoff generated by the local topography, i.e., Cima Dome (Ludwig et al. 2005).

Temporally, perennials fractional cover appears to be consistent over periods lasting several years. A relatively high fractional cover characterizes 1987 to 1994, with the exception of 1992. The latter may be a lagged response to the 1989–1991 drought (Hereford et al. 2006). Following that, 1995 to 2007 features low perennial fractional cover, generally <5%. McAuliffe and Hamerlynck (2010) reported considerable mortality of small, drought-deciduous perennial sub-shrubs during this period, caused by the late 1990s to early 2000s episodic drought. From 2008 to 2010 is highly variable, which may suggest another regime shift between wet and dry conditions. In summary, the long-term pattern of perennial fractional cover corresponds to the decadal variability and regime shift between wet and dry conditions.

2.5.4.1: Perennials Trend Analysis

Figure 15 shows the monotonic trend for perennial fractional cover and the statistically significant pixels. Overall, 32% of the MNP show increase in perennial fractional cover and 68% show a decrease. The magnitude of change ranges from -3.06% to 1.73% for negative and positive trends, respectively. Areas showing a positive trend

are not significant, whereas 11.8% of pixels with negative trends are statistically significant. The latter include the two areas showing relatively high fractional cover. Several reasons may contribute to the negative trend identified in these areas: (1) Our algorithm considers only green canopies, whereas many of the short-lived perennial appear grayish in the field; (2) the overall low cover identified by our algorithm for most years; (3) the relative high cover in 1987 (beginning point of our analysis), followed by the climate transition into a dry period; and (4) images might not represent the peak of greenness for every year.

In addition to water availability, temperature plays a significant role in the phenology of perennial sub-shrubs (Reynolds et al. 2004). The long-term increased temperature from the 1970s to the 2000s (Guida et al. 2013), coupled with the dry precipitation regime (Hereford et al. 2006), may have lead to reduced soil moisture, including from the 20–40cm depth layer where most perennials roots are located (Reynolds et al. 2004). Over the long-term, this feedback mechanism leads to mortality of perennials that shows as a negative trend.

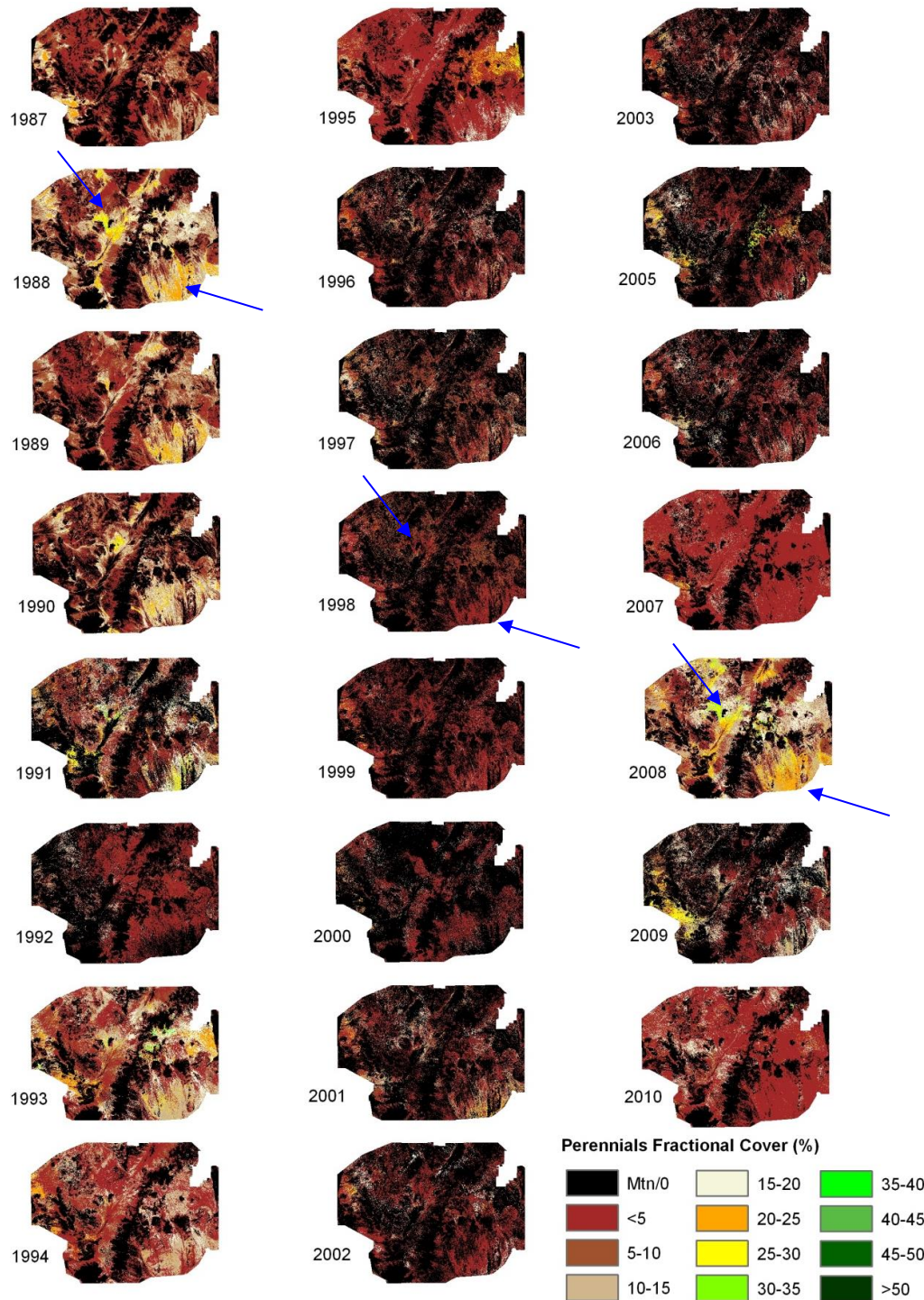


Figure 14. Yearly perennials fractional cover. Arrows represent areas characterized by high fractional cover during favorable conditions. Dynamics follows long term decadal climate and regime shifts identified by Hereford et al. (2006).

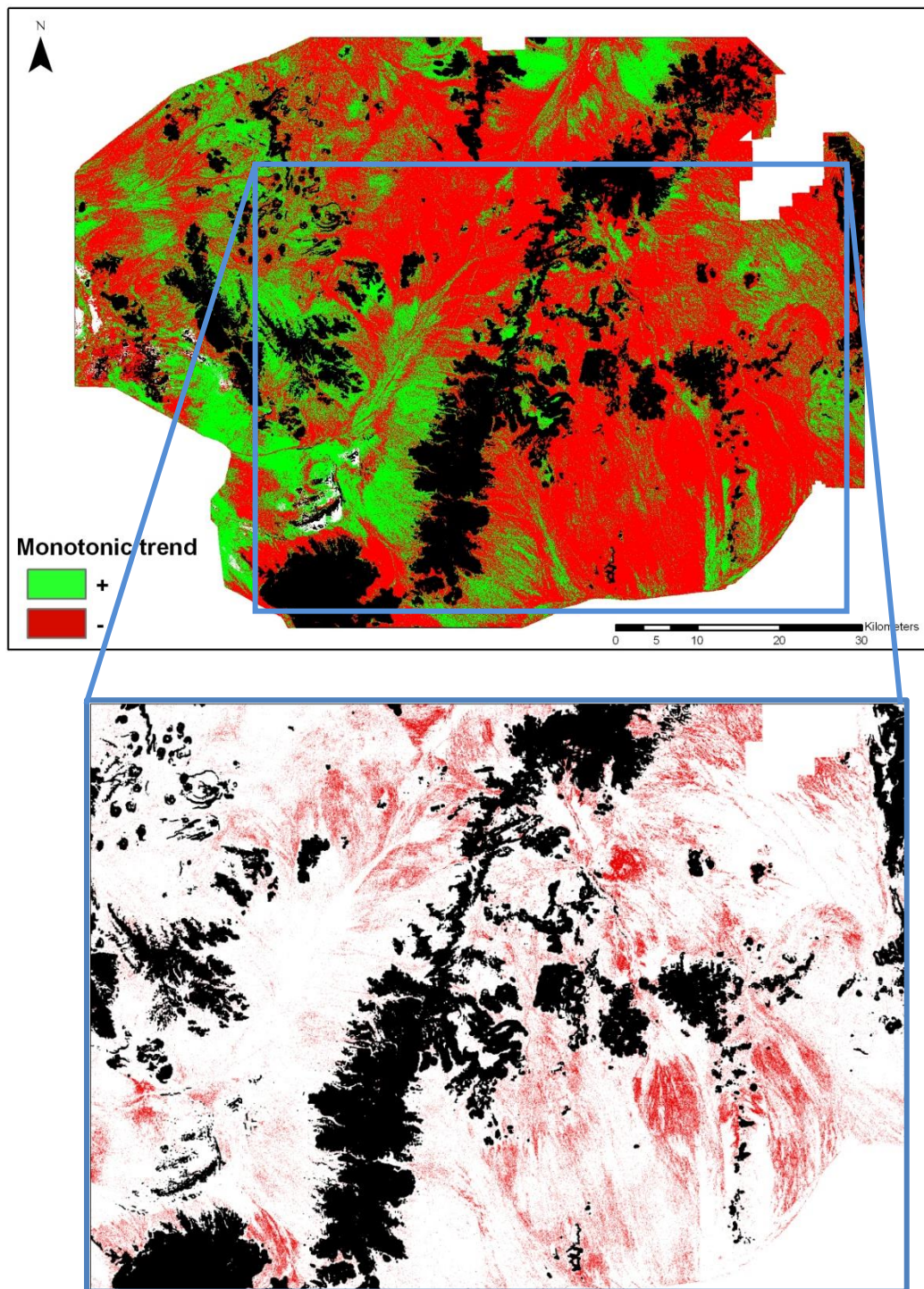


Figure 15. Up – 1987-2010 MK trend for perennial vegetation; down – areas with statistically significant changes at the 0.05 level. Note that similar to annual vegetation, areas with significant changes are located at piedmont and alluvial terraces.

2.5.5: Evergreens

As the dominant vegetative component of the MNP ecosystem, evergreen fractional cover is an indicator of the ecosystem health. Evergreen cover affects soil moisture availability, potential evapotranspiration, soil-crust development, erosion potential, and condition of wildlife habitat (Wallace et al. 2008).

As expected, evergreen vegetation has the highest and most stable fractional cover amongst all different vegetation functional types (Figure 16). Reynolds et al. (2004) concluded that a consistent aboveground biomass enables evergreen vegetation to take advantage of winter precipitation. Most of the MNP has an evergreen fractional cover above 10%, with many areas consistently above 20% cover. Examples of high fractional cover are the Cima Dome and Cinder Cone volcanic fields, as well as the alluvial piedmonts around the Providence Mountains. Field visits and data indicate that Joshua trees and Yucca dominate the Cima Dome, and creosote dominates the cinder cone and piedmonts. These are the main species from which the end-members for evergreen vegetation were derived, and they have been found to have relatively large, dense, and green canopies with a strong signal. For many widely spread species, such as creosote bush, Miriti et al. (2007) and Guida et al. (2013) reported little distribution changes over the last three decades in the Mojave. It should be noted that a cluster of low cover (<5%) in the center of the MNP appeared in 2005. This cluster is attributed to the Midhills campground fire that occurred in June 2005. The fire was a result of lightning and the high vegetation cover (Juniper and Pinyon) following the wet winter of that year. The fire scar is consistent for 2005 through 2008, with signs of rehabilitation appearing in 2009–2010.

2.5.5.1: Evergreen Trend Analysis

Most of the MNP show increase in evergreen fractional cover over time (Figure 17). Overall, 68% show a positive trend, and 32% show a negative trend. Their trend slope indicate magnitude of changes ranges -1.87% to 3.6%. Statistical analysis showed 23.6% areas with positive changes to be significant. These areas show a consistent average change of ~1% per year, and their majority is located along active washes. We hypothesize that low slope and high water availability due to the proximity to the wash promote water infiltration. The deeper rooting system of the evergreen vegetation enables it to use this moisture to maintain and even increase their canopy during the current prevailing dry regime conditions (Hereford et al. 2006). Other areas with similar geomorphic characteristics, however, are not significant, indicating that need a more in-depth analysis at the local scale to determine the driving force for these changes.

Most areas with negative trends are comparable to those identified by Wallace et al. (2008) as having high evergreen/perennial cover. Analysis of Figures 16 suggests these areas had relatively high evergreen cover at the beginning of our time series (end of 1980s), and that they are highly variable. In summary, our results suggest little change in evergreen fractional cover over the last three decades. The long life span, high drought tolerance, and consistent aboveground biomass enable evergreen vegetation to maintain itself in the highly variable desert climate.

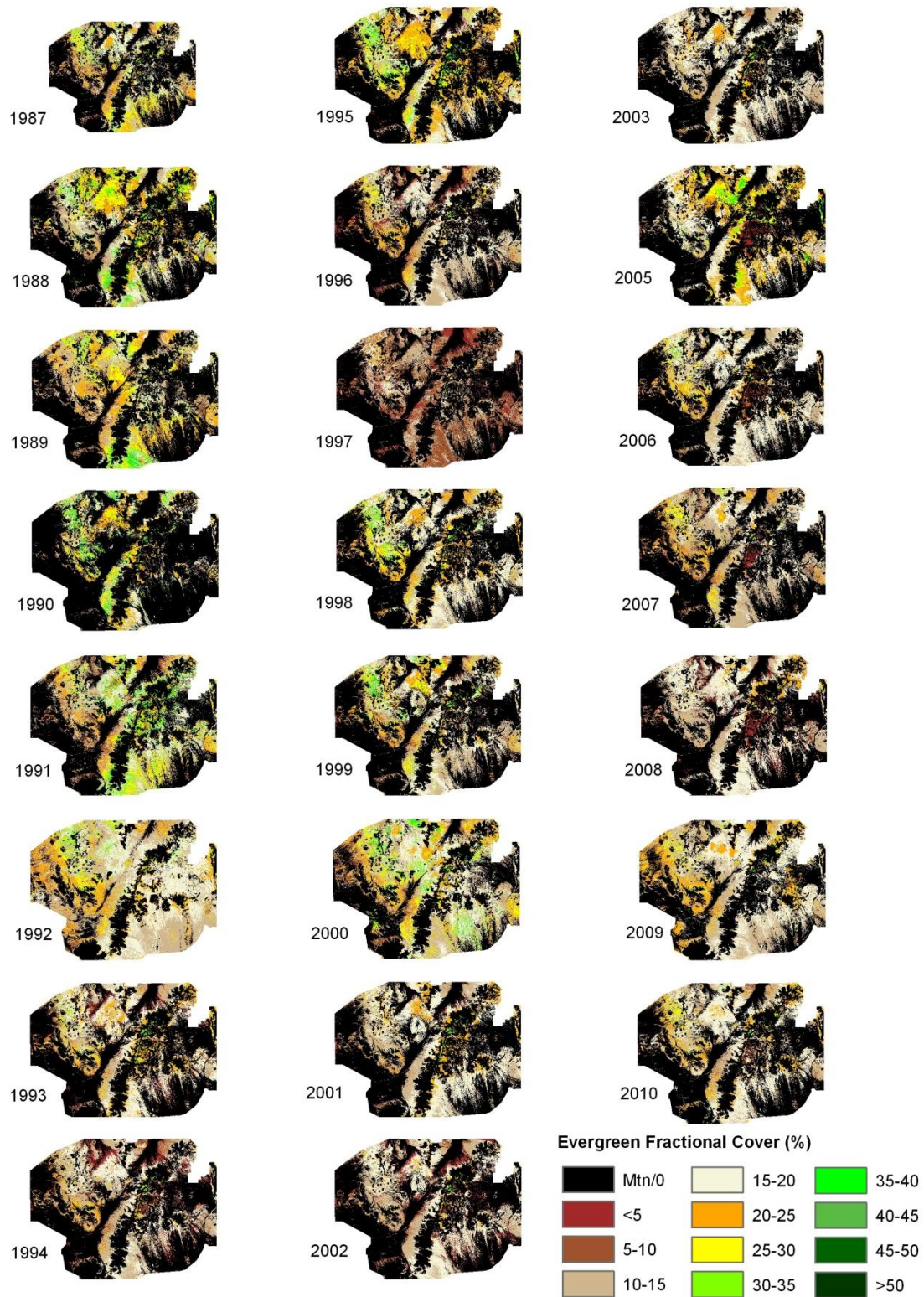


Figure 16. Yearly evergreen fractional cover.

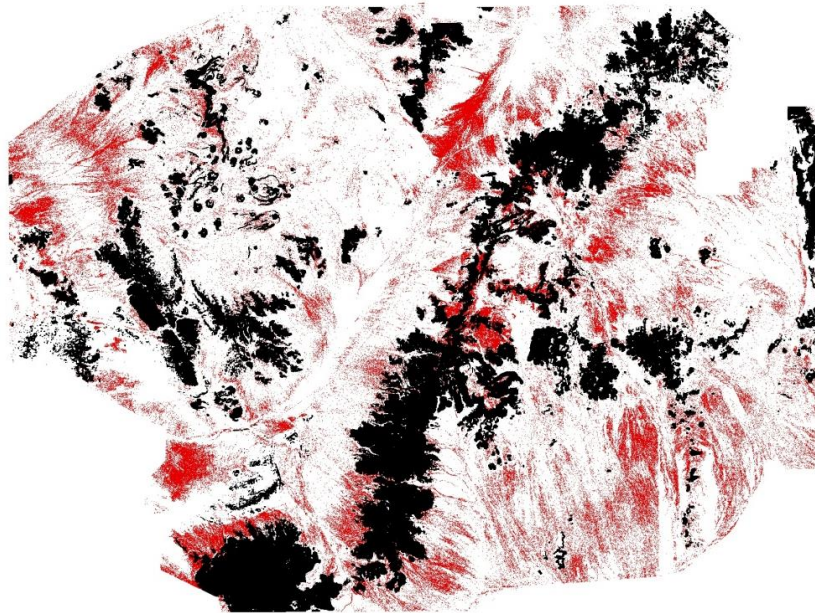
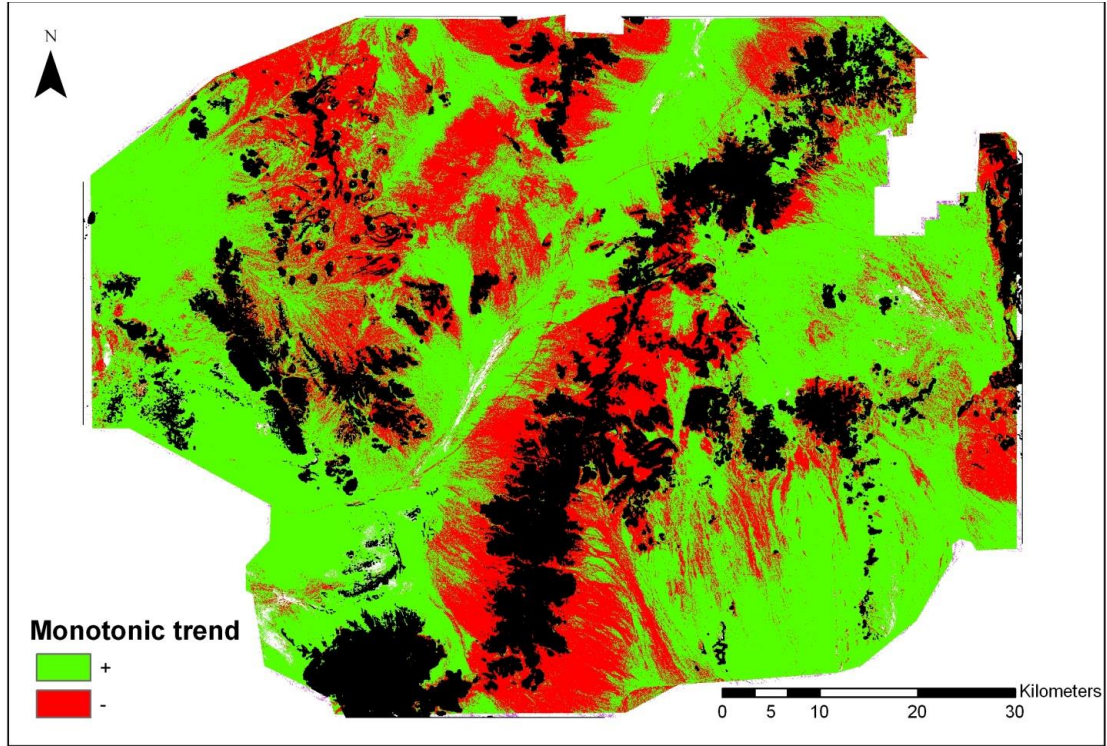


Figure 17. Top - 1987-2010 monotonic (MK) trend for evergreen fractional cover; bottom – areas of statistically significant change (in red).

2.6: Remaining Uncertainties

Technical uncertainties relate to pre-processing, MESMA, and trend analysis steps. While all images were radiometrically and atmospherically calibrated, uncertainties due to miscalibration in single band or for single images cannot be ruled out entirely in the pre-processing scheme. The MESMA algorithm minimizes error by accounting for the different number and type of end-members, yet some uncertainties still exist related to the representation of vegetation and soil components by spectral signatures: different signatures might give different results. Hostert et al. (2003) pointed out the uncertainties associated with dead biomass and nonlinearity. Part of this was overcome by including NPV as an end-member in MESMA. The nonlinear relationship between vegetation cover and reflectance remains an uncertainty and may result in slightly different vegetation fraction estimates (Elvidge 1990). Our results show good agreement with field data; we need more field observations to fully validate and calibrate the model. The trend analysis used in this paper is nonparametric and thus is robust to outliers. Yet, the magnitude of change as evaluated by Thiel's regression is smaller than the model's RMSE. In addition, the first point (first image) of the time series may influence the direction of the trend, however. We selected acquisition times based upon a conceptual model and high quality availability. Some images do not necessarily represent the peak cover for each functional type. Some growth of perennials and evergreen may still occur during early spring, and some annuals may grow during wet summers.

2.7: Summary and Conclusions

In this study, we quantified and characterizing natural desert vegetation spatio-temporal variability and changes in response to climate at the functional-type level using remote sensing. Methodologically, this study represents a proof of concept for applying MESMA, phenology, and non-parametric trend analysis to estimate functional type cover and changes at local-to-regional scale throughout the Mojave Desert. The resulting functional types and trend maps enhance vegetation distribution and ecosystem monitoring efforts by identifying areas where local forces operate. Identifying areas where different forces operate can inform ongoing and future scientific investigation and management efforts related to preserving the natural desert environment. Furthermore, the method proposed here allows us to look simultaneously at both local and regional scales and provide insight on the relationship between changes of different functional types. This approach can be extended to other arid regions and other vegetation associations, adding to our knowledge of their phenology.

We conclude that the spatiotemporal variability of vegetation functional types during the period of 1987-2010 is attributed to patterns of water availability, which, in turn, is determined by precipitation spatiotemporal patterns, local soil properties, and underlying geomorphology. Annuals' cover was consistently low and highly variable, both spatially and temporally. We identified no regional change in the response of annuals to drought over time. Perennials' cover was found to be highly variable spatially, with two areas showing increased cover due to local geomorphology and soil characteristics that promote higher soil moisture content in the 20-40cm horizon. Temporally, perennials are consistent on a time scale of several years to decades, following climate regime shifts

between wet and drought conditions. Evergreen vegetation is the dominant functional type and has the highest (>30%) and most spatially consistent fractional cover. With regard to climate, we concluded evergreen growth is disconnected from short-term climate variability.

Regionally, evergreen shows a dominance of positive trend while perennials and annuals show a negative trend, suggesting land degradation in the form of shrub encroachment. For most areas, the changes are not significant over time; however, the existence of a monotonic trend may distinguish between rehabilitation and degradation. No relationship was found between clusters of significant vegetation trend to clusters of significant climate trend. To fully understand the local driving forces and why some locations change while others do not requires additional fieldwork.

2.8: Acknowledgements

We would like to thank Dr. Kathrin Tomas and Dr. Cynthia Wallace (USGS) for providing field data. We also thank Dr. Debra Hughson (National Park Service) for her help getting the research permit and providing insights on the Mojave National Preserve vegetation dynamics. The Matthew G. Bailey Scholarship awarded to Shai Kaplan funded some of the fieldwork for this study.

2.9: References

- Archer, S.R. and K.I. Predick, 2008. Climate Change and Ecosystems of the Southwestern United States. *Rangelands*, 30, 23-28.
- Baldwin, M. P., L. J. Gray, T. J. Dunkerton, K. Hamilton, P. H. Haynes, W. J. Randel, J. R. Holton, M. J. Alexander, I. Hirota, T. Horinouchi, D. B. A. Jones, J. S. Kinnersley, C. Marquardt, K. Sato, and M. Takahashi, 2001. The quasi-biennial oscillation. *Reviews of Geophysics*, 39, 179-229.
- Beatley J.C. 1974. Phenological events and their environmental triggers in Mojave-Desert. *Ecosystem Ecology*, 55, 856–863.
- Beatley, J.C., 1979, Shrub and tree data for plant associations across the Mojave/Great Basin desert transition of the Nevada Test Site, 1963-1975, Springfield, VA, National Technical Information Service, DOE/EV/2307-15 U-48, 52 p.
- Bonan, G.B., 2002. Ecological climatology – concepts and applications. Cambridge university press, United Kingdom, pp 678.
- Buyantuyev, A. and J. Wu, 2009. Urbanization alters spatiotemporal patterns of ecosystem primary production, a case study of the Phoenix metropolitan region, USA. *Journal of Arid Environment* 73, 512-520.
- Casady, G.M., W.J. van Leeuwen, and B.C. Reed, 2013. Estimating winter annual biomass in the Sonoran and Mojave Deserts with satellite- and Ground-Based observations. *Remote Sensing*, 5, 909-926; doi:10.3390/rs5020909.
- Chapin, F.S., P.A. Matson, and H.A. Mooney, Principles of Terrestrial Ecosystem Ecology, 2002. Springer-Verlag Press, NY.
- Chavez, P.S. Jr., 1996 Image-based atmospheric corrections – revised and improved. *Photogrammetric Engineering and Remote Sensing*, 62, 1025-1036.
- CLIMAS: Climate Assessment for the Southwest. 2012. Available at: <http://www.climas.arizona.edu> (accessed Jan. 18, 2013).
- Daniel, W.W. 1990. *Applied nonparametric statistics*. Duxbury, Pacific Grove, California, USA.
- Dennison, P. E. and D.A. Roberts, 2003. Endmember Selection for Multiple Endmember Spectral Mixture Analysis using Endmember Average RSME, *Remote Sensing of Environment*, 87,123-135.

- Ehleringer, J.R. 1985. Annuals and perennials of warm deserts. pp.162-180. In Chabot B.F. and Mooney, H.A. (eds.) *Physiological ecology of North American Plant Communities*. Chapman and Hall, New-York.
- Elmore, A.J., J.F. Mustard, S.J. Manning, and D.B. Lobell, 2000. Quantifying vegetation change in semiarid environments: precision and accuracy of spectral mixture analysis and the normalized difference vegetation index. *Remote Sensing of Environment*, 73, 87-102.
- Elvidge, C.D., 1990. Visible and infrared reflectance characteristics of dry plant materials. *International Journal of Remote Sensing*, 12, 1775–1795.
- Guida, R.J., S.R. Abella, W.J. Smith jr., H. Stephen, and C.L. Roberts, 2013. Climatic change and desert vegetation distribution: assessing thirty years of change in southern Nevada's Mojave Desert. *The Professional Geographer*. doi: 10.1080/00330124.2013.787007
- Hereford, R., R.H. Webb, and C.I. Longpre, 2006. Precipitation history and ecosystem response to multidecadal precipitation variability in the Mojave Desert region, 1983-2001. *Journal of Arid Environments* 67, 13-34.
- Hostert, P., A. Roder, and J. Hill, 2003. Coupling spectral unmixing and trend analysis for monitoring of long-term vegetation dynamics in Mediterranean rangelands. *Remote Sensing of Environment*, 87, 183-197.
- IPCC (Intergovernmental Panel on Climate Change), 2007. Summary for policymakers. In: *Climate Change 2007: The Physical Science Basis*. Contribution of Working Group I to the Fourth Assessment Report of the Intergovernmental Panel on Climate Change [Solomon, S., D. Qin, M. Manning, Z. Chen, M. Marquis, K.B. Averyt, M. Tignor, and H.L. Miller (Eds.)]. Cambridge University Press, Cambridge, UK, and New York, pp. 1-18.
- Loik M.E., D.D. Breshears, W.K. Lauenroth, and J. Belnap, 2004. A multi-scale perspective of water pulses in dryland ecosystems: climatology and ecohydrology of the western USA. *Oecologia*, 141, 269–281.
- Ludwig, J.A., B.P. Wilcox, D.D. Breshears, D.J. Tongway, and A.C. Imeson, 2005. Vegetation patches and runoff erosion as interacting ecohydrological processes in semiarid landscapes. *Ecology*, 86, 308-319.
- McAuliffe, J.R. and E.P. Hamerlynck, 2010. Perennial plant mortality in the Sonoran and Mojave deserts in response to severe, multi-year drought. *Journal of Arid Environments*, 74, 885-896.
- Miriti, M.N., S. Rodriguez-Buritica, S.J. Wright, and H.F. Howe, 2007. Episodic death across species of desert shrubs. *Ecology*, 88, 32-36.

Mojave National Preserve, 2002. General Management Plan. Available at: <http://www.nps.gov/moja/parkmgmt/gmp.html> (accessed Nov. 19, 2013).

Myint, S.W., and G.S. Okin, 2009. Modeling land-cover types using multiple endmember spectral mixture analysis in a desert city, *International Journal of Remote Sensing*, 30, 2237–2257.

Newman, B. D., B.P. Wilcox, S.R. Archer, D.D. Breshears, C.N. Dahm, C.J. Duffy, N.G. McDowell, F.M. Phillips, B.R. Scanlon, and E.R. Vivoni, 2006: Ecohydrology of water-limited environments: A scientific vision. *Water Resources Research*, 42, w06302.

Nimmo, J.R., K.S. Perkins, K.M. Schmidt, D.M. Miller, J.D. Stock, and K. Singha, 2009. Hydrologic characterization of desert soils with varying degrees of pedogenesis: 1. Field experiments evaluating plant-relevant soil water behavior. *Vadose Zone Journal*, 8, 480-495.

Ogle, K., and J.F. Reynolds, 2004. Plant response to precipitation in desert ecosystems: integrating functional types, pulses, thresholds and delays. *Oecologia* 141, 282-294.

Pennington, D., & S. Collins, 2007: Response of an aridland ecosystem to interannual climate variability and prolonged drought. *Landscape Ecology*, 22, 897-910.

Reynolds, J.F., P.R. Kemp, K. Ogle, and R.J. Fernandez, 2004. Modifying the ‘pulse-reserve paradigm for deserts of North America: precipitation pulses, soil water, and plant responses. *Oecologia*, 141, 194-210.

Roderick, M.L., I.R. Nobel and S.W. Cridland, 1999. Estimating woody and herbaceous vegetation cover from time series satellite observations. *Global Ecology and Biogeography*, 8, 501-508.

Rundel P.W. and A.C. Gibson, 1996. *Ecological communities and processes in a Mojave desert ecosystem: Rock Valley*, Nevada. Cambridge University press.

Shoshany, M. and T. Svoray, 2002. Multidate adaptive unmixing and its application to analysis of ecosystem transitions along a climatic gradient. *Remote Sensing of Environments* 82, 5-20.

Smith, S.D., C.A. Herr, K.L. Leary, and J.M. Piorkowski, 1995. Soil-plant water relations in a Mojave Desert mixed shrub community: a comparison of three geomorphic surfaces. *Journal of Arid Environments*, 29, 339-351.

Sonnenschein, R., T. Kuemmerle, T. Udelhoven, M. Stellmes, and P. Hostert, 2011. Differences in Landsat based trend analyses in drylands due to the choice of vegetation estimate. *Remote Sensing of Environment*, 115, 1408-1420.

Troch, P. A., G.F. Martinez, V.R.N. Pauwels, M. Durcik, M. Sivapalan, C. Harman, P.D. Brooks, H. Gupta, and T. Huxman, 2009. Climate and vegetation water use efficiency at catchment scales. *Hydrological Processes*, 23, 2409-2414.

Ustin, S.L. and J.A. Gamon, 2010. Remote sensing of plant functional types. *New Phytologist*, 186, 795-816.

Wallace, S.A., and K.A. Thomas, 2008. An annual plant growth proxy in the Mojave Desert using MODIS-EVI data. *Sensors* 8, 7792-7808.

Wallace, S.A., R.H. Webb, and K.A. Thomas, 2008. Estimation of perennial vegetation cover distribution in the Mojave Desert using MODIS-EVI. *GIScience & Remote Sensing* 45, 167-187.

Wilhite, D. A. 2000. Drought as a nature hazard. *Drought. A Global Assessment*. London, Routledge. 1, 1-18.

CHAPTER 3: RESPONSE OF URBAN AND NON-URBAN LAND-COVER IN SEMI-
ARID ECOSYSTEM TO SUMMER PRECIPITATION VARIABILITY¹

3.1: Abstract

Vegetation response to precipitation variability is an important climate-ecosystem-hydrology feedback. Anthropogenic impacts coupled by changes in seasonal and annual precipitation patterns can have a dramatic and large spatial effect on ecosystem structure and functioning, especially in water limited environments. While the natural Sonoran desert is water limited, Phoenix metropolitan area is constantly being irrigated to support human activities. The aim of this research is to study how urban areas differ from their natural surroundings ecosystems in their phenology and response to summer water inputs. Rain use efficiency (RUE), inter-annual and intra-annual vegetation phenology and above-ground net primary production (ANPP) of the two land cover types and their response to summer precipitation have been analyzed. In addition, a soil water balance model is used to simulate the Horton index (H) as a measure land cover response to climate variability. Results show that the urban environment has a year round constant, high productivity with high variability in RUE. The desert has lower productivity and responds strongly to summer water. Furthermore, the desert ecosystem convergences towards $H=1$ and $RUE \sim 133 \text{ MJ/m}^2 \cdot \text{hour mm}^{-1}$. Based on the RUE and ANPP it was calculated that 295 mm of water input are necessary to sustain the urban tree biomass. Unlike natural ecosystems, urban areas RUE do not converges to a common

¹ This manuscript was submitted to Journal of the Arizona-Nevada Academy of Science in October 2011 and published in March 2012.

maximum value, suggesting that inter annual variability in hydrological partitioning over urban and desert land-cover is consistent with the water use efficiency concept.

3.2: Introduction

The scope of human's role as major ecological and climatic agents of Earth's ecosystems change is gaining recognition, and it is important to understand how specific forms of human-induced land transformation affect the dynamics of Earth's physical and biological systems (Vitousek and Mooney, 1997). Recently, more attention has been paid to urbanization as it constitutes one of the more ecologically disturbing land transformation processes (Grimm et al. 2008; Imhoff et al 2000). This is especially important in water limited environment, as they have been shown to be highly sensitive to any form of change (Whilhite, 2000; Newman et al. 2006) and contain fast growing urban centers.

One of the most important components of arid and semi-arid ecosystems is vegetation. Ecosystem processes in arid landscape such as vegetation productivity, measured as the above-ground net primary production (ANPP), vary in response to precipitation (Buyantuyev and Wu, 2009; Pennington and Collins 2007). Changes in vegetation response to precipitation changes are an important climate-ecosystem-hydrology feedback as they influence carbon, water and energy allocation at the land surface (Troch et al. 2009). Webb et al. (1986) showed ANPP and evapotranspiration are strongly correlated, and since evapotranspiration is considered the largest component of the water balance, its inter-annual variability is strongly related to ecosystem function and productivity. Over the short timescale vegetation can adapt to climate variations

(Troch et al. 2009). Nevertheless, changes in seasonal and annual precipitation patterns can have a dramatic and large spatial effect, that coupled by anthropogenic impacts (i.e. Irrigation, temperature, higher CO₂) can change ecosystem structure and functioning. While this is true for natural vegetation, Buyantuyev and wu, (2010) have shown urban and agriculture vegetation dynamics do not respond to temporal and spatial precipitation patterns due to irrigation and fertilization. Furthermore, Neil et al. (2010) demonstrated that natural desert vegetaion has higher inter-annual variability in response to precipitation amount and timing compare to the non-native urban vegetation.

One of the indicators to measure vegetation response to climate changes is the Rain Use Efficiency (RUE) which is defined as the ratio between ANPP and precipitation, thus informs us on evapotranspiration. Huxman et al. (2004) showed all ecosystems persist within some range of climate variability and that under dry conditions (drought) the ecosystem Rain Use Efficiency (RUE) converges toward $0.42\text{gm}^{-2}\text{yr}^{-1}$ – the value of semi-arid ecosystems. Troch et al. 2009 demonstrated the same concept by plotting RUE versus the Horton index (H), which is defined as the ratio between actual evapotranspiration and catchment wetting (precipitation minus infiltration excess runoff). Result from Troch et al. (2009) showed that in water limited regions, vegetation is more efficient in its water use and H approaches 1, meaning all the water available for evaporation were vaporized through soil evaporation, interception and vegetation evapotranspiration. Following these results, the authors concluded the use of Horton index will help refine the partitioning of precipitation between soil and vegetation processes. However, Huxman et al. (2004) and Troch et al. (2009) studies refer to natural ecosystems at the catchment scale. They do not take into account land-use land cover

changes, such as urbanization – an ecosystem shaped and controlled at all of its parts, especially vegetation, by human activities.

Urban vegetation often varies substantially from native ecosystems surrounding the city. In recent decades many of the world's drylands experienced high rate of urbanization (Brazel et al. 2000). Given the water limitation of the natural desert on the one hand and the constant availability of water via irrigation in the city, the overall aim of the research is to study how urban areas differ from their natural surroundings ecosystems in terms of their phenology and response to summer water inputs as a first step in understanding the ecohydrological consequences of land cover changes in general, and specifically urbanization. To achieve this and outline implications to vegetation water use efficiency, inter-annual and intra-annual vegetation phenology and ANPP of the different land cover types and their response to summer precipitation have been analyzed.

Driven by the paper of Troch et al. (2009), two hypotheses are offered:

1. Urban landscape will have lower variability in the NPP response to precipitation compare to the desert.
2. The desert RUE will vary, and as drought condition develops, it will follow the Troch et al. (2009) convergence towards $H=1$. The RUE over the urban landscape, on the other hand, will not change during drought years thus will not converge to the semi arid RUE and will stay constant due to irrigation.

The analysis of the urban vegetation compare to the natural vegetation will enable us to test the effect of irrigation and can lead to a more sustainable management of the water resources.

3.3: Study Area

This study will focus on the Phoenix metropolitan region (Figure 18); An area that has undergone extensive modification to its landscape during the 20th century, following rapid population growth and expansion of the urban land cover on the account of semi arid natural desert shrubland. As urbanization in this region is predicted to continue and increase, the influence of land cover changes on the hydrological cycle and ecological system in these regions will also intensify (Imhoff et al 2000).

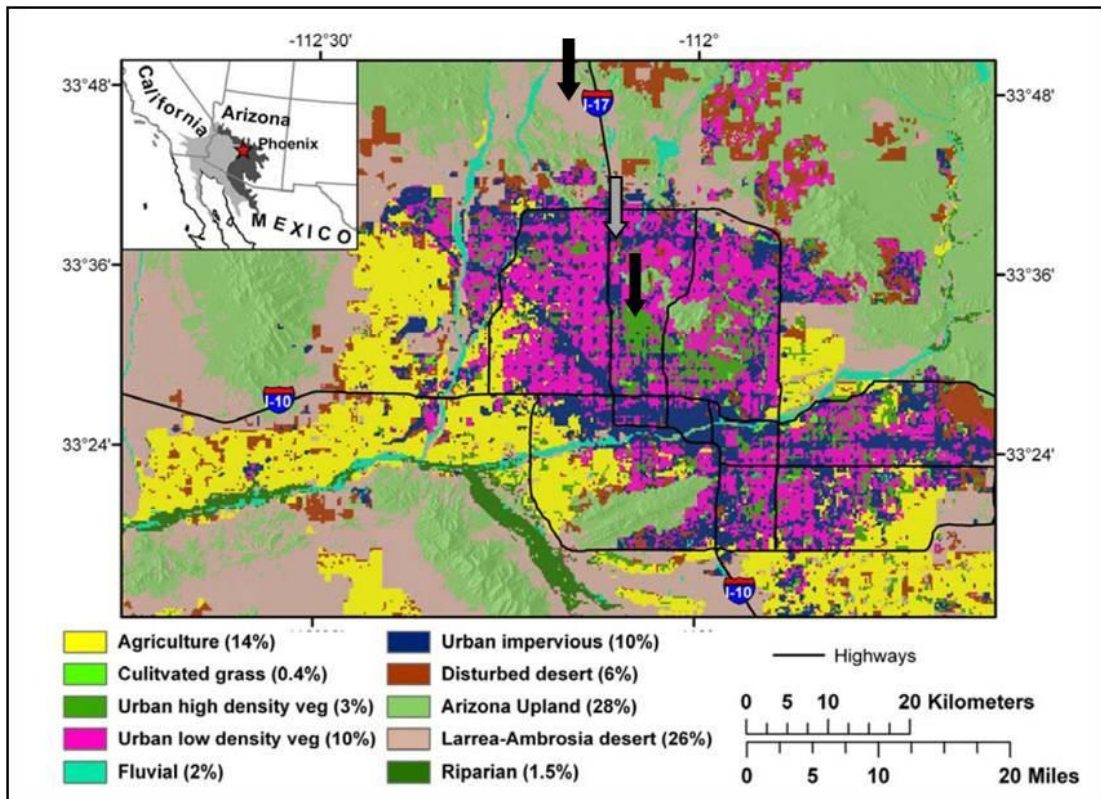


Figure 18. Map of the study area land cover (Buyantuyev and Wu, 2009). Black arrows point the locations selected for comparison. Gray arrow indicates the meteorological station location.

Climatologically, the region is classified as a semi-arid hot desert. Mean summer temperature is 30.8°C with mean summer high temperature of 40°C. Mean annual precipitation is 193 mm, falling in two distinct wet seasons: one in the winter and the other in summer. Over 40% of rainfall occurs during spring and summer (May - October) as a result of the influence of the southwest monsoon (Shepherd, 2006). Soils are a mixture of clay-loam and sandy loam (USDA soil survey; <http://websoilsurvey.nrcs.usda.gov>). The region has two main ecosystems, which are subdivisions of the Sonoran Desert scrub: (1) Arizona upland – characterized by a mix of Palo-Verde trees and cacti series; and (2) lower Colorado River with creosote bush series. This study will focus on a comparison of the vegetation response to climate variability between the core urban area with high density vegetation (trees) and the lower Colorado River ecosystem (figure 18) for the period of 2000-2009.

3.4: Data and Methodology

3.4.1: Remote Sensing Data

Satellite remote sensing techniques provide successful tools for environmental monitoring over long time periods and large spatial scale (Ballone et al. 2009). Taking a remote sensing approach, this study uses 16 day, 250m resolution MODIS-NDVI (MOD13A1 product) images for the 2000-2009 period were obtained from CAP-LTER (years 2000 -2005) and Oak Ridge National Laboratory (<http://daac.ornl.gov/MODIS/modis.htm>; years 2006 - 2009). The NDVI is defined:

$$NDVI = \frac{(NIR-RED)}{(NIR+RED)} \quad (3.1)$$

where RED and NIR are atmospherically-corrected surface reflectance values in red and infrared bands, respectively.

Based on the land-cover map presented in figure 18, two pixels, each representing the urban and desert land cover were selected:

1. Urban (residential with high density vegetation) – 33° 32' 56.07" N/112° 04' 51.65" W
2. Desert - 33° 48' 26.51" N/112° 13' 58.17" W

For each pixel the monthly mean NDVI was calculated and each month was averaged over the entire period of 2000-2009 to identify seasonality. NDVI seasonality was later compared to precipitation seasonality to identify vegetation response to seasonal precipitation.

NDVI data were used to calculate ANPP for the growing season May 1st - October 31st (based on Troch et al, 2009) using the model suggested by Buyantuyev and Wu (2009):

$$ANPP = \int NDVI * PAR \quad (3.2)$$

where PAR is the fraction of incoming solar radiation between 400 and 700 nm in MJ/m²*hour . Following Buyantuyev and Wu a fixed value of PAR=0.47 was used. Because MODIS-NDVI product has a temporal resolution of 16 day, each NDVI value was multiplied by 16 and then by the spatial resolution (250m²). For example the 2005 ANPP for the desert area is 5448.24 MJ/m²*hour and the urban ANPP is 8495.16 MJ/m²*hour (Figure 19).

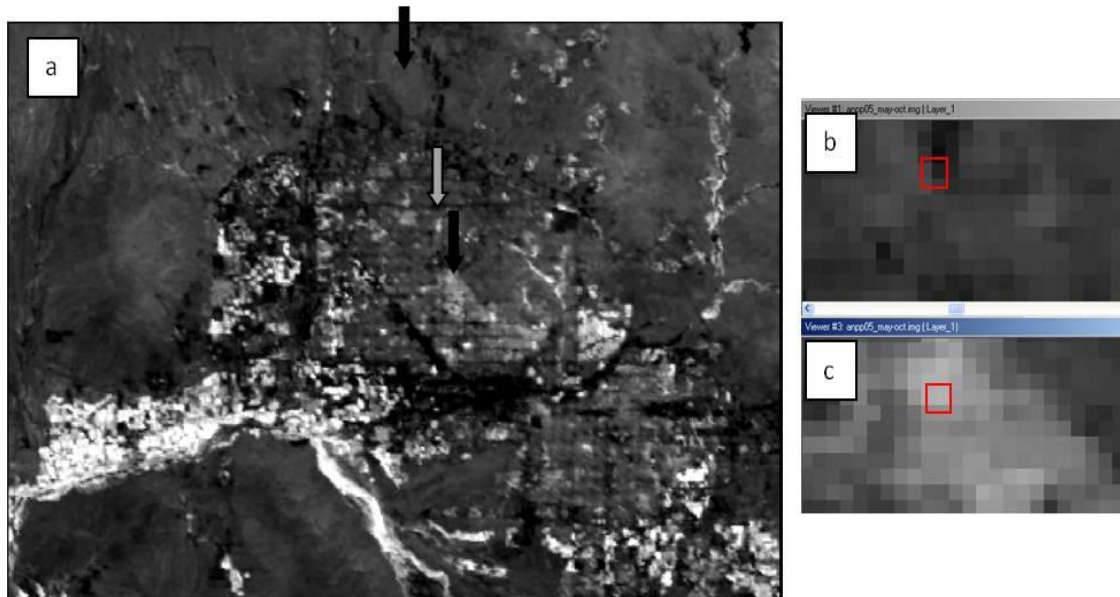


Figure 19. a) Grayscale image of the 2005 growing season ANPP. Black arrows point selected pixels; Gray marks Greenway meteorological station; b) Zoom of the desert pixel; c) Zoom of the urban pixel. Whiter and darker pixels represent higher and lower ANPP, respectively.

3.4.2: Precipitation Data

Precipitation data for the Phoenix Greenway meteorological station were obtained from CAP-LTER (<http://caplter.asu.edu>). This station represents climate of the northern part of the phoenix metropolitan area; and it is a station relatively close to the city edge so it can be regarded as representative for both the city and the desert. Daily data were transformed to monthly total and each month was averaged over the entire period of 2000-2009 to suggest trends in seasonality. Total annual rainfall was also computed.

3.4.3: Horton Index Simulation

Based on Troch et al. (2009), Horton index can be defined in modern hydrology terms as:

$$H = \frac{V}{W} \quad (3.3)$$

Where V is the sum of vaporization, interception and plant evapotranspiration, and W is the total water available for vaporization. In their paper, Troch et al. (2009) derive H from precipitation, stream flow, base flow and runoff. Those data are not available at the land cover level or at the point scale. Therefore we simulated the Horton index using the soil water balance (SWB) model from Laio et al. (2001) coded in MATLAB by Dr. Enrique Vivoni. V is equal to the SWB model $\langle et \rangle$, and W was considered as the difference between precipitation to runoff (Q). Leakage is assumed to be negligible. The SWB model and the corresponding parameters used to calculate H by Troch et al. are described in figure 20.

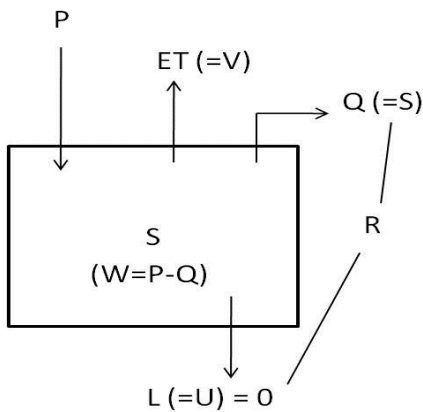


Figure 20. The Soil Water Balance model. P – precipitation; ET - evapotranspiration; Q - runoff; L - leakage (assumed to be zero); R = stream flow. Letters in parenthesis are the corresponding representation of Troch et al. 2009.

Input parameters for the SWB: The monthly precipitation event depth (α) and frequency (λ) were calculated for each month and used as input for the SWB stochastic rainfall generator (table 2). Soil parameters for loam were obtained from Laio et al. (2001). Two vegetation types were used: trees and creosote bush, representing the urban and desert ecosystem, respectively. The parameters used for each are listed in Table 3.

Table 2. Monthly mean storm depth (α) and mean arrival time (λ) for the years of study.

Year	2000	2001	2002	2003	2004	2005	2006	2007	2008	2009
	α									
Jan	0.254	8.672	1.524	3.810	1.727	9.616	0.000	3.747	9.017	3.302
Feb	4.318	2.572	0.000	12.859	13.970	6.277	0.000	2.946	1.575	4.267
Mar	7.334	7.239	0.000	5.630	5.461	1.016	13.123	7.197	0.000	0.254
Apr	0.000	4.509	0.000	5.334	9.208	7.874	0.000	2.540	0.000	8.890
May	0.000	0.762	0.000	0.000	0.000	0.000	0.254	0.254	1.185	3.556
Jun	4.826	0.508	0.000	0.000	0.000	0.508	0.254	0.000	0.000	0.000
Jul	1.334	4.445	3.471	13.970	3.556	6.054	3.912	5.283	8.788	0.677
Aug	3.612	2.709	0.664	4.267	7.874	7.842	5.546	1.270	5.207	3.387
Sep	1.873	0.000	4.911	0.677	12.319	14.224	16.320	2.794	4.826	3.556
Oct	6.816	0.000	8.128	2.286	7.959	4.318	2.985	0.000	0.000	1.270
Nov	0.699	2.667	6.350	8.509	6.655	0.000	0.000	42.926	3.895	0.000
Dec	0.254	4.953	1.727	3.302	8.839	0.000	1.588	3.429	4.572	11.430
	λ									
Jan	0.032	0.226	0.032	0.097	0.161	0.226	0.226	0.129	0.194	0.097
Feb	0.034	0.286	0.000	0.286	0.069	0.500	0.226	0.179	0.172	0.179
Mar	0.226	0.065	0.000	0.194	0.194	0.226	0.097	0.097	0.194	0.032
Apr	0.000	0.133	0.000	0.033	0.133	0.032	0.226	0.100	0.194	0.065
May	0.000	0.032	0.000	0.033	0.133	0.032	0.032	0.032	0.097	0.097
Jun	0.100	0.033	0.000	0.033	0.133	0.032	0.033	0.032	0.097	0.000
Jul	0.129	0.129	0.387	0.032	0.097	0.194	0.161	0.161	0.161	0.097
Aug	0.290	0.194	0.419	0.161	0.065	0.258	0.194	0.032	0.323	0.097
Sep	0.267	0.000	0.200	0.100	0.067	0.097	0.133	0.067	0.033	0.067
Oct	0.387	0.000	0.097	0.032	0.097	0.097	0.129	0.067	0.033	0.032
Nov	0.133	0.067	0.067	0.133	0.167	0.097	0.226	0.033	0.100	0.000
Dec	0.032	0.129	0.161	0.065	0.161	0.097	0.129	0.194	0.290	0.065

Table 3. Input parameters for the Soil Water Balance model for two vegetation types representing desert and urban ecosystems.

Parameter	Vegetation type	
	Creosote bush (Desert)	Trees (urban)
Interception (mm)	Delta_interc = 1.5	Delta_interc = 2
rooting depth (mm)	Z _r = 700	Z _r = 1200
Maximum Evaporation rate (mm/day)	E _{max} = 4.59	E _{max} = 4.5
Evaporation at wilting point (mm/day)	E _w = 0.1	E _w = 0.2

Each year was simulated for a 10 year period with its calculated monthly α and λ parameters. Vegetation seasonality was not considered. Nevertheless, E_{max} for the desert land cover was varied annually based on total precipitation. Three situations were considered: wet, normal and dry years. Maximum value for wet years was 4.59 mm/day. For dry years value was based on the linear relationship of ANPP, found to be ANPP_{min}=0.75ANPP_{max}. Minimum (dry years) and ‘median’ (averaged precipitation) values for the desert were E_{max}=3.5 and E_{max}=4.05, respectively. The urban vegetation is always irrigated, therefore only the maximum value reported above was considered. The final index was calculated at the ratio: ET/W.

3.5: Results and Discussion

3.5.1: Precipitation Analysis

Total annual rainfall time series was calculated (Figure 21). The multi-year average was 197mm/year with high variability (Standard deviation = 63mm; coefficient of variance = 32%). Range of precipitation was also large: minimum precipitation

occurred in 2009 – 99.8 mm, and maximum precipitation occurred in 2005 – 309.88 mm. 5 out of the 10 years had below average precipitation with two (2002 and 2009) lower than 1 standard deviation less than the multi—year average.

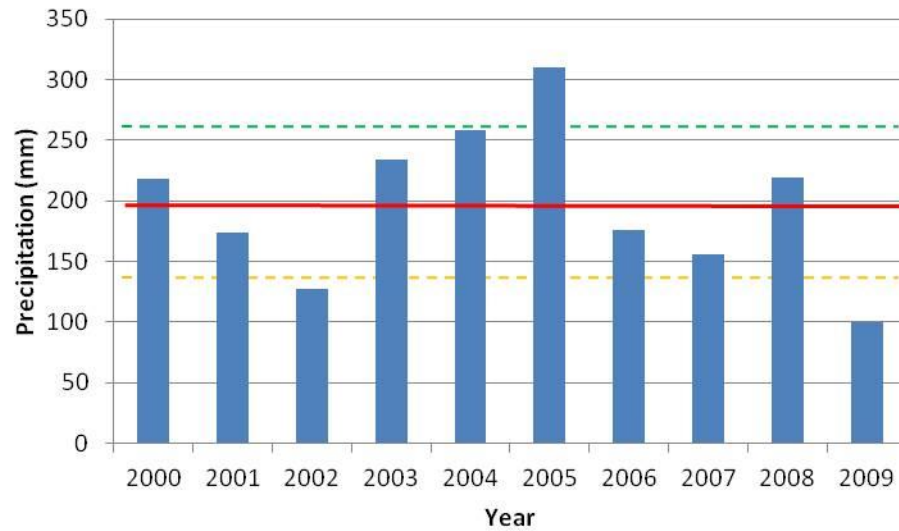


Figure 21. Yearly precipitation. Red line is the multi-year average, and dashed lines are 1 standard deviation from that mean.

Summer growing season precipitation (May – October) were also calculated (Figure 22). The summer rain average is 83.9 mm/year, with very high variability (standard deviation = 47 mm; coefficient of variance = 57%). It is important to note that the trends of summer precipitation do not correspond to the total annual precipitation. Some years (i.e. 2002) were classified as drought, yet had high summer precipitation. Other years experienced above average total precipitation and had low summer precipitation (i.e. 2003, 2004)

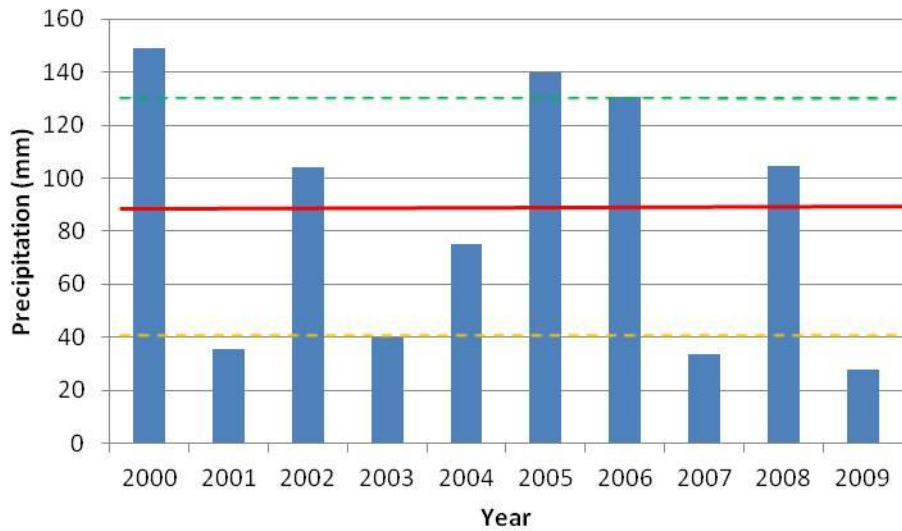


Figure 22. Yearly summer/growing season (May – October) precipitation. Red line is the multi-year average, and dashed lines are 1 standard deviation from that mean.

To represent the trend in seasonality, monthly precipitation data were computed, and each month was averaged over the entire period of record (Figure 23). Monthly precipitation show strong bi-modal pattern with two distinct wet seasons: winter (December – February; 57% of precipitation) and summer (July-September; 43% of precipitation). The dryer period lasts from May to June, where both months have less than 2 mm of rain. February is the wettest winter month (28.75 mm) and August is the wettest summer month (25.4 mm). The average monthly rainfall calculated over all months was 16.4 mm with a coefficient of variation of 53%. This analysis suggests that the variations between years can be a result of changes in either season.

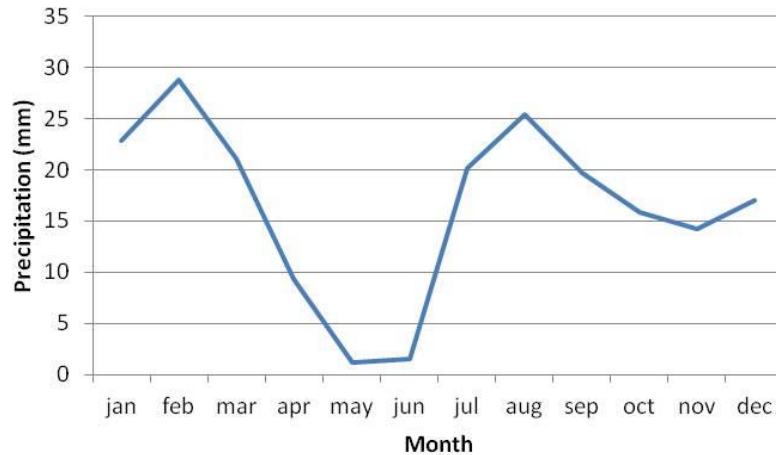


Figure 23. Average monthly precipitation for the Greenway meteorological station (2000 – 2009)

3.5.2: Response of Different Land-Cover Types to Seasonal Precipitation

To see how vegetation responds to summer precipitation, monthly averaged NDVI was plotted over seasonal precipitation for each year. Figure 24 shows an example of the vegetation dynamics and precipitation for the year 2000 growing season at the two selected urban and desert land covers pixels. As hypothesized, the urban vegetation show only small variations in response to precipitation while the natural desert vegetation has a lagged increase in the NDVI signal in respond to precipitation input.

Notice the response to summer precipitation is much stronger than to winter precipitation. A possible explanation is that temperatures during summer are more favorable for greenness-onset. The small lagged increase following winter precipitation may be attributed to plants with deeper roots such as the creosote bush. This vegetation functional type uses the soil moisture from winter to generate growth during the dry period, thus gaining competitive advantage compare to other natural desert functional types with shallow root system (Ogle and Reynolds, 2004).

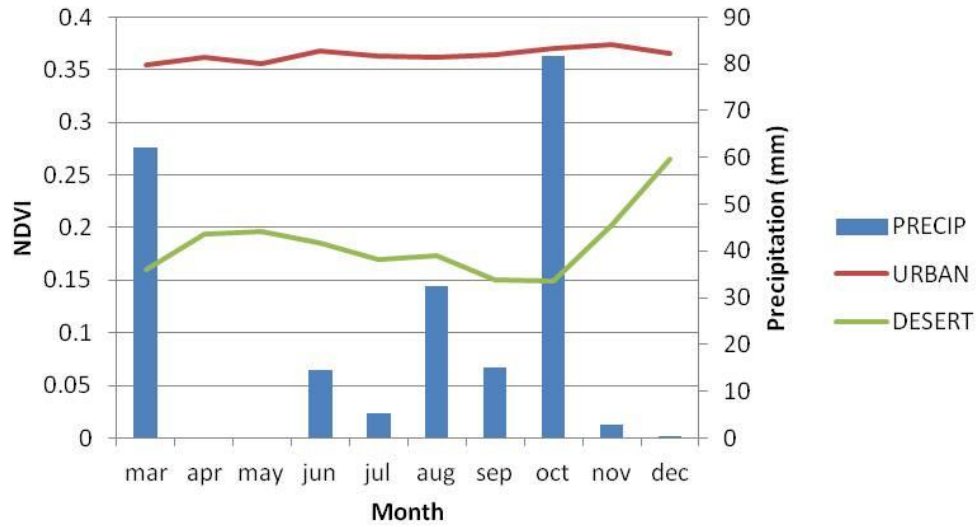


Figure 24. Vegetation dynamics in response to precipitation for the year 2000.

To measure different land cover sensitivity to summer precipitation, growing season ANPP was plotted against precipitation (Figure 25). The year of 2006 was identified as an outlier, therefore removed from the rest of the analysis. It can be seen from figure 25 that the urban land-cover has a much higher ANPP and it is less sensitive to precipitation (smaller slope). The multi-year average ANPP for the desert was found to be 3944 MJ/m²*hour (standard deviation = 876; coefficient of variance 22%). The multi-year average ANPP for the urban land-cover was found to be 8283 MJ/m²*hour (standard deviation = 589.5; coefficient of variance 7%). As we assume both land-cover types receive the same precipitation, these results indicate the impact of irrigation in the urban areas.

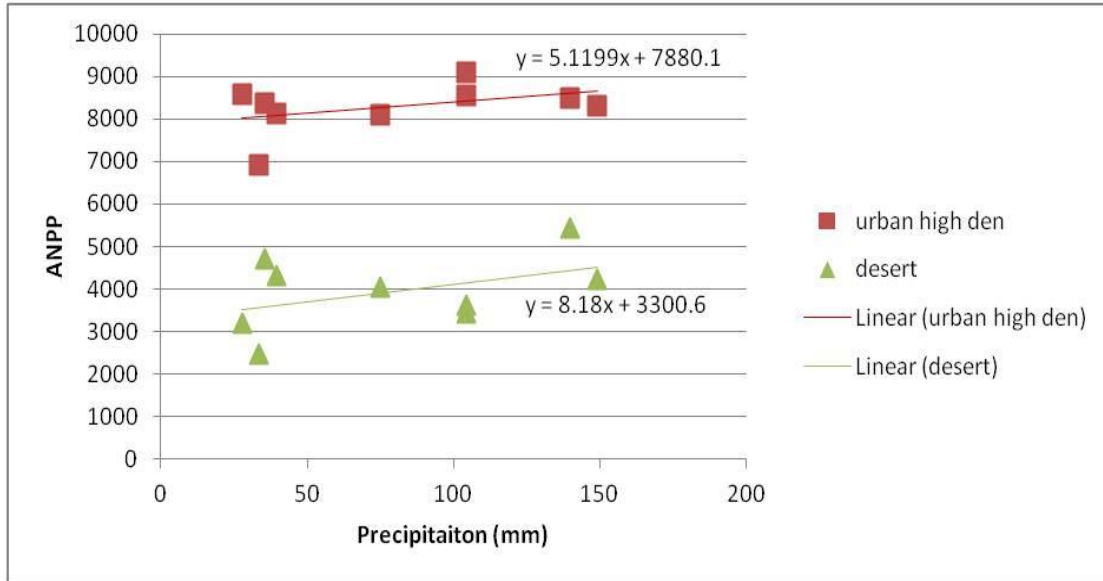


Figure 25. ANPP as a function of Precipitation for three land cover types.

3.5.3: Rain Use Efficiency and Irrigation

Another indicator to measure vegetation response to climate changes is the Rain Use Efficiency (RUE). Precipitation data and ANPP results were combined to calculate RUE:

$$RUE = \frac{ANPP}{P} \quad (3.4)$$

Comparing the RUE of the urban and desert, under the same precipitation is really just a comparison of ANPP and yield higher RUE for the urban area. This contradicts the basic concept of the RUE that environments with lower rainfall are more efficient in using it for biomass production. Therefore to calculate the actual RUE for the urban area, irrigation needs to be considered.

Figure 25 indicate the ANPP is relatively constant in the urban area. Giving the climatic conditions of the Phoenix region, we assume urban areas are always irrigated. Hence we can treat the city as having, for the low boundary, the RUE as the year with

highest precipitation in the desert. This means that the ANPP units per 1 mm of rain are the lowest. Using the RUE values for the best year in the desert (28) imply that in order to keep a relatively constant green biomass ($8283 \text{ MJ/m}^2\text{xh}$) there is a need for 295mm of water, on average, over the growing season. This means every month gets on average 49mm of water input. Based on the seasonal precipitation analysis, and the assumption people irrigate regardless of specific summer rain events, irrigation scenario was assumed to be 3 days of irrigation per week for May and June (3.6mm/event) and twice a week for the remaining months. The actual urban RUE was calculated based on the sum of daily irrigation and precipitation for each growing season. Figure 26 shows the differences between urban and desert land cover RUE.

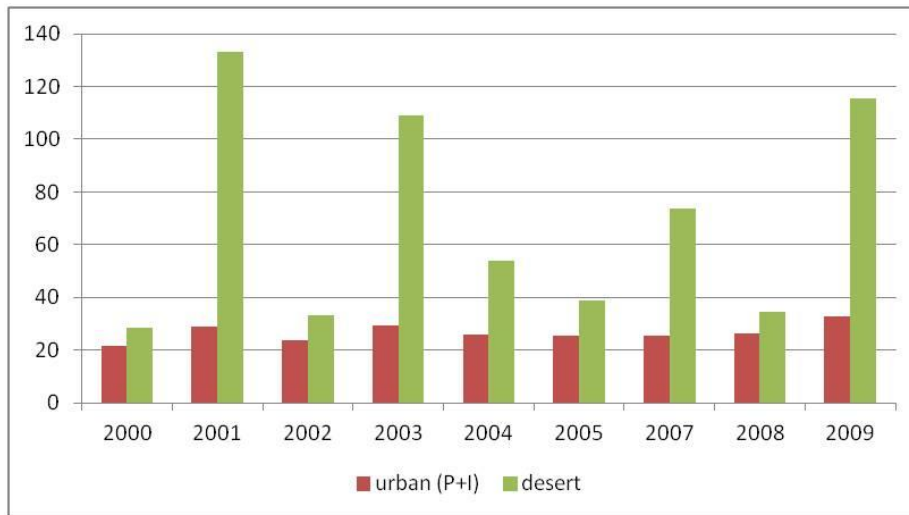


Figure 26. RUE for urban and desert land cover. Note the desert rain use efficiency is much higher and vary more, emphasizing the role of the constant fixed irrigation that keeps the same greenness and biomass throughout the year, thus constant RUE.

3.5.4: Implication for Vegetation RUE

ANPP has been shown to be related to plant evapotranspiration (Webb et al. 1996) thus we can compare growing season RUE to the Horton index in order to measure each land cover response to climate variations. Figure 27 shows the point scale vegetation RUE for urban and desert land-cover versus the inter-annual variability of the Horton index.

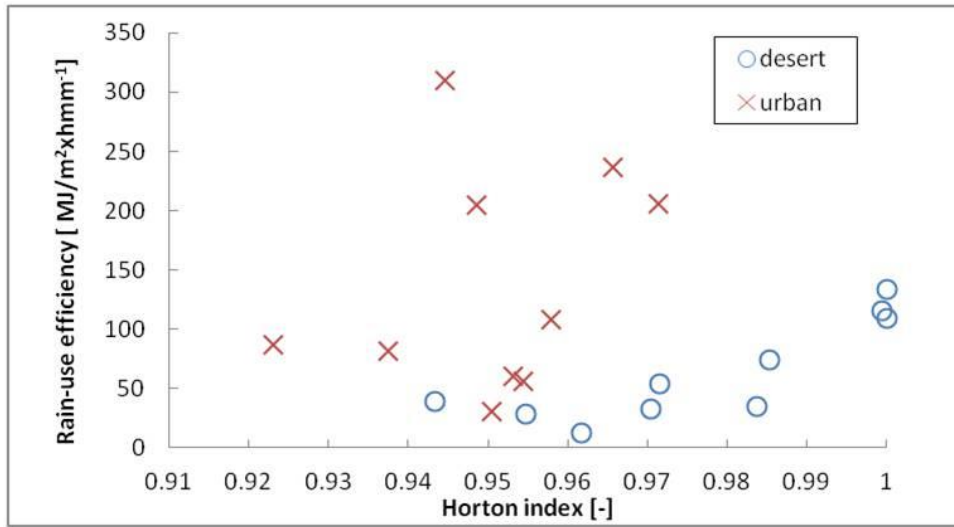


Figure 27. Vegetation rain-use efficiency vs. the Horton index variability for urban and desert land cover in the Phoenix metropolitan area.

The results indicate that the desert ecosystem convergences towards $H=1$ and $RUE \sim 133 \text{ MJ/m}^2 \cdot \text{hour mm}^{-1}$. The urban land cover, however, varies considerably in its RUE and has a relatively constant H (~ 0.95). When comparing the Horton index of each land cover type for each year (table 4), the values for the desert are constantly higher, indicating its dryness compare to the urban area.

This analysis follows the conclusions of Troch et al. (2009) that in dryer years natural ecosystems tend to converge towards a common maximum RUE. Additionally,

the analysis imply different land cover types, have a detectable signal that may help us understand the role of vegetation in the hydrological partitioning across different land cover types, especially those controlled by man,.

Table 4. Precipitation and Horton index for urban and desert land-cover

Year	Precip.	desert	urban
2000	149.098	0.9548	0.9544
2001	35.306	1	0.9656
2002	104.14	0.9704	0.9374
2003	39.624	1	0.9485
2004	74.93	0.9716	0.9579
2005	139.7	0.9434	0.9532
2006	130.556	0.9617	0.9504
2007	33.528	0.9854	0.9714
2008	104.394	0.9837	0.9231
2009	27.686	0.9994	0.9446
Average	83.8962	0.97704	0.95065

3.6: Conclusions

The analysis presented in this study focused on understanding the response of vegetation to seasonal summer precipitation over different land cover types, and the implication to RUE. It was found that the desert vegetation responds strongly to summer water input compare to winter water input. Urban vegetation is not sensitive to any climate water input due to irrigation. Using the RUE and ANPP calculated from remote

sensing data it was possible to calculate that 295 mm of water input are necessary to sustain the urban tree biomass.

Inter annual variability in hydrological partitioning over urban and desert land-cover seems to be consistent with the concept of the RUE that vegetation becomes more efficient in its water use as water availability decreases. Results also show that unlike natural ecosystems, as reported by Troch et al. (2009) and Huxman et al. (2004), urban areas RUE do not converge to a common maximum value.

Of course the approach presented in this study has several limitations and will need to be verified and tested over larger data sets (more pixels). One way to improve the analysis is to consider all land-cover types. Such information would provide a more accurate and complete spatial picture.

3.7: References

- Bellone, T., P. Boccoardo, and F. Perez, 2009. Investigation of vegetation dynamics using long term Normalized Difference Vegetation Index time series. *American Journal of Environmental Sciences*, 5, 460-466.
- Buyantuyev, A. and J. Wu, 2009. Urbanization alters spatiotemporal patterns of ecosystem primary production: a case study of the Phoenix metropolitan region, USA. *Journal of Arid Environment*, 73, 512-520.
- Buyantuyev, A. and J. Wu, 2010. Urban heat island and landscape heterogeneity: linking spatiotemporal variations in surface temperature to land-cover and socioeconomic patterns. *Landscape Ecology*, 25, 17-33.
- Grimm, N. B., S.H. Faeth, N.E. Golubiewski, C.L. Redman, J. Wu, X. Bai, and J.M. Briggs, 2008. Global Change and the Ecology of Cities. *Science*, 319, 756-760.
- Huxman, T. E., M.O. Smith, P.A. Fay, A.K. Knapp, M.R. Shaw, M.E. Loik, S.D. Smith, D.T. Tissue, J.C. Zak, J.F. Weltzin, W.T. Pockman, O.E. Sala, B.M. Haddad, J. Harte, G.W. Koch, Su. Schwinning, E.E. Small, and D.G. Williams, 2004. Convergence across biomes to a common rain-use efficiency. *Nature*, 429, 651-654.
- Imhoff, M. L., C.J.Tucker, W.T. Lawrence, and D.C. Stutzer, 2000. The use of multisource satellite and geospatial data to study the effect of urbanization on primary productivity in the United States. *IEEE Transactions on Geoscience and Remote Sensing*, 38, 2549-2556.
- Laio, F., A. Porporato, L. Ridolfi, and I. Rodriguez-Iturbe, 2001. Plants in water controlled ecosystems: active role in hydrologic processes and response to water stress II. Probabilistic soil moisture dynamics. *Advances in Water Resources*, 24, 707-723.
- Neil, K. L., L. Landrum, and J. Wu, 2010. Effects of urbanization on flowering phenology in the metropolitan phoenix region of USA: Findings from herbarium records. *Journal of Arid Environment*, 74, 440-444.
- Newman, B. D., B.P. Wilcox, S.R. Archer, D.D. Breshears, C.N. Dahm, C.J. Duffy, N.G. McDowell, F.M. Phillips, B.R. Scanlon and E.R. Vivoni, 2006. Ecohydrology of water-limited environments: A scientific vision. *Water Resources Research*, 42, w06302.
- Ogle, K., and J.F. Reynolds, 2004. Plant response to precipitation in desert ecosystems: integrating functional types, pulses, thresholds and delays. *Oecologia*, 141, 282-294.
- Pennington D.D., and S. Collins, 2007. Response of an aridland ecosystem to interannual climate variability and prolonged drought. *Landscape Ecology* 22, 897-910.

Shepherd, J. M., 2006. Evidence of urban-induced precipitation variability in arid climate regimes. *Journal of Arid Environment*, 67, 607-628.

Troch, P. A., G.F. Martinez, V.R.N. Pauwels, M. Durcik, M. Sivapalan, C. Harman, P.D. Brooks, H. Gupta, and T. Huxman, 2009. Climate and vegetation water use efficiency at catchment scales. *Hydrological Processes* 23, 2409-2414.

Vitousek, P. M. and H.A. Mooney, 1997. Human domination of Earth's ecosystems. *Science*, 277, 494-499.

Webb, W., S. Szarek, W. Lauenroth, R. Kinerson, , and M. Smith, 1978. Primary productivity and water use in native forest, grassland, and desert ecosystems. *Ecology*, 59, 1239-1247.

Wilhite, D. A. 2000. Drought as a nature hazard. *Drought. A Global Assessment*. London, Routledge. pp. 1, 1-18.

CHAPTER 4: ESTIMATING IRRIGATED AGRICULTURE WATER USE THROUGH
LANDSAT TM AND A SIMPLIFIED SURFACE ENERGY BALANCE MODELING
IN THE SEMI-ARID ENVIRONMENTS OF ARIZONA²

4.1: Abstract

Quantifying evapotranspiration (ET) is a key element for achieving better water management, especially in regions where agriculture is the main water consumer. A hybrid model combining the SEBAL and ReSET models (S-ReSET) was developed to effectively estimate actual ET (water use) of the agriculture sector around the phoenix metropolitan area. To examine how irrigated agriculture water consumption varies with climate, the S-ReSET model was applied under wet and dry climatic conditions. Results show that the average ET for active agriculture is 9.3mm/day (± 3.8 mm/day) during the study period. Seasonal water use was 438 mm for 2000 (drought) and 494 mm for 2008 (wet). Based on the seasonal ET we concluded that farmers in arid region use the same amount of water regardless of climatic conditions, implying that the agriculture sector as a whole may not be sensitive to drought as long as there is sufficient water from irrigation. This finding carries significant implications for the region's water security.

4.2: Introduction

Current pressure of global change, including both climatic and societal, continuously elevates competitions for fresh water between different uses. Monitoring water consumption has become a critical tool in water resources management, especially

² This manuscript was co-authored with Soe W. Myint and was published in PE&RS in August 2012.

in arid environments where water is scarce, droughts are frequent, and climate is predicted to become warmer and drier (Mariotto et al. 2011; IPCC, 2007). Evapotranspiration is considered to be one of the key elements in the water cycle that needs to be quantified to achieve better water management.

Evapotranspiration (ET) is defined as the sum of evaporation from soil surface, plant surface, and transpiration from plants. Controlled mainly by solar radiation, ET is a major component of the hydrological cycle and energy transport between the biosphere, atmosphere, and hydrosphere (Idso et al. 1975; Liu et al. 2007). Globally, ET from land surface accounts for 60% of average precipitation (Zhao-Liang et al. 2009). Of the water which falls over the continental USA, 70% - 90% is believed to return to the atmosphere by evapotranspiration (Rosenberg, 1974). This return replenishes atmospheric moisture and leads to precipitation recycling. However, ET is probably the most difficult water cycle components to measure due to its wide spatial variation and invisibility (Mariotto et al. 2011; Allen 2008). Quantifying spatial and temporal variability of ET over large areas is important to understand water cycle, climate dynamics and ecological processes. Understanding these issues can help us better manage and improve water resources planning, water regulations and water use efficiency; especially in regions where agriculture plays an important role. In such regions ET is the largest water consumer, and irrigation is generally a key source for ET (Bastiaanssen, 2000; Allen et al. 2007; Sun et al. 2009).

Traditional methods for ET estimations, such as lysimeter, Bowen ratio system or eddy covariance system, are time consuming and expensive. Moreover, these methods are point based. Remote sensing can estimate ET as a residual of the energy balance, thus

reduces the need for ground data while providing regional coverage and information on the spatial and temporal variability of actual consumption (Elhaddad and Garcia, 2008; Bastiaanssen et al 1998a; Kustas and Norman, 1996). Over the last two decades there have been ongoing developments of energy balance models utilizing remote sensing data for ET estimations. A comprehensive review of models can be found in Kustas and Norman (1996) and Zhao-Liang et al. (2009).

The most widely used models are SEBAL and METRIC - one-source models that consider soil and plants as a single component (Mariotto et al. 2011). They are designed to minimize the use of ground data by using two extreme conditions – “hot” (bare soil) and “cold” (full vegetation cover). Allen et al. (2007) described the procedure required to calculate actual ET using the surface energy balance method that employs the “hot” and “cold” pixel approach developed by Bastiaanssen et al. (1998a; 1998b). SEBAL has been widely validated for irrigated agriculture in Egypt (Bastiaanssen et al. 1996), Spain (Pelgrum and Bastiaanssen, 1996), Turkey (Bastiaanssen 2000) and several others. Roerink et al (1997) and Bastiaanssen et al. (2001) combine SEBAL with field data to assess irrigation scheme, crop ET, and soil moisture and biomass growth in Argentina and Brazil. METRIC uses an internal calibration by utilizing daily weather station alfalfa reference ET (ET_{ref}). Using reference ET along with wind speed and air temperature from local weather stations better incorporate local/regional conditions (Allen et al. 2007). For seasonal estimations, METRIC interpolates between different image dates, thus taking into account ET temporal variability. Folhes et al. (2009) reported daily ET estimation using METRIC averaged +12% compared to the Eddy covariance measurements with values range from 0 to 9 mm. Similar results were obtained by Allen

et al. (2005) when comparing METRIC to lysimeter over sugar beet crop in Idaho. Within individual fields, spatial variability of 24h ET reached 8mm/day, emphasizing the benefit of using high spatial resolution satellite data. The same study also indicates that during the driest and hottest months 80% of the water flowing into the fields has been utilized for ET, indicating the effectiveness of water use. METRIC's ET estimations error were reported to be 10-25% for daily ET and 1-4% for seasonal estimates (Conrad et al. 2007). Gowda et al. (2008) suggested that some errors could result from the assumption that maximum ET (at the cold pixel) is 5% more than the reference ET used for calibration, the assumption of a linear relationship between surface temperature (T_s) and the surface-air temperature difference (dT) as well as from the linear interpolation between dates.

The recently developed remote sensing of evapotranspiration (ReSET) model (Elhaddad and Garcia, 2008) improves METRIC by using interpolated grids of wind run and calibration data from several weather stations in a consumptive model, thus taking into account both temporal and spatial variability of weather. The spatial variability of ET and the non-linear temporal interpolation affect the seasonal ET estimates. Elhaddad et al. (2011) compared ReSET results with lysimeter measurements, and showed that the difference between daily ET estimations and ReSET was within 11.16% to 13.6%. The same study showed that for seasonal estimations of Alfalfa the differences were reduced to 1.5-9.1%. However, the incorporation of interpolated wind speed might suggest a non-constant linear relationship between surface and near-surface air temperature; a crucial assumption used in all surface energy balance models for estimating ET with remote sensing (Allen et al. 2007). Furthermore, the use of reference ET from several

meteorological stations already takes into account spatial variations in climate as reference ET at each station is calculated using local parameters including winds. The current study employs a SEBAL like model for daily estimates of ET and a simplified ReSET approach for seasonal estimations, i.e. without wind run interpolation and independent of a consumptive model suggested by Elhaddad and Garcia (2008); thus making it more applicable to a wider community. The model we introduced in this study is hereafter referred to as S-ReSET (simplified ReSET).

We focus on the agricultural sector around Phoenix, Arizona - a unique case of an arid region where, given the unique climatic conditions, the agricultural crop production is based on blue water (Thenkabail, 2010), mainly ground water and a canal system that delivers water from other watersheds. The overall aim of this research is to quantify the regional water consumption by agriculture using remote sensing and geospatial information technologies. More specifically: (a) quantify ET_{actual} (water use) over active agricultural fields for the Central Arizona - Phoenix Long-Term Ecological Research (CAP-LTER) region using Landsat TM data; and (b) compare and contrast regional water use (ET_{actual}) from agricultural areas between a wet year (2008) and a drought year (2000). By comparing water consumption of wet and drought years we were able to examine agriculture sensitivity to drought as well as farmers resilience in the context of water usage. In light of the reliance on blue water, these may have important implications for the region's water security.

4.3: Data and Study area

4.3.1: Study Area

This study focuses on the Phoenix metropolitan region (CAP-LTER) (Figure 28); an area that has undergone extensive modification to its landscape during the 20th century, following rapid population growth. As a result, large areas of the previously semi arid natural desert shrubland are now dominated by urban, active and non-active agriculture land covers (Imhoff et al. 2000). A recent study by Buyantuyev and Wu (2009) indicates that agriculture (both active and non-active) comprises 28% of the land cover and is used mainly for growing Alfalfa, Cotton, and Corn (NASS 2009). The context for this rapid modification is of a desert biome - 193 mm yr⁻¹ precipitation falling in two distinct wet seasons (~60% winter and 40% summer) and 2,000 mm yr⁻¹ potential evapotranspiration (Baker et al. 2002) - in which climate change models suggest a future that is warmer and drier, with more extreme climatic events (IPCC 2007). Soils are a mixture of clay-loam and sandy loam (USDA soil survey; <http://websoilsurvey.nrcs.usda.gov>). As a result from these conditions, the only feasible way to support any kind of human activity is to rely on blue water use (Thenkabail, 2010).

According to Arizona Department of Water Resources (ADWR) irrigated agriculture consumes approximately 70% of Arizona's water (ADWR, 2010). Of this total, on average, 49% are drawn from ground water, 25% are being diverted from the Colorado River (the Central Arizona Project canal), 18% are decreed, 2% are effluent, and 6% are from other surface water sources. Recent estimates indicate that the urban growth, coupled with the region's aridity exerts pressure on agriculture, indicating the

need for more efficient and sustainable agricultural practice. Therefore, quantifying spatio-temporal evapotranspiration (ET) from active agricultural fields is important for water resource management in this arid region.

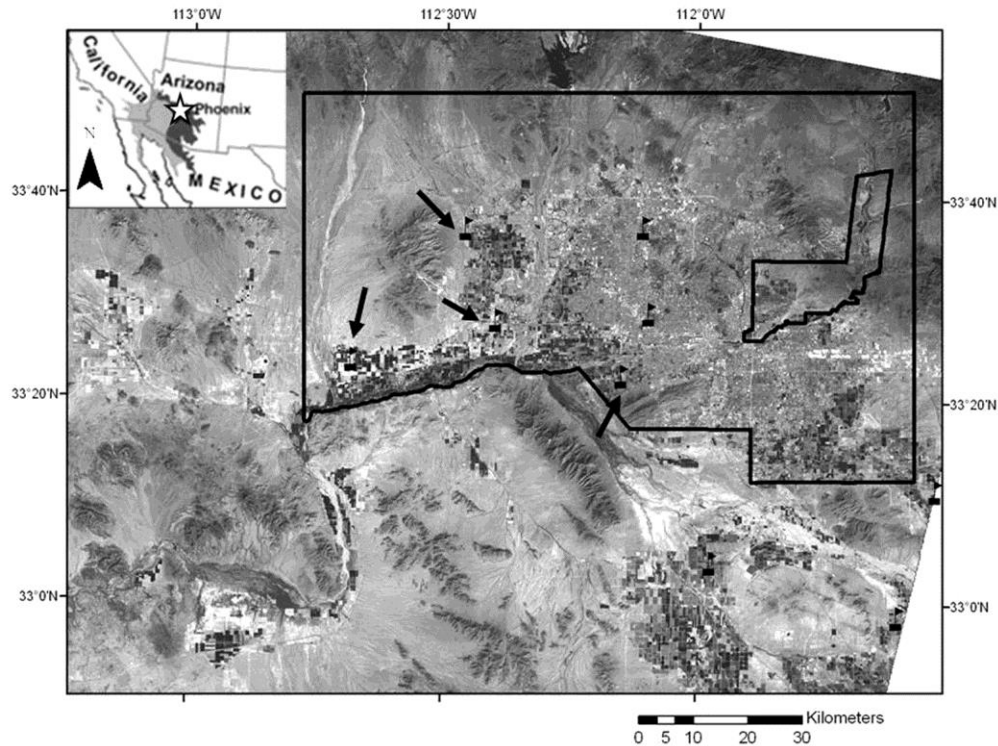


Figure 28. The CAP-LTER study area as seen by Landsat 5. Flags represent location of the meteorological stations. Arrows indicate the stations used for validation.

4.3.2: Data

Landsat 5 TM image data with seven bands were used in this study. The seven bands include six bands ranging from blue to the short-wave IR portion of the spectrum (bands 1-5 and 7; 0.45-2.35 μm) at 30 m resolution, and a thermal band (band 6; 10.4-12.5 μm) at 120 m resolution. Landsat is the only operational satellite with a thermal band and a pixel size small enough to map ET for individual fields. The Landsat scenes were obtained in

raw format and processed using ERDAS Imagine software. Image bands 1-5 and 7 were atmospherically corrected and converted to reflectance values using the COS-T model (Chavez, 1996). The thermal band was resampled to 30 m by the United States Geological Survey (USGS), and converted to surface temperature following Markham and Barker (1986).

Two years were considered: 2000 as a drought year and 2008 as a wet year, with winter precipitation of 63mm and 114mm, respectively. Seven Landsat 5 TM images were acquired in order to cover the 2000 growing season between March and June. The March-June time span was selected for two reasons: (1) low rain frequency; and (2) the availability of cloud free image. As a result we can assume most water lost to ET is from irrigation. For 2008, being a wet year with frequent cloud cover, only four cloud free images were available for the same time period. These images cover the time span of April 1 through May 19. Given image availability limitation, only the overlapping time was considered for comparison. Furthermore, the bi-modal rainfall distribution of the area indicates April-May to be the driest period of the year. Hence, any differences in water consumption in response to drought can be more evident during this time frame.

Other data used in this study were DEM of the research area, and reference ET data from 11 AZmet meteorological network stations within and around the study area. Using Kriging interpolation, reference ET grids were generated for each day during the growing season. These grids were used later for interpolation between dates.

4.4: Methodology

4.4.1: Land Use/Land Cover Mapping

An object oriented classification approach was used to delineate land use and land cover for each year using Landsat 5 TM. Four general land categories were identified: Urban, Desert, Active- and Non-active agriculture. The advantage of using object oriented approach is the ability to merge and reclassify data or pixels having similar spectral and spatial signatures into meaningful objects; resulting in a more homogenous classification across the image. The image was segmented using the multiresolution segmentation in Definiens Developer software. The segmentation is controlled by the values of three key parameters, namely shape, compactness, and scale. The shape parameter adjusts spectral homogeneity vs. shape of objects, whereas the compactness parameter balances the object shape between smooth boundaries and compact edges (Liu and Xia, 2010). Compactness and shape were set to 0.5 and 0.1 respectively. Scale parameter, which is an indicator of how big an object is allowed to grow (object size), was set to 5. Only a single segmentation was performed. A set of decision rules was established to identify the urban area, active agricultural fields, non-active fields and desert land covers. The nearest neighbor algorithm was used to delineate urban and non urban areas as the two parent classes. All seven bands were included in the object-based analysis.

Proceeding a priori, active agriculture fields were classified using two parameters - Soil Adjusted Vegetation Index (SAVI) and object's area. From the initial segmentation, merging, and growing of objects within the non-urban class was initiated for active and non active agriculture. The merged objects were then classified using membership function classifier based on their areas, where large area with $SAVI > 0.4$

corresponded to active agriculture. Similar merging and growing procedure using Albedo values was employed to identify non-active agricultural areas. These areas are usually bare soil with high Albedo and similar size to the active fields. Inactive agriculture proved more difficult to classify and showed some confusion with the non-urban natural desert. While this may lead to some errors in the land use map, for our purpose it is less critical as we assume inactive agriculture has $ET = 0$ (bare soil).

For accuracy assessment, a stratified random sample approach was used. This approach assumes that the sample points selected are the true representation of the map being evaluated, thus an improperly gathered sample will produce meaningless information on the map accuracy (Congalton and Green, 1999; Jensen, 2005; Lillesand et al., 2008). High resolution imagery on Google earth and the original image with the local area knowledge were used as references. A total of 250 points with a minimum of 30 points per class were selected. For each classification an error matrix was produced and the accuracy for each class was analyzed. From the error matrix, overall accuracy, producer's accuracy, user's accuracy, and the Kappa Coefficient were generated (Story and Congalton, 1986; Congalton, 1991). Overall accuracy for the year of 2000 was 94.8% with Kappa 0.93. For 2008, overall accuracy was 89.2% with Kappa of 0.85. Both classified output maps are presented in figure 29. Histogram analysis (figure 30) indicates land cover percentage estimations are consistent with results reported by Buyantuyev and Wu (2009). The only land cover that increased is the urban; where most expansion took place on the account of natural desert area and non-active agriculture. Active agriculture shows only 1% decrease, equivalent to approximately 64km^2 .

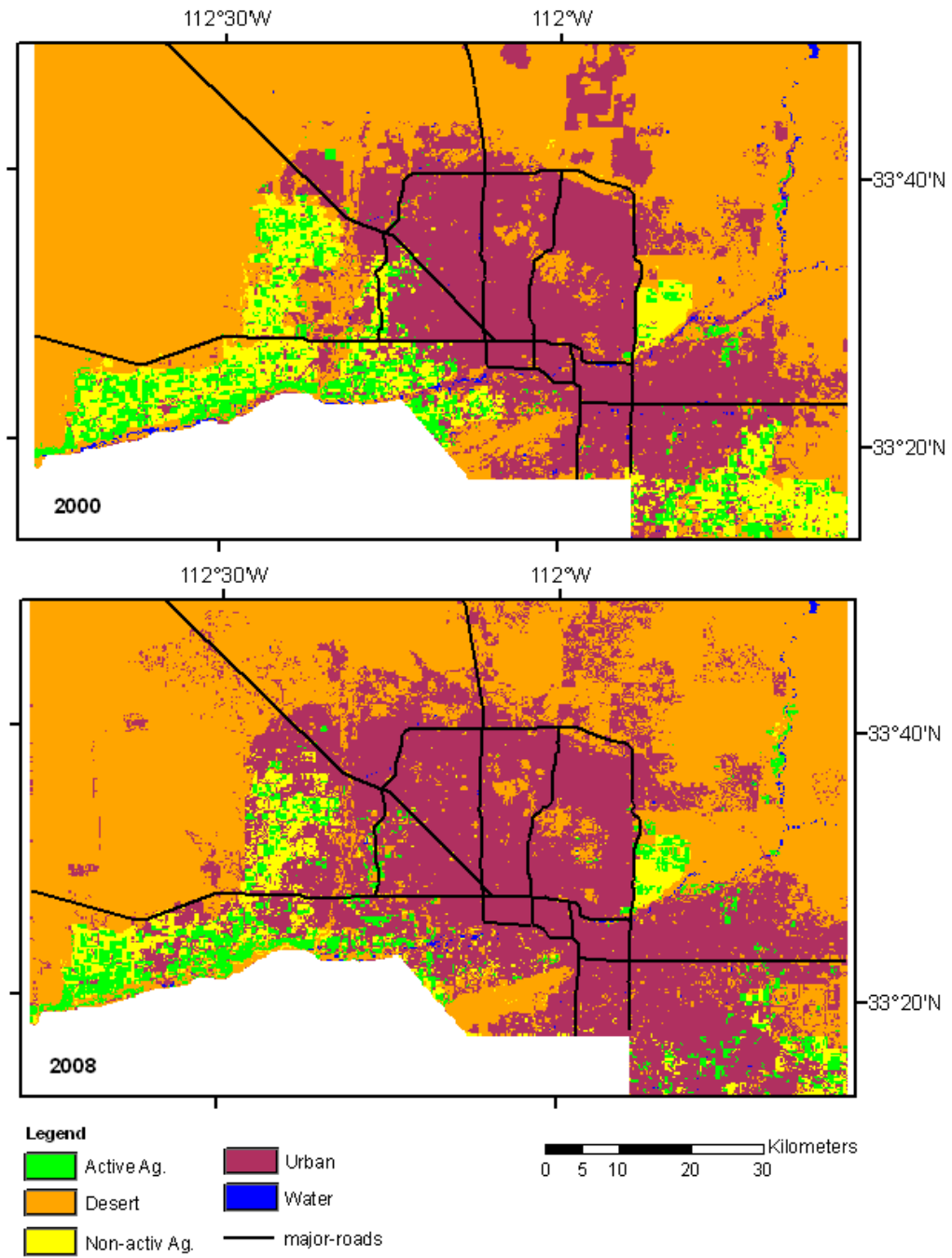


Figure 29. Land use/land cover classification of the study area for 2000 (top) and 2008 (bottom).

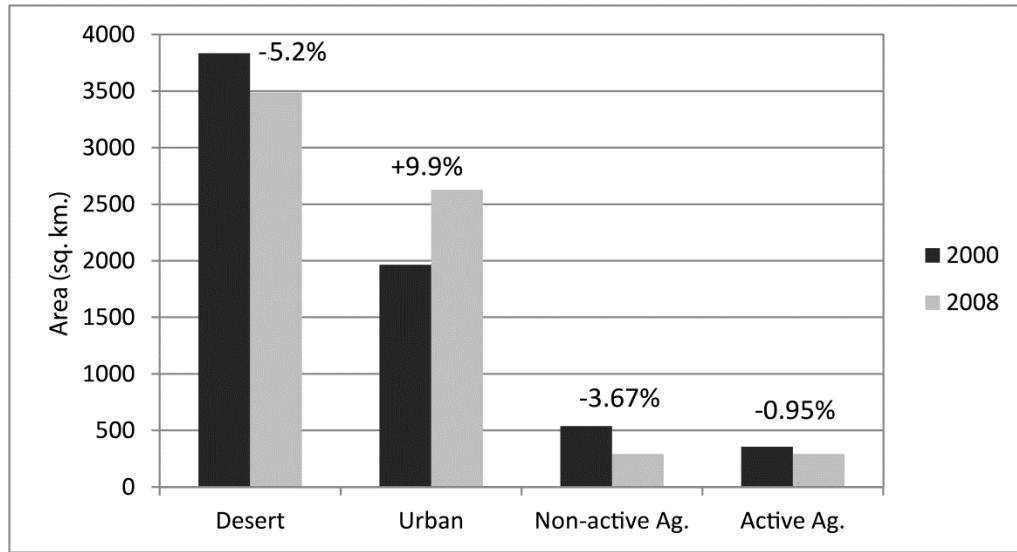


Figure 30. Changes in land cover area between 2000 and 2008. Labels indicate change in class cover percentage.

4.4.2: The S-ReSET Model

ET is generally determined from satellite imagery by applying an energy balance at the surface, where energy consumed by ET is calculated for each pixel as a residual of the surface energy balance:

$$LE = \lambda ET = R_n - G - H \quad (4.1)$$

Where LE = latent heat flux; ET = evapotranspiration; λ = latent heat of vaporization ($2272 \cdot 10^3$ J/kg); R_n = net radiation; G = soil heat flux; H = sensible heat flux. Parameters are in Wm^{-2} . Using equation 1, actual ET can be calculated so that reductions of ET caused by water shortage in the soil are captured. The ET calculations are only accurate as the R_n , G and H estimations. The procedure used here follows the one detailed in Allen et al. (2007). All functions were calculated using the ERDAS spatial modeler.

Net radiation (R_n) is computed by subtracting all the sum of outgoing solar radiation from total incoming:

$$R_n = (1 - \alpha)R_s^\downarrow + R_L^\downarrow - R_L^\uparrow - (1 - \varepsilon_0)R_L^\downarrow \quad (4.2)$$

Where R_s^\downarrow =incoming short-wave radiation (Wm^{-2}); α =surface albedo; R_L^\downarrow = incoming long-wave radiation (Wm^{-2}); R_L^\uparrow = outgoing long-wave radiation (Wm^{-2}); ε_0 = broadband surface thermal emissivity. The $(1 - \varepsilon_0)R_L^\downarrow$ term represents the fraction of incoming long wave radiation reflected from the surface. The different parameters were calculated based on Allen et al. (2007) for a “flat” terrain; however, this model was adjusted for turbidity as the Phoenix atmosphere is assumed to have higher dust content. Soil heat flux, is calculated using an empirical equation developed by Bastiaanssen (2000) as a function of R_n :

$$G = R_n * (T_s - 273.15)(0.0038 + 0.0074\alpha)(1 - 0.98NDVI^4) \quad (4.3)$$

Where T_s = surface temperature (K); α = surface Albedo, and NDVI is the normalized difference vegetation index. The sensible heat flux (H) is estimated using the following equation:

$$H = \rho_{air} C_p \frac{dT}{r_{ah}} \quad (4.4)$$

Where ρ_{air} = air density ($kg\ m^{-3}$); C_p = specific heat of air at constant pressure ($J\ kg^{-1}\ K^{-1}$); and r_{ah} =aerodynamic resistance ($s\ m^{-1}$) between two near surface heights: Z_1 - aerodynamic roughness and Z_2 - 3m; and dt = near-surface temperature difference between Z_1 and Z_2 .

Aerodynamic resistance (r_{ah}) is strongly affected by boundary layer buoyancy and driven by the sensible heat flux rate. Because both r_{ah} and H are unknown at each

pixel, an iterative solution is required. In the current study, r_{ah} calculations uses wind speed extrapolated from a blending height of 100m above surface, and an iterative stability correction based on the Monin-Obukov function (As detailed in Allen et al. 2007). During the first iteration, r_{ah} is computed assuming natural stability:

$$r_{ah} = \frac{\ln(Z_1/Z_2)}{U_*k} \quad (4.5)$$

Where Z_1 and Z_2 = heights above the zero-plane displacement of vegetation where the end point of dT is defined and k = von Karman's constant (0.41). U_* = friction velocity (m/sec), is computed using the logarithmic wind law for neutral atmospheric conditions:

$$U_* = \frac{KU_{100}}{\ln(100/Z_{om})} \quad (4.6)$$

Where U_{100} = wind speed at a blending height of 100m assumed to be constant for the image, and Z_{om} = momentum roughness length. Z_{om} is calculated for each pixel using Bastianssen (2000) equation:

$$Z_{om} = \exp(-5.809 + 5.62SAVI) \quad (4.7)$$

Where SAVI= Soil Adjusted Vegetation Index. SAVI can be independent from plant height; that is, different plants that are equally tall may yield different SAVI values depending on canopy density and structure. However, this relationship has been developed using several crops types (Cotton, grapes and olive trees), at various locations including Arizona. U_{100} is calculated as:

$$U_{100} = \frac{U_w \ln(100/Z_{om})}{\ln(Z_x/Z_{om})} \quad (4.8)$$

Where U_w = averaged wind speed at the weather stations within the study area for the satellite overpass time, and Z_{om} = the averaged momentum roughness for the weather stations surface (as calculated from eq. 4.7). Z_x represents the height above the surface at

which wind speed is measured (usually 2-3m). By using a single value, the assumption of a constant linear relationship between T_s and dT can be kept (Allen et al., 2007).

Following Bastiaanssen (1995) the dT (K) and surface temperature (T_s) are assumed to have a linear relationship t:

$$dT = a + bT_s \quad (4.9)$$

The approach for determining dT and consequently H and LE that yields instantaneous ET is based on selecting two anchor locations: (1) a cold (wet) pixel where dT is minimal and water vapor is assumed to be released solely according to atmospheric requirement. Under such conditions, $H = 0$ and $LE = R_n - G$; (2) a hot pixel where ET is assumed to be zero; thus $H = R_n - G$. Following Allen et al. (2007), a bare soil/non-active agriculture field is selected as the hot pixel for each image. For the cold pixel, a well irrigated full cover pixel within an active agricultural field was selected. As no past actual ET measurements (i.e. lysimeter, eddy tower etc.) are available for this study area, we did not use the METRIC internal calibration of $H = 1.05 * ET_{ref}$. This omission allows us to compare the S-ReSET daily estimates with the daily ET_{ref} recorded by the meteorological stations. Using the assumption that $dT = 0$ at the wet pixel, an initial dT function can be determined and the value of H can be calculated at the dry pixel. An assumed air temperature of $25^\circ C$ is used to calculate the initial dT function. To account for the instability of air conditions an iterative solution is necessary. Stability characteristics influence the aerodynamic resistance, which directly influences the calculation of H (equation 4). The procedure for the iterative solution of r_{ah} and H is outlined in Allen et al. (2007) and Liu et al. (2007). This procedure updates values for r_{ah} , dT and H at each iteration. The final values are determined when $dT < 1^\circ$ and dR_{ah}/R_{ah}

<0.05. On average it took 5-7 iteration for each image to converge. Once H values for both extreme locations are known, the value of LE can be calculated for those locations. The rest of the image pixels were stretched between these two values. At the next step the instantaneous ET fraction is computed following Elhaddad and Garcia (2008):

$$ET_{\text{inst-frac}} = LE/(R_n - G) \quad (4.10)$$

where LE , R_n and G are all instantaneous. The 24h ET is computed using:

$$ET_{24} = 86,400 * ET_{\text{inst-frac}} * (R_{n24} - G_{24})/L \quad (4.11)$$

Where 86,400 = time conversion from seconds to days; R_{n24} = 24-h net radiation calculated using the Bastiaanssen (2000) equation; G_{24} = 24-h soil heat flux (assumed to be zero); and L = latent heat of vaporization used to convert the energy to mm of evaporation.

$$L = (2.501 - 0.00236 * (T_s - 273.16)) * 10^6 \quad (4.12)$$

where T_s = surface temperature in K.

The cumulative seasonal ET for the defined period was calculated using the GIS algorithm developed by Elhaddad and Garcia (2008). Using ordinary Kriging on the reference ET data from the meteorological station, a daily grid of reference ET was created. Using the ratio between the remote sensing ET and the interpolated reference ET at the beginning and end of the interpolation period (scene dates), a correction factor was calculated. The correction factor was then used to produce a modified ET grid that changes from day to day depending on two variables: location of the date between the scenes and the daily grid of interpolated weather station ET values for that date. The seasonal cumulative ET is the sum of the modified ET grids. Using this methodology takes into account both spatial and temporal dynamics of ET.

4.5: Results and discussion

4.5.1: Model Validation

The S-ReSET empirical equations were based on the well validated SEBAL (Bastiaanssen , 1998) and METRIC (Allen et al. 2007). Seasonal algorithm was based on the ReSET model (Elahddad and Garcia, 2011). As there were no ET field measurements for the area, daily estimations were plotted against alfalfa reference ET from four meteorological stations in agricultural settings (figure 31). Because we did not use ET_{ref} to constrain maximum ET ($LE_{cold} = Rn-G-1.05*ET_{ref}*\lambda$; as in METRIC) we were able to compare the meteorologically derived ET_{ref} with the model results. As can be seen from figure 31, a strong relationship was observed ($R = 0.71$).

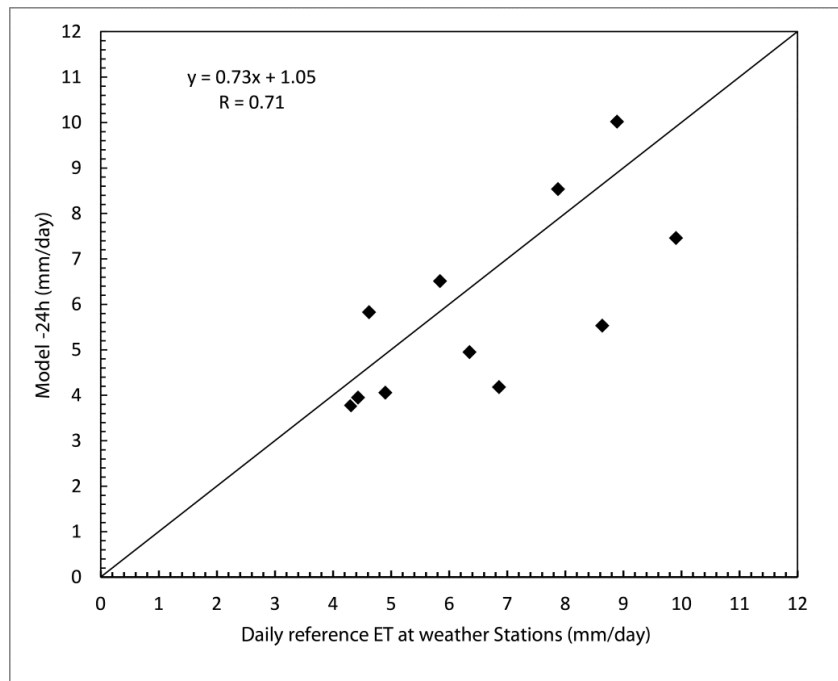


Figure 31. Comparison between S-ReSET predicted ET_{actual} and weather stations reference ET.

To further validate daily estimations, a statistical procedure was carried out: A crop map developed by NASA for 2008 (NASS 2009) was used to identify Alfalfa fields. For each scene date, S-ReSET ET estimates over active alfalfa fields were identified, and a random sample of 50 points were collected. The sample statistical distribution properties were compared to those of reference ET measured by the AZmet meteorological stations. To avoid field edge effects, points were collected from the middle of fields. Because only 11 weather station ET data were available, A Mann-Whitney test was performed to compare the weather station and the samples from the model values distribution ($H_0: M_{mod} = M_{ws}$; $H_1: M_{mod} \neq M_{ws}$). The Mann-Whitney is a non-parametric test that takes into account not only the observation location compare to the median but also its magnitude (Daniel, 1990). Results indicate that for all dates we do not have sufficient evidence to reject the null hypothesis (P-value > 0.05 for all dates), i.e. the S-ReSET estimations are not different from the reference ET (table 5).

Table 6 presents the comparison between S-ReSET estimations and seasonal reference ET means of the AZmet meteorological stations (Brown, 2005). As can be seen, for all three locations the S-ReSET underestimates actual ET. The highest difference is observed in Waddell. This -16% difference could be due to the fact that the weather station is located in a transition zone between urban and natural desert. These results are similar to those reported in the literature for several surface energy balance models (Elhaddad and Garcia 2011; Senay 2007; Conrad et al. 2007; Gowda et al. 2008).

The underestimation of the S-ReSET can be attributed to the scaling mechanism from instantaneous LE to daily ET, which is based on evaporative fraction $[LE/(R_n-G)]$. ET fraction is assumed to be the same at both the observation time and for the 24h period.

This method was found to be highly accurate for scaling instantaneous LE to daily ET, especially for arid regions (Colaizzi et. al, 2006). However, according to Allen et al. (2007) this assumption can lead to under-prediction of daily ET. Furthermore, the interpolation between the ET data across space was based on small number meteorological stations. The semi-variogram fitted in the Kriging might have deviated from the true spatial variation in some cases. Additionally, some of the stations used for interpolation are in urban settings, which may have caused different microclimate conditions that affect ET estimations.

Table 5. Median, standard error and Mann-Whitney P-value for comparison of model and weather station ET estimations. P-values indicate that results are not significantly different

	1/4/2008		17/4/2008		3/5/2008		19/5/2008	
	S-ReSET	WS	S-ReSET	WS	S-ReSET	WS	S-ReSET	WS
median	3.52	5.72	6.81	7.11	7.74	7.75	6.31	9.27
SE	0.20	0.15	0.35	0.14	0.39	0.15	0.34	0.23
P-value	0.09		0.27		0.34		0.06	

Table 6. Comparison between the seasonal ET estimated by S-ReSET and the AZmet report by Brown (2005).

Location	Seasonal ET from S-ReSET (mm/50day)	Seasonal ET from Azmet report (mm/50day)	Difference (%)
Buckeye	320.4	341.7	-6.64
Litchfield	328.3	335.3	-2.14
Waddle	276.5	321.6	-16.3

As the main water source for the region is ground water, we also utilized ground-water pump data from the Buckeye, Roosevelt, Adman and Maricopa irrigation districts (ADWR, 2010) as an additional validation. Data on water quantity drawn from the wells are collected once a year; therefore, we calculated the daily average and multiplied by 50 to make it comparable to the S-ReSET seasonal estimations. Two complications arise from this method: other water sources may contribute to irrigation and ground-water can be drawn for non-irrigation purposes. However, results at all four locations indicate a very strong correlation and predictive power (Figure 32).

Similar to the way all energy balance models function, some biases result from the use of empirical functions to estimate some components. The most important ones are net radiation calculations, the surface temperature from the thermal band and its associated temperature gradient function used to calculate the sensible heat flux (The sensible heat flux is sensitive to radiometric temperature errors that are non-linear in true kinetic temperature) (Mariotto et al. 2011).

Additional biases and uncertainties may result from the use of satellite imagery as the primary spatial information resource. While most satellites are 700km above Earth, the heat and vapor transport occur close to the surface, and are influenced by aerodynamic processes including turbulence and buoyancy. Other uncertainties and limitations may be related to the cold and hot pixels selection and availability of several meteorological stations in a region.

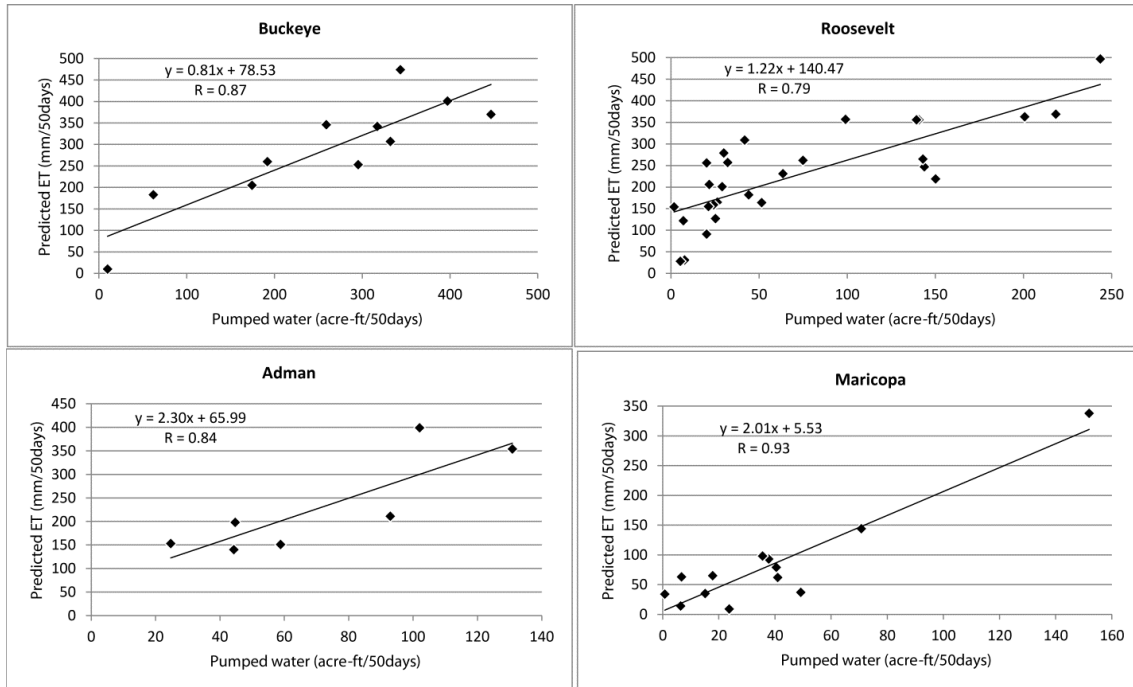


Figure 32: S-ReSET seasonal ET estimations compared to ground water wells data at four different irrigation and water districts across the region.

4.5.2: Water Consumption and Drought Effect

Desert and non-active agriculture land covers were characterized by daily ET < 5.4 mm/day. Active agriculture showed an average ET of 9.3 mm/day, ranging from 2 to 17+ mm/day. This high variability was due to two factors, irrigation schedule and soil and crop characteristics (e.g., crop type, height, growth-stage). Figure 33 shows the S-ReSET daily estimates for May 19, 2008.

To evaluate the effect of crop type on water consumption, data for the Roosevelt irrigation district were analyzed. Following Teixeira (2010) approach, the NASS (2009) crop map was overlaid with the seasonal ET image for 2008.

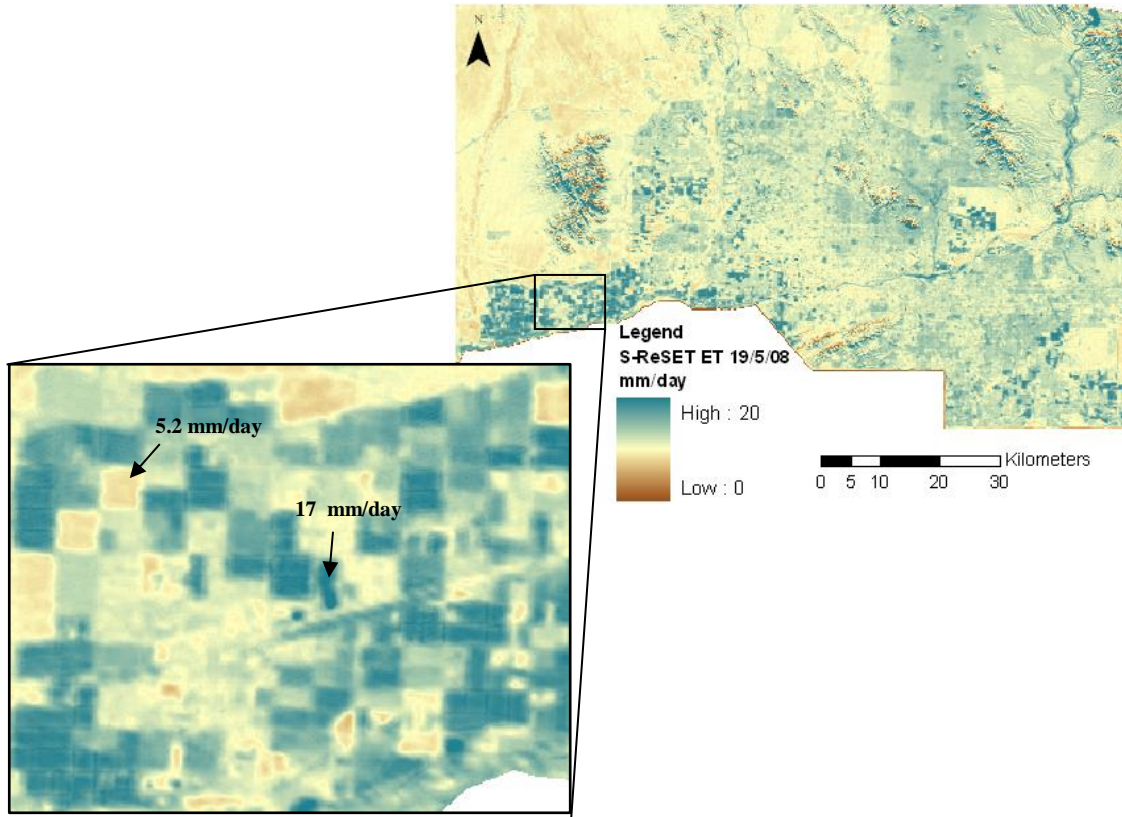


Figure 33. Daily ET for the Central Arizona Phoenix Long Term Ecological Research area, and a subset depicting agricultural areas (active and fallow).

Table 7 shows a summary of statistics for Alfalfa, Cotton, and Corn - the three main irrigated crops in the region. These data follow the data in USDA (1982) and Masoner et al. (2003). Table 7 also suggests that Cotton consumes similar amount of water per area compare to Alfalfa. This result is supported by Masoner et al. (2003) who reported Cotton and Alfalfa to have comparable water requirements in semi arid environments (Oklahoma and Texas). However, considering that Alfalfa is harvested every few months while cotton and corn are restricted to a single season, it can be concluded that Alfalfa consumed more water per area than Cotton and Corn.

Table 7. Area of the main irrigated crops and seasonal actual ET in 2008 for the Roosevelt irrigation district.

Crop	Area (ha)	ΣET (mm/50 days)	Average ET (mm/km²)
Alfalfa	3003	10475697	3488
Cotton	2540	1563416	3217
Corn	643	8,171,067	2428

Comparing the seasonal (April 1st – May 19th) ET estimations (figure 34) revealed the effect of drought. Because our objective was to estimate water use for agriculture, only those objects classified as active agricultural fields were considered for comparison. Although crop type is highly important for estimating water consumption, no spatially referenced crop map exists for Arizona prior to the year 2008. Therefore we focused our drought sensitivity analysis on the agricultural sector as a whole, and not specific crops. While most active agricultural fields show seasonal ET of over 400 mm for both years, the desert and urban land cover experienced lower ET during drought (<300 mm). Drought effect was also seen in some of the inactive agricultural field where in wet years ET was slightly higher. This is possibly explained by annual plants growth on the exposed soil.

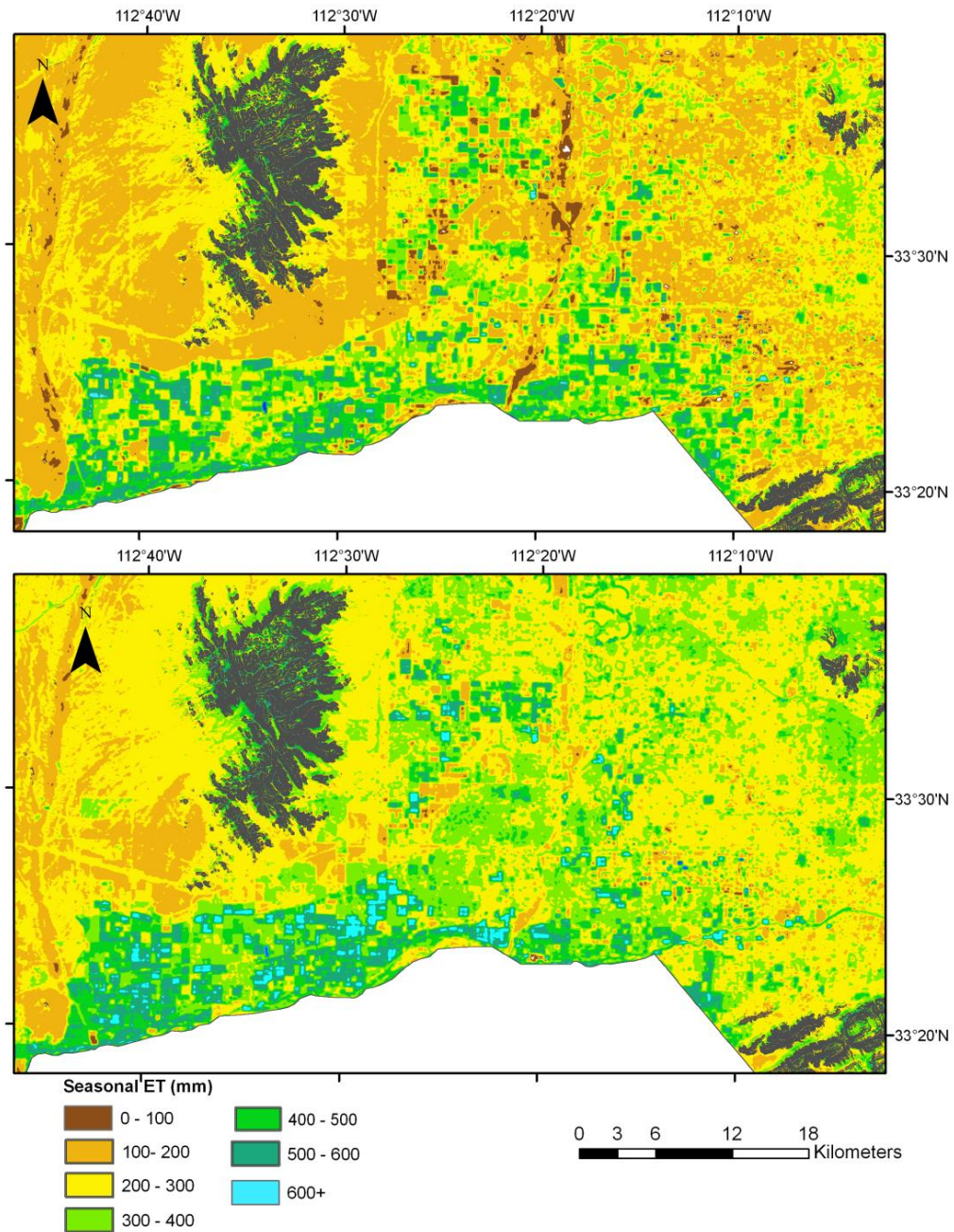


Figure 34. Seasonal ET for drought year (top) and wet year (bottom).

Within each year, active agricultural fields showed high variability in their ET. The S-ReSET was able to identify individual fields where high water consumption was identified ($ET > 700$ mm /50 days ~ 7000 m³ /ha). Total water usage of the entire

agricultural sector was $117 \times 10^6 \text{ m}^3$ and $103 \times 10^6 \text{ m}^3$ for 2000 and 2008, respectively. However, considering land use changes, the precipitation equivalent water addition was 336 mm/m^2 during 2000 and 354 mm/m^2 during 2008. Statistical analysis (F-test: P-value=0.19) indicates water usage distribution across active fields is not significantly different between drought and wet years. A possible explanation is that farmers use the same amount of water regardless of climate conditions during the previous season. The small difference of 18 mm/m^2 over 50 days, can be attributed to the difference in precipitation timing and amount (114.5 mm in October 2007 – May 2008 winter vs. 62.5 mm in October 1999 – May 2000), leading to higher soil water content on April 1st of the wet year. This could probably be due to the fact that the study period is relatively short. Other factors such as wind speed and temperature can also contribute. The decision to use the same water input to the field regardless of climatic conditions is not surprising given the high variance of precipitation between years and the desire to maximize yield.

The comparison to wells data of ground water suggests that although other sources of water have been developed to address water issue with regards to climate conditions (CAP canal brings water from the Colorado river, Salt and Verde rivers project), ground water are still a main source for irrigation. Other sources are used mainly by municipal, industrial, and other sectors to support population growth and activities. Given the low precipitation and the consequence low recharge of ground water, our analysis indicates an ongoing depletion of the region's only local source. As more droughts are projected, urbanization taking over agriculture, and the Colorado discharge decreasing, ground water is crucial for sustainable development of the region.

4.6: Conclusions

At a time water supply and security are major national and global concerns, the ability to monitor actual evapotranspiration (ET_{actual}) or water use over time and space by agricultural crops provides critical information and new insights on water consumption. A hybrid model combining the SEBAL and ReSET models (S-ReSET) was developed and applied to estimate the agriculture sector water consumption in the Central Arizona Phoenix Long Term Ecological Research region. The images covered a period of 50 days (April 1 – May 19) for two years - 2000 (drought) and 2008 (wet). For the wet year, the S-ReSET was able to explain 0.7 to 0.87 of the variance of ground water usage in four irrigation districts within the region. These results indicate that the S-ReSET model can effectively quantify the spatio-temporal distribution of ET_{actual} , providing there are number of meteorological stations with reference ET data. For the drought year, S-ReSET underestimates ET_{actual} of agricultural crops by 2-16% when compared with alfalfa $ET_{\text{reference}}$. These errors were similar to those reported in the literature for remote sensing surface energy balance models (Bastiaanssen et al. 1998a; Allen et al. 2007; Elhaddad et al. 2011). The results were rather encouraging considering that only remote sensing derived parameters together with interpolated data of reference ET are necessary, without the need of crop classification. Nevertheless, additional evaluation is needed over longer time periods, with field measurements under various climatic conditions and different crop types to fully assess the S-ReSET capability to accurately estimate spatially distributed water consumption.

This study focusing on the Phoenix metro area showed that for the period of April – May, desert lands and fallow agricultural fields are characterized by water use or

$ET_{\text{actual}} < 5.4$ mm/day during drought years. During wet years, ET for these land covers can reach to about 7 mm/day, suggesting high variability between drought and wet years for the desert lands and fallow croplands. In contrast, agricultural cropland water use (ET_{actual}) was on average 8.8 mm/day (± 3.9) during drought and 9.9 mm/day (± 3.6) during the wet year. Agricultural water use, however, remains constant during dry and wet years, because the water requirements of crops are met by adequate irrigation. Of all the crops Alfalfa consumes most water with as high as 17 mm/day during its peak growth.

Seasonal estimations yielded water input to the fields equivalent to 438 mm/m² during the year of 2000 (drought) and 494 mm/m² during the year of 2008 (wet). Although we expect that under drought condition farmers will use more water for irrigation, our results indicate that the plants consumed less water during the year of 2000 compare to the year of 2008. Lower water consumption during drought year may have simply meant that the crops had less available water. Thus, we concluded that there is no variation in ET estimates between drought and wet years for the entire agriculture as a whole and that farmers use similar amount of water regardless of climatic conditions (drought/wet) during the study period. This implies that the agriculture sector as a whole may not be drought sensitive. Although further analysis considering all the different sectors is needed, this research has shown that one significant way to protect the region's water security is to encourage the agricultural sector to adjust their irrigation schemes to climatic conditions. The S-ReSET approach proposed in this study is computationally simple, conceptually straight forward, and easy to handle. We have demonstrated that the S-ReSET model is effective and has potential for global application to determine

agricultural crop water use. The model can also help us make an historical evaluation of the ET_{actual} , identify cropland areas that consume different amounts of water and thus inform water management decision makers and promote regional and global water security.

4.7: Acknowledgments

The authors wish to thank Barbara Trapido-Lurie for her cartographic input and advice.

4.8: References

- Allen T.G., 2008. Why do we care about ET? *Southwest Hydrology*, 7, 18-19.
- Allen, R. G., M. Tasumi, A. Morse, and R. Trezza, 2005. A Landsat based energy balance and evapotranspiration model in western U.S. water rights regulation and planning. *Irrigation and Drainage Systems*, 19, 251–268.
- Allen, R. G., M. Tasumi, A. Morse, and R. Trezza, , 2007. Satellite-based energy balance for mapping evapotranspiration with internalized calibration (METRIC) – model, *Journal of Irrigation and Drainage Engineering*, 133, 380-394.
- ADWR, 2010. Available at: <http://www.azwater.gov> (accessed: 12 October 2011).
- Baker, L.A., A.J. Brazel, N. Selover, C. Martin, N. McIntyre, F. Steiner, A. Nelson, and L. Musacchio., 2002. Urbanization and warming of Phoenix (Arizona, USA): impacts, feedbacks, and mitigation, *Urban Ecosystems*, 6, 183-203.
- Bastiaanssen, W.G.M., 2000. SEBAL based sensible and latent heat fluxes in the irrigated Gedez Basin, Turkey, *Journal of Hydrology*, 229, 87–100.
- Bastiaanssen, W.G.M., T. Van der Wal, T.N.M. Visser, 1996. Diagnosis of regional evaporation by remote sensing to support irrigation performance assessments, *Irrigation and Drainage Systems*, 10, 1-23.
- Bastiaanssen, W.G.M., R.A.L Brito., M.G., Bos., R. Souza, E.B. Cavalcanti, and M.M Bakker, 2001. Low cost satellite data applied to monthly irrigation performance monitoring; benchmarks of Nilo Coelho, Brazil, *Irrigation and Drainage Systems*, 15, 53-79
- Bastiaanssen, W. G. M., H. Pelgrum, J. Wang, Y. Ma, J.F. Moreno, G.J. Roerink, and T. Van der val, 1998a. Remote sensing surface energy balance algorithm for land (SEBAL): 2. Validation. *Journal of Hydrology*, 212, 213–229.
- Bastiaanssen, W. G. M., M. Menenti, R.A. Feddes, and A.A.M Holtslag, 1998b. Remote sensing surface energy balance algorithm for land (SEBAL): 1. Formulation. *Journal of Hydrology*, 213, 198–212.
- Brown, P.W., 2005. Standardized reference evapotranspiration: a new procedure for estimating reference evapotranspiration in Arizona. [rfwww:Cals.arizona.edu/pubs/water/az1324.pdf](http://www.Cals.arizona.edu/pubs/water/az1324.pdf).
- Buyantuyev, A., and J. Wu, 2009. Urbanization alters spatiotemporal patterns of ecosystem primary production: a case study of the Phoenix metropolitan region, USA, *Journal of Arid Environments*, 73, 512-520.

Chavez, P. S. jr. 1996. Image-based atmospheric corrections - Revisited and Improved. *Photogrammetric Engineering and Remote Sensing*, 62, 1025-1036.

Colaizzi, P.D., S.R. Evett, T.A. Howell, and J.A. Tolck, 2006. Comparison of five models to scale daily evapotranspiration from one-time-of-day measurements, *Trans. ASABE*, 49, 1409-1417.

Congalton, R.G. and K. Green, 1999. *Assessing the Accuracy of Remotely Sensed Data: Principles and Practices*, Lewis Publishers, Boca Raton, Florida, 137 p.

Congalton, R.G. 1991. A review of assessing the accuracy of classifications of remotely sensed data. *Remote Sensing of Environment*, 37, 35-46.

Conrad, C., S.W. Dech, M. Hafeez, J. Lamers, C. Martins, and G. Strunz, 2007. Mapping and assessing water use in a Central Asian irrigation system by utilizing MODIS remote sensing products. *Irrigation and Drainage Systems*, 21, 197-218.

Daniel, W. 1990. Applied nonparametric statistics, second edition, Brooks/Cole, Pacific Grove, CA, USA, 635 P.

Elhaddad, A and L.A. Gracia, 2008. Surface energy balance-based model for estimating evapotranspiration taking into account spatial variability in weather, *Journal of Irrigation and Drainage Engineering*, 134, 681-689.

Elhaddad, A., L.A. Gracia, and J.L. Chaves, 2011. Using a surface energy balance-based model to calculate distributed actual evapotranspiration, *Journal of Irrigation and Drainage Engineering*, 137, 17-26.

Folhes, M.T., C.D. Renno, and J.V. Soares, 2009. Remote sensing for irrigation management in the semi-arid northeast of Brazil, *Agricultural Water Management*, 96, 1398-1408.

Gowda, P.H., J.L. Chavez, T.A. Howell, T.H. Marek, and L.L. New, 2008. Surface energy balance based evapotranspiration mapping in the Texas high plains. *Sensors*, 8, 5186-5201.

Idso, S.B., R.D. Jackson, and R.J. Reginato, 1975. Estimating evaporation: a technique adaptable to remote sensing. *Science*, 189, 991-992.

Imhoff, M.L., C.J. Tucker, W.T. Lawrence, and D.C. Stutzer, 2000. The use of multisource satellite and geospatial data to study the effect of urbanization on primary productivity in the United States, *IEEE Transactions on Geoscience and Remote Sensing*, 38, 2549-2556.

IPCC, 2007. Climate Change 2007: The Physical Science Basis. Contribution of Working Group I to the Fourth Assessment Report of the Intergovernmental Panel on Climate Change [Solomon, S., D. Qin, M. Manning, Z. Chen, M. Marquis, K.B. Averyt, M. Tignor and H.L. Miller (eds.)], Cambridge University Press, Cambridge, United Kingdom and New York, NY, USA, 996 pp.

Jensen, J.R. 2005. *Introductory Digital Image Processing: A Remote Sensing Perspective*, 3rd Edition, Upper Saddle River: Prentice-Hall, 526 p.

Kustas, W.P., and J.M. Norman, 1996. Use of remote sensing for evapotranspiration monitoring over land surfaces, *Hydrological Sciences Journal*, 41, 495-516.

Lillesand, M. R.W. Kiefer and J.W. Chipman, 2008. *Remote sensing and image interpretation*, John Wiley & Sons, Inc., New York.

Liu, D. and F. Xia, 2010. Assessing object-based classification: advantages and limitations. *Remote Sensing Letters*, 1, 187-194.

Liu, S., Hu, G., Lu, L. and Mao, D, 2007. Estimation of regional evapotranspiration by TM/ETM+ data over heterogeneous surfaces. *Photogrammetric Engineering & Remote Sensing*, 73, 1169-1178.

Mariotto, I., V.P. Gutschick, and D.L. Clason, 2011. Mapping evapotranspiration from ASTER data through GIS spatial integration of vegetation and terrain features. *Photogrammetric Engineering & Remote Sensing*, 77(5), 483-493.

Markham, B. L. and J.L. Barker, 1986. Landsat MSS and TM Post-Calibration Dynamic Ranges, Exoatmospheric Reflectances and At-Satellite Temperatures, EOSAT Landsat Technical Notes, No. 1, August 1986.

Masoner, J.R., C.S. Mladinich, A.M Konduris and S.J Smith, 2003. Comparison of irrigation water use estimates calculated from remotely sensed irrigated acres and state reported irrigated acres in the Lake Altus drainage basin, Oklahoma and Texas, 2000 growing season. *Water-Resources Investigations Report 03-4155*. USGS. ([url: http://pubs.usgs.gov/wri/wri034155/pdf/wri034155.pdf](http://pubs.usgs.gov/wri/wri034155/pdf/wri034155.pdf))

NASS, 2009. 2008 Arizona Cropland Data Layer, USDA, Washington, D.C.

Norman, J., W. Kustas, and K. Humes, 1995. A two-source approach for estimating soil and vegetation energy fluxes from observations of directional radiometric surface temperature. *Agricultural and Forest Meteorology*, 77, 263-293.

Pelgrum, H. and W.G.M. Bastiaanssen, 1996. An intercomparison of techniques to determine the area-averaged latent heat flux from individual in-situ observations: A remote sensing approach using the European Field Experiment in a Desertification-Threatened Area data, *Water Resources Research*, 32, 2775-2786.

Roerink, G.J., W.G.M. Bastiaanssen, J. Chambouleyron, and M. Menenti, 1997. Relating crop water consumption to irrigation supply by remote sensing, *Water Resources Management*, 11, 445-465.

Roerink, G.J., Z. Su, and M. Menenti, 2000. S-SEBI: a simple remote sensing algorithm to estimate the surface energy balance, *Phys. Chem. Earth (B)*, 25, 147-157.

Rosenberg, N.J., 1974. *Microclimate: the biological environment*, John Wiley and Sons, New-York, 315 p.

Senay, G.B., M. Budde, J.P. Verdin, and A.M. Melesse, 2007. A Coupled Remote Sensing and Simplified Surface Energy Balance Approach to Estimate Actual Evapotranspiration from Irrigated Fields, *Sensors*, 7, 979-1000.

Story, M., and R.G. Congalton, 1986. Accuracy Assessment: A User's Perspective, *Photogrammetric Engineering and Remote Sensing*, 52, 397-399

Sun, Z., Q. Wang, B. Matsushita, T. Fukushima, Z. Quyang, and M. Watanabe, 2009. Development of a simple remote sensing evapotranspiration model (Sim-ReSET): algorithm and model test, *Journal of Hydrology*, 376, 476-485.

Teixeria, A.H., 2010. Determining regional actual evapotranspiration of irrigated crops and natural vegetation in the Sao Francisco River basin (Brazil) using remote sensing and Penman-Monteith equation. *Remote Sensing*, 2, 1287-1319

Thenkabail, T.S., 2010. Global croplands and their importance for water and food security in the twenty-first century: towards an ever green revolution that combines a second green revolution with a blue revolution. *Remote Sensing*, 2, 2305-2312.

USDA, May 1982. Consumption use of water by major crops in the Southwestern United States. *ARS Conservation Research Report 29*.

Zhao-Liang, L., T. Ronglin, W. Zhengming, B. Yuyun, Z. Chenghu, T. Bohui, Y. Guangjian, and Z. Xiaoyu, 2009. A Review of current methodologies for regional evapotranspiration estimation from remotely sensed data, *Sensors*, 9, 3801-3853.

Zwart, S.J. and L.M.C. Leclert, , 2010. A remote sensing based irrigation performance assessment: a case study of the Office du Niger in Mali, *Irrigation Science*, 28, 371-385.

CHAPTER 5: QUANTIFYING OUTDOOR WATER CONSUMPTION OF URBAN
LAND USE/LAND COVER: SENSITIVITY TO DROUGHT³

5.1: Abstract

Outdoor water use is a key component in arid city water systems for achieving sustainable water use and ensuring water security. Using evapotranspiration (ET) calculations as a proxy for outdoor water consumption, the objectives of this research are to quantify outdoor water consumption of different land use and land cover types, and compare the spatio-temporal variation of water consumption between drought and wet years. An energy balance model was applied to Landsat 5 TM time series images to estimate daily and seasonal ET for the Central Arizona Phoenix – Long Term Ecological Research region (CAP-LTER). Modeled ET estimations were correlated with water use data in 49 parks within CAP-LTER and showed good agreement ($r^2=0.77$), indicating model effectiveness to capture the variations across park water consumption. Seasonally, active agriculture shows high ET (>500 mm) for both wet and dry conditions, while the desert and urban land cover types experienced lower ET during drought (<300 mm). Within urban locales of CAP-LTER, xeric neighborhoods show significant differences from year to year, while mesic neighborhoods retain their ET values (400-500 mm) during drought, implying considerable use of irrigation to sustain their greenness. Considering the potentially limiting water availability of this region in the future due to large population increases and the threat of a warming and drying climate, maintaining large water-consuming, irrigated landscapes challenges sustainable practices of water

³ This manuscript was co-authored with Soe W. Myint, Anthony J. Brazel, and Chao Fan. It was submitted to Environmental Management in November 2013.

conservation and the need to provide amenities of this desert area for enhancing quality of life.

5.2: Introduction

Many of the world arid regions contain fast growing urban centers- one of the most disturbing land transformation processes, as it alters natural biophysical processes including local surface energy balances and the hydrological cycle (Imhoff et al 2000; Pielke, 2001; Grimm et al. 2008). As a result, the urban environment tends to be hotter than its surroundings - a phenomenon known as the urban heat island effect (UHI). The UHI phenomenon has been well documented in the scientific literature and is attributed to impervious surfaces and built structures (e.g., Balling & Brazel 1987; Brazel et al. 2000; Baker et al. 2002; Hawkins et al. 2004; Fast et al. 2005). Implications of the UHI effect for urban residents, particularly in arid regions, are manifold: increasing energy demand for air conditioning, aggravating air pollution, reducing human comfort, and augmenting vulnerability to extreme heat events (Harlan et al. 2006, Sarrat et al. 2006, Grimmond 2007, Hart & Sailor 2009). Using water for outdoor irrigation allows the population to sustain a 'greener' landscape and mitigate the effects of the urban heat island (UHI). However, adding vegetation in water stressed arid regions comes with a cost of increased irrigation requirements.

Water availability and land use/land cover (LULC) properties in urban areas are driven by socio-economic conditions and human forces (Buyantuyev and Wu 2010; Brazel et al. 2007). In Phoenix, 45% of the city's municipal total water deliveries are for outdoor usage, i.e., irrigation to support landscaping (City of Phoenix 2011). For

residential water consumption it is estimated that between 60 and 74% is used for the outdoors. This water is sensitive to climate variations (Mayer and DeOreo, 1999). Residential landscapes can be generally characterized as mesic and xeric or some mixture of each. The former refers to the use of non-native vegetation (e.g., Bermuda grass and broad-leaf trees) that requires intensive irrigation, while the latter refers to landscaping that reduces water usage through best practices (i.e., desert vegetation that requires little or no irrigation such as Palo-Verde, Cactai and Mesquite trees). Irrigated mesic landscapes reduce temperature through evaporative cooling and shading from vegetation making plants an important cooling agent in arid environments (Bonan, 2000). The magnitude of the cooling effect depends on local climate, water availability, and land cover properties – specifically the extent of vegetation cover and vegetation composition (Buyantuyev and Wu, 2010; Gober et al. 2012). Increased outdoor water usage raises concerns about production of cooling as an ecosystem service, and long term sustainability of the urban environment in an arid climate, specifically water security (Gober et al. 2011).

In the absence of direct observation, evapotranspiration (ET) can be used to provide a measure of outdoor water usage. ET is the sum of evaporation from soil surface and transpiration from plants. ET is the second most important (after precipitation) component of the water cycle and a controlling factor of energy transport between the biosphere, atmosphere and hydrosphere (Idso et al. 1975). By definition, ET is a measure of the plants water uptake/consumption and can be regarded as a lower boundary for outdoor water usage. In this paper, actual ET (hereafter referred to as ET) derived from a surface energy balance model is used as a proxy for water consumption. Using ET

enables us to quantify outdoor water consumption of different LULC types within the Central Arizona Phoenix Long-Term Ecological Region (CAP-LTER). Quantifying ET over areas undergoing bio-physical changes (e.g., urban expansion) is important in understanding the water cycle, climate dynamics and ecological processes. Understanding these can influence water resources planning, water regulations and water use efficiency, especially in water limited areas where atmospheric demand is high and ET is the largest water consumer (Bastiaanssen, 2000; Allen et al. 2007; Sun et al. 2009). The spatio-temporal variation of ET can help us understand the role of vegetation in the hydrological partitioning across different LULC types, especially types dominated by human impacts.

Traditional methods for ET estimation such as the use of eddy flux towers and lysimeters, are time consuming, require large amounts of field data that is often unavailable, expensive and point based. These issues are even more critical considering the highly heterogeneous LULC in urban environments (Liu et al. 2010). Remote sensing methods often include estimates of ET as a residual of the energy balance, thus reducing the need for ground data while providing information on critical hydrological components such as vegetation, soil, and topographic data. Furthermore, remote sensing provides regional coverage information on the spatial and temporal variability of ET (Bastiaanssen et al 1998; Elhaddad and Garcia, 2008). While remote sensing surface energy balance studies minimize the use of ground data, they were designed and applied almost specifically for agricultural use and natural vegetation (e.g., Teixeira, 2010; Hankerson et al. 2012; Ruhoff et al. 2012). Several studies (e.g., Liu et al. 2007; Liu et al. 2010) used a remote sensing based energy balance approach to map ET over

heterogeneous surfaces. These studies, focusing on daily temporal scale, show that different LULC experience significantly different ET in urban regions and that the higher the ET the lower the development level in urban regions. More recently, Jenerette et al. (2011) used a simplified energy balance model where the sensible heat flux was estimated by the temperature differential between canopy and air. The authors used Sky-Harbor airport as the sole source for meteorological data whereas these can vary considerably over the metropolitan area. Here, we extend their approach by taking into consideration the spatial variability of meteorological conditions, aerodynamics resistance and surface roughness variation across the landscape. The current study takes a direct observation approach utilizing remote sensing data and readily available weather data needed to apply the S-ReSET model (Kaplan and Myint, 2012) and overcome some of the above limitations.

Given recent decade's urban growth in Phoenix metropolitan area, coupled with the region's climatic conditions and water sources, the overall aim of this study is to explore different outdoor water consumption patterns associated with various LULC types and how the results vary under drought and wet conditions. In the past, water development focused on the supply in order to support economic development. Recently more attention has been given to studying water demand, more specifically water usage. Gober (2010) identified outdoor water usage as a critical component for the region's water security. In the tradeoffs between outdoor and indoor water usage under different climatic scenarios, some of the outcomes can be reduced by changing outdoor lifestyle toward a dense urban environment with xeric landscape and pool usage limitations.

This paper thus considers the effect of urbanization on ET by comparing different LULC to the surrounding natural desert ecosystem that represent the baseline conditions. Our specific objectives are to: (a) estimate ET_a as an indicator for outdoor water usage, and determine its variation across different LULC types within urban settings; (b) explore LULC sensitivity to drought; and (c) identify changes in outdoor water usage driven by climate. In the arid southwest United States of America, where water resources are scarce and finite, temperatures are high and are expected to continue rising (Kunkel et al. 2013), information on sensitivity to drought and outdoor water consumption will support more knowledgeable decisions for water use and urban planning. Illustrating the effect of drought on water consumption can provide additional insight on the long term sustainability of different urban landscapes and regional water security. Generally, water security is defined as the ability of a water system to meet environmental and societal needs. In the context of this paper, as per the case of Phoenix, water security means supporting the quality of life and standard of living without diminishing over time.

5.3: Study Area

This study focuses on the Central Arizona Phoenix Long Term Ecological Research area (CAP-LTER) (Figure 35). The CAP-LTER Phoenix metropolitan region is located in the arid southwest USA and includes both natural desert environments and human controlled environments (urban and agriculture). The southwest region and the Phoenix metropolitan area in particular, have undergone extensive modification to its landscape during the 20th century following rapid population growth. The Phoenix metropolitan is comprised of 25 municipalities and diverse land use and land cover

classes, including urban and suburban neighborhoods (commercial, industrial, and residential segments with different densities) as well as desert landscape, unmanaged soil, and undeveloped areas. Jenerette et al. (2011) reported that approximately 40% of the population is ethnic minorities, and concluded that residential segregation plays a key factor in neighborhoods landscape design. .

To sustain human activities in the region, extensive water supply projects and large ground water reserves have been built, including the CAP canal that brings water from the Colorado River, and the Salt and Verde projects that collect runoff from the river basins in to reservoirs. In the last decade, urban growth has increased outdoor water usage as more urban landscapes require irrigation. Currently, the increased usage for urban activities is supported by the water previously allocated to agricultural land on which the new urban area was built. Further growth may threaten the sustainability of water supply sources, especially groundwater (Gober et al. 2011).

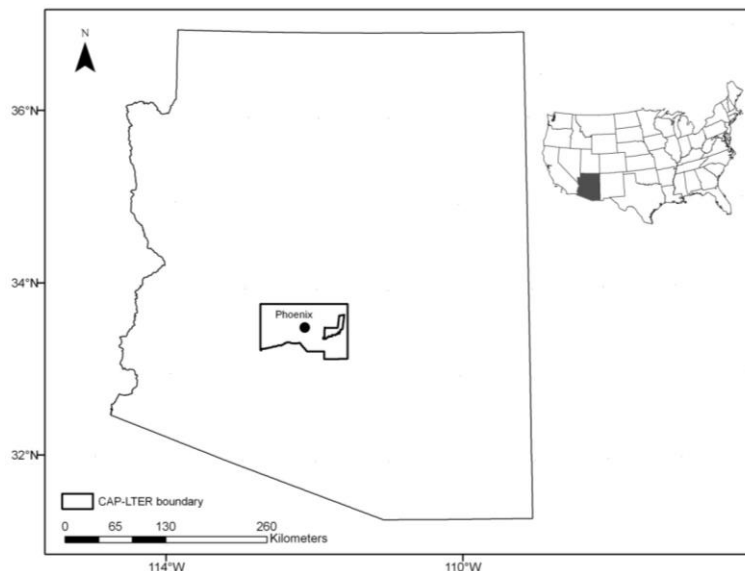


Figure 35. Location map for the Central Arizona Phoenix Long Term Ecological Research study area. Map on the right indicates the location of Arizona within the continental USA

5.4: Data and Methods

5.4.1: Satellite and weather data

In this study, we used level 1G Landsat 5 Thematic Mapper (TM) images that have 30 m resolution with 7 channels – blue (0.42-0.52 μm), green (0.52-0.6 μm), red (0.63-0.69 μm), near infrared (0.75-0.90 μm), mid infrared (1.55-1.75 μm), thermal infrared (10.4-2.50 μm) and mid infrared (2.09-2.35 μm). The thermal infrared channel, which measures thermal radiation, has a 120m resolution that was resampled to 30m by the United States Geological Survey (USGS). The Landsat scenes were obtained in raw format and processed using ERDAS Imagine® software. Image bands 1 to 5 and 7 were atmospherically corrected and converted to reflectance values using the COS-T model (Chavez, 1996). The thermal band was converted to surface temperature following procedures after Markham and Barker (1986).

A total of nine Landsat 5 TM images were acquired covering the time span of April- May of 2000 and 2008 (Table 8). Only the overlapping dates were considered for the final analysis, i.e., April 1 to May 19. The April-May time span was selected for two reasons: (1) Low rainfall frequency and temperatures that do not usually require adjustment of irrigation schedule and amount, thus we can assume most water lost to ET is from irrigation; (2) cloud free image availability. ET cannot be estimated for cloud covered locations because clouds drop the thermal band readings considerably and lead to large errors in sensible heat flux calculations.

Table 8. Dates (Day/Month) of Landsat 5 TM used to estimate ET. Final time span considered only overlapping dates – April 1 to May 19.

2000	2008
26/3	1/4
11/4	17/4
27/4	3/5
13/5	19/5
29/5	

Weather data were obtained from an automated and readily available Arizona meteorological network called AZmet. Three variables were included: air temperature, wind speed and reference ET. The air temperature and wind speed were used to estimate the daily ET. Reference ET was used to interpolate between images, using the algorithm developed by Elhaddad and Garcia (2008), to obtain seasonal values.

To evaluate the effect of drought, we examined and compared two years: 2000 as a drought year, and 2008 as a wet year. Due to the bi-modal rainfall distribution of the region, only winter precipitation (October-May) was considered for the definition of drought (Figure 36). Widespread drought conditions have been recorded in the paleo record (Sheppard et al. 1999) and can be reasonably expected to occur again. Moreover, given the rainfall amount and distribution during 2000, and the consistently higher temperatures, these drought conditions may be considered to represent projected climate conditions for the southwest USA. Several scenarios project a warmer and drier climate, along with an increase in extreme weather events in which seasonal precipitation frequency decreases while their intensity increases (IPCC, 2007; Kunkel 2013).

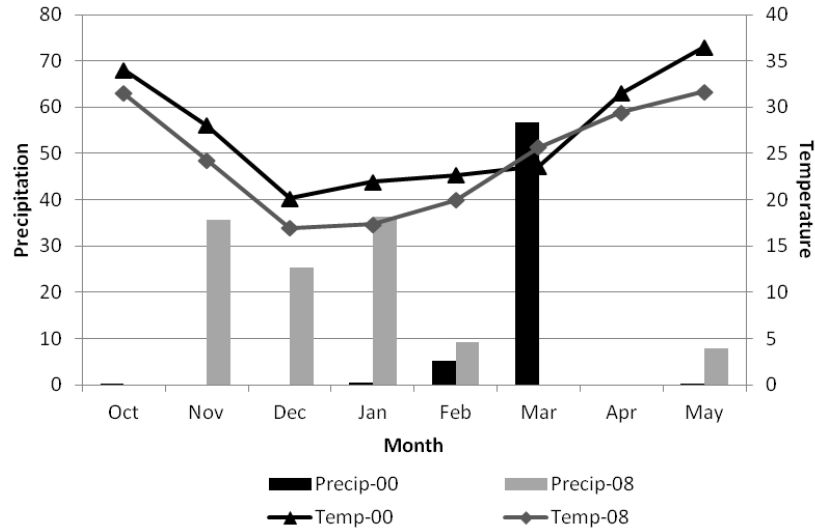


Figure 36: Monthly Precipitation and maximum average Temperature for 2000 and 2008. Note that: (1) While temperatures trends are very similar, values for 2000 are consistently higher; and (2) the year of 2008 had a total of 114.5 mm of rainfall well distributed across the winter season, while the year of 2000 had only 62.5mm of rainfall most of which fell during March.

5.4.2: Evapotranspiration and water use

In this study, a surface energy balance ET algorithm was implemented to estimate actual ET using Landsat 5 satellite images (30m resolution). Using the S-ReSET model (Kaplan and Myint, 2012), ET is calculated for each pixel as a residual of the surface energy balance:

$$LE = \lambda ET = R_n - G - H \quad (5.1)$$

Where LE= latent heat flux, ET=evapotranspiration, λ = latent heat of vaporization (2272*103 J/kg), R_n = net radiation, G= soil heat flux, H= sensible heat flux. Parameters are all in Wm^{-2} .

Most applications of the surface energy model are for monitoring agricultural crops water consumption. The METRIC (Allen et al. 2007) and ReSET (Elhaddad and Garcia 2008) use the alfalfa reference ET to calculate the seasonal water consumption while considering the spatio-temporal variability of weather conditions across the landscape. To adjust the model to the urban environment, we used the grass reference. The use of the grass potential ET rather than alfalfa is more suitable to the urban environment as most of the vegetation is grass (lawns, golf courses, parks) and desert vegetation which has lower potential ET due to physiological adaptation (Rundel and Gibson, 1996). Urban trees, though potentially can have high ET, are usually irrigated less than agricultural crops. Therefore our results can be considered as a lower boundary for trees.

Following Allen et al. (2007) net radiation (Rn) was calculated from remote sensing as the balance between incoming and outgoing solar radiation:

$$Rn = (1 - \alpha)R_s^\downarrow + R_L^\downarrow - R_L^\uparrow - (1 - \varepsilon_0)R_L^\downarrow \quad (5.2)$$

Where R_s^\downarrow =incoming short-wave radiation (Wm^{-2}), α =surface albedo, R_L^\downarrow = incoming long-wave radiation (Wm^{-2}), R_L^\uparrow = outgoing long-wave radiation (Wm^{-2}), ε_0 = broadband surface thermal emissivity. The $(1 - \varepsilon_0)R_L^\downarrow$ term represents the fraction of incoming long wave radiation reflected from the surface, calculated using the Stephan-Boltzmann equation, and the surface temperature derived from Landsat band 6 (10.4-12.5 μ m) following Markham and Barker (1986). The full detailed equations used to derive the different parameters appear in Allen et al. (2007). Soil heat flux (G) was estimated as a

function of R_n , surface temperature (T_s), albedo (α) and vegetation cover (represented by the normalized difference vegetation index- NDVI):

$$G = R_n * (T_s - 273.15)(0.0038 + 0.0074\alpha)(1 - 0.98NDVI^4) \quad (5.3)$$

The NDVI is a measure of vegetation greenness, and is calculated using the red and near-infrared

$$(NIR) \text{ bands of Landsat as: } \quad (NIR-red)/(NIR+red) \quad (5.4)$$

The sensible heat flux (H) was estimated based on the surface - air temperature difference (dT) and aerodynamic resistance (r_{ah}):

$$H = \rho_{air} C_p \frac{dT}{r_{ah}} \quad (5.5)$$

Where ρ_{air} = air density (kg m^{-3}), C_p = specific heat of air at constant pressure ($\text{J kg}^{-1} \text{K}^{-1}$). Aerodynamic resistance calculations use wind speed extrapolated from a blending height of 100m above surface, and an iterative stability correction based on the Monin-Obukov function (As detailed in Allen et al. 2007). Surface – air temperature difference was estimated using Bastiaanssen (1998b) approach.

To solve the sensible heat flux, many of the remote sensing energy balance models use fully vegetated, well irrigated fields as the wet edge. In this study we used Tempe Town Lake ($33^\circ 25' 59''\text{N } 111^\circ 55' 06''\text{W}$) as the wet edge to calibrate the model. The lake is within the urban environment and despite the UHI effect it is still expected to have $dT=0$. Furthermore, it is not subjected to seasonal changes or to irrigation and can be used as the cold pixel for all the images, providing a fixed point of

reference. For the hot pixel (dry edge) in each image, a different bare soil /non active agriculture pixel with minimum NDVI and maximum surface temperature was selected. For these locations we assumed there was no latent heat flux. Commercial/industrial and asphalt/concrete classes were masked and given a value of $ET=0$. We assumed there is no connectivity (water flow) between pixels and that water are distributed evenly across a pixel.

5.4.3: Land use/land cover data

To spatially link ET with different LULC types, ET estimations were overlaid with the CAP-LTER mixed land use/land cover map developed by Buyantuyev (2007). The same map was used for both 2000 and 2008. With an overall accuracy of 83%, the categories used in this land use/land cover map are ecologically associated with dominant vegetation types and net primary production. Vegetation type and net primary production directly affect ET (Bonan, 2002; Buyantuyev and Wu, 2009). To account for LULC changes (LULCC between 2000 and 2008, areas that have undergone change were excluded. The distribution of land use/land cover after excluding areas undergone change is presented in Table 9.

The coefficient of variation (CV) was used to assess the heterogeneity of land cover and to evaluate how the spatial structure of ET in each land cover differs between wet and dry years. The CV was also used to compare and contrast the different land covers.

Table 9. Land Use/Land Cover classification distribution within the study area, after excluding areas that have undergone change (Modified from Buyantuyev, 2007).

Class name	Area (km²)	Percent
Cultivated vegetation (Active Agriculture)	279.39	4.53
Cultivated Grass	18.47	0.30
Soil (Prior Agricultural. Use)	334.46	5.43
Vegetation	748.15	12.14
Commercial/Industrial	428.34	6.95
Asphalt and Concrete	280.50	4.55
Undisturbed (Desert)	2774.11	45.00
Compacted soil	112.35	1.82
Mesic Residential	400.05	6.49
Xeric Residential	760.11	12.33
Water	28.25	0.46

5.5: Results and discussion

5.5.1: Model validation

The S-Reset model was developed and validated for agricultural fields in the CAP-LTER region (Kaplan and Myint 2012). To validate the S-Reset estimations for the urban environment, total ET values for the year 2008 for parks were compared against the park's actual water usage data (City of Phoenix Parks and Recreation – unpublished data, 2011). Generally, the Phoenix city parks are a mix of desert landscaping, water features and turf grass. As the data do not specify the final usage of the water, we excluded all those parks with open water features. The average turf cover for the parks used for validation was 91.5%. This also supports our usage of the grass reference ET in

the model. To adjust our results to turf water use the averaged crop coefficient (K_c) for April and May was used, where $K_c=0.765$ (AZMET 2012).

Park areas were identified using Google Earth and classified 2.4 m spatial resolution Quickbird imagery of the City of Phoenix (approximately 1300 km²). The classification includes 7 land covers (buildings, other impervious surfaces, grass, trees, soil, water and pools) with an overall accuracy of 89%. Based on the classified Quickbird dataset a polygon was drawn for each park. The polygons were then overlaid on the ET maps derived from the S-Reset in order to extract total ET values for each park. The total ET for a park is defined as the sum of all pixels that fall within the polygon.

Total ET was then plotted against actual water usage for each park (Figure 37). Because water use is collected in hundreds of cubic feet (CCF), while the energy balance models estimate ET in mm, and because the data are not normally distributed, we used the natural log (Ln) transformation. The correlation was found to be statistically significant with an $R^2=0.7$ (P-value<0.001). Note that the regression suggests our model overestimates compared to the amount of water actually consumed by the park's vegetation (mostly grass). A couple of explanations are: (a) over irrigation – given the climate and current water regulations, many of the parks are irrigated beyond the actual vegetation needs. In addition, many parks are irrigated by flooding. When using flood irrigation, part of the water evaporates before consumed by the plants, and some infiltrate without being consumed; (b) other water usage allocations - while parks with water bodies have been excluded, all parks have additional water usage such as drinking water, toilets, and play grounds. The latter may also explain the higher disparity between water usage and our ET estimation in the lower part of the data range. Other factors that

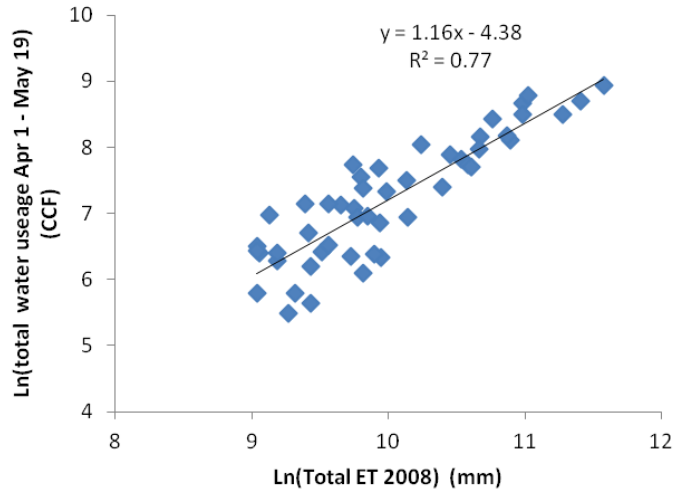


Figure 37. Correlation between the S-ReSET predicted ET and actual water usage from parks, golf courses and sports and recreation facilities across the metropolitan area (n=49).

may contribute to the higher disparity are that our model does not account for advection, the effects of surrounding land cover types, difference in grass/turf and other vegetation types, and consequently difference in resistance and/or k-factor (we assumed both constant)

The strong correlation observed indicates that the S-ReSET model can be effectively used to estimate outdoor water usage. Mayer and DeOreo (1999) studied 12 cities across north America, including several cities within CAP-LTER. The authors found that on average, ET explains 59% of the spatial variation of outdoor water use. The higher R^2 in our model is a result of Phoenix's climate conditions, and its unique landscape and life style choice: wide streets, many open spaces in both the municipal level (i.e., parks) and private (private lawns), and the single family housing. In areas where high rise buildings provide shade and block the satellite view of the vegetation at

street level, such as the Phoenix downtown area, the model is much less effective. In other cities such as New York City for example, the model will not be able to detect the vegetation in the narrow streets.

5.5.2: Seasonal ET estimates

Seasonally accumulated ET estimations for a drought and wet year are presented in Figure 38. The seasonal ET estimates indicate that regionally, the cumulative ET is significantly higher in a wet year than that in a drought year. This is reasonable because both precipitation and irrigation intensify the ET process and thus lead to high ET. Balling and Gober (2007) concluded there is a statistically significant relationship between climatic conditions and water use in Phoenix and point out the importance of outdoor water use. Our comparison of seasonal ET estimates between the drought year and wet conditions revealed that LULC types have diverse drought-sensitivity patterns. The seasonal ET maps coupled with the land use map for 2008 suggest consistent high ET for controlled landscapes regardless of the climate conditions. Results indicate that for mesic residential, the cumulative ET was greater than 250 mm for both years and even greater than 450 mm for cultivated vegetation and grass. These results follow Balling et al. (2008) who reported greater change in outdoor water use for neighborhoods with a high portion of mesic landscaping.

The desert and xeric residential areas yield lower ET than controlled landscapes for both the drought year and wet year due to less vegetation and less or no irrigation. The desert and xeric land cover both show similar differences between wet and dry years, with cumulative ET less than 200 mm during drought and ~250 mm for the wet year. Assuming no major changes in vegetation properties (i.e., density, area, extent, type), these differences can be attributed to the difference in precipitation between the years: 62.5 mm during 2000 (drought year) and 114.5 mm during 2008 (wet year).

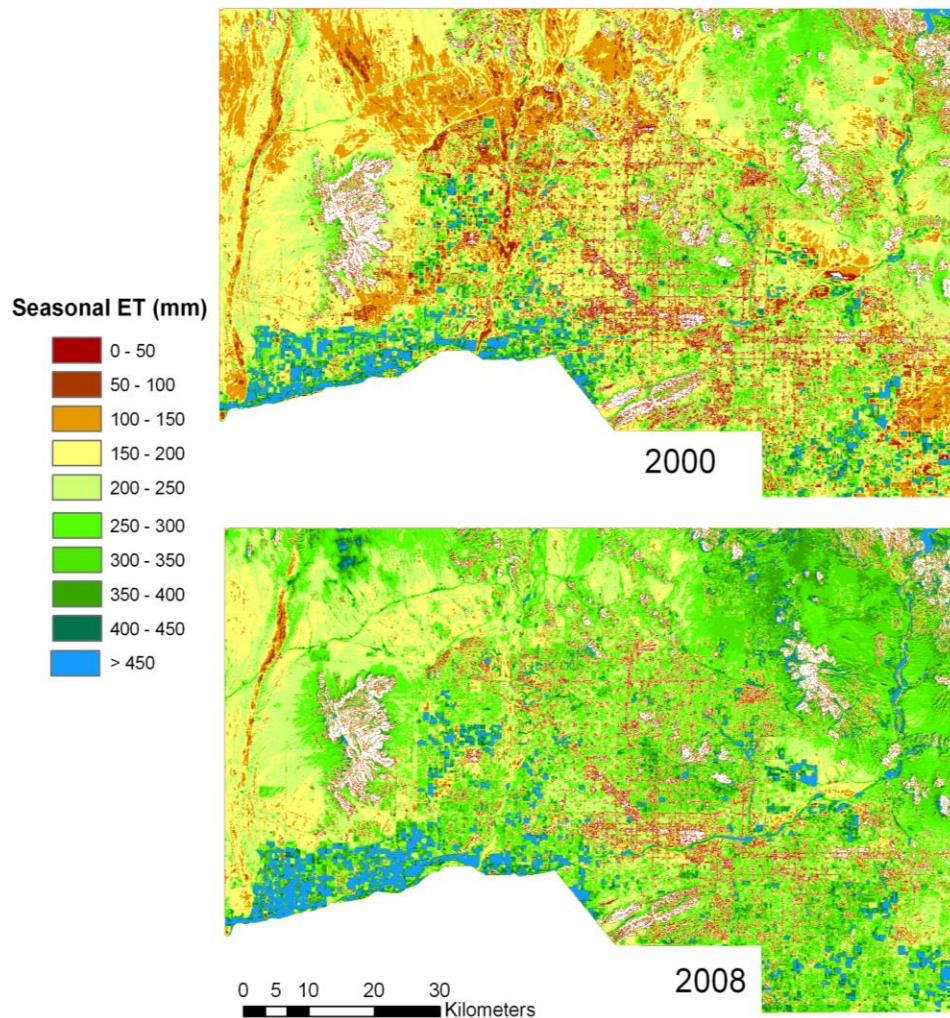


Figure 38. Seasonal ET for a dry year (2000) and a wet year (2008); the effect of drought.

5.5.3: ET coefficient of variance for wet and drought years

To analyze the variation in ET across the entire study area, according to land cover type, we calculated the coefficient of variance (CV). The ET CV was calculated for both wet and drought years for comparison purposes. Results are shown in Figure 39. Analysis of these results indicates that drought leads to consistently higher ET CV regardless of land cover types. Note that there is no striking difference in the ET CV between drought and wet years for controlled (irrigated) landscapes as there is for undisturbed (desert) and xeric residential areas. This confirms our finding based on the seasonal ET estimates that controlled landscapes are not as sensitive to drought as unmanaged landscapes. Specifically, mesic residential and cultivated grass exhibit homogeneously low ET CV across years while compacted soil reveals considerably different patterns in ET between wet and drought conditions.

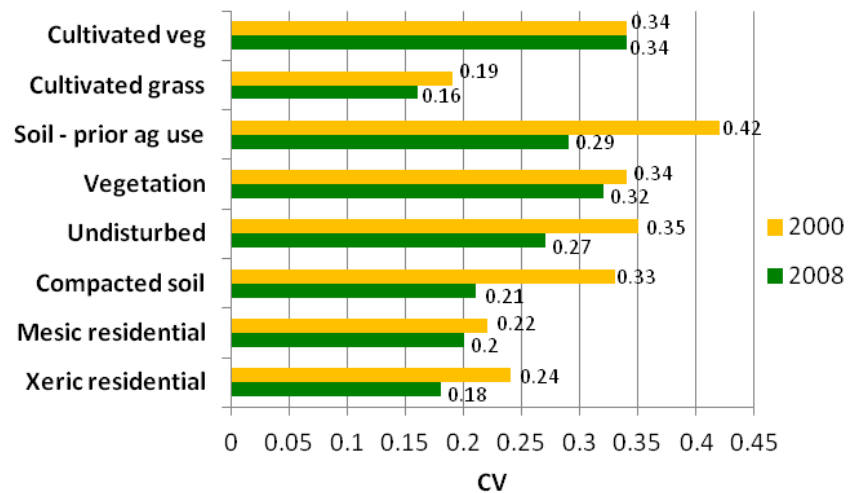


Figure 39. ET coefficient of variance of wet (2008) and dry (2000) years for different land use/land cover types.

5.5.4: Water consumption for major urban land covers

Water consumption for three major LULC types - mesic residential, xeric residential and cultivated grass, was further examined (Figure 40). Results show that drought years have consistently higher water consumption for all LULC types. It is noteworthy that cultivated grass is the most water-consuming land cover among the three and that the amount of water consumed by cultivated grass is very similar regardless of climatic conditions. This is mainly attributable to the irrigation routine and land use: most cultivated grasses are parks, recreation areas and golf courses. As such, they are kept in constant soil moisture levels (i.e., field capacity), thus ET is at its maximum and is limited by physiological properties rather than climate.

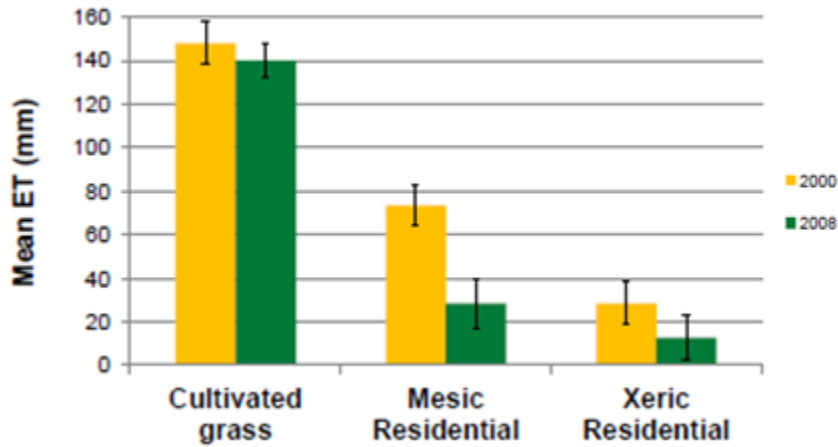


Figure 40. Mean ET (water consumption) of main urban land covers (Apr 1 – May 19).

Mesic residential areas show significantly higher water consumption during drought, indicating that mesic residential areas are more sensitive to drought. Xeric residential consumes the least amount of water for both climatic conditions and the water

consumption does not vary greatly between wet and dry years across the study area. Similar results were reported in several studies (Balling et al. 2008; Balling and Cubaque, 2009), which showed that change in water consumption is related to percent mesic land use and socio-economic parameters. More recently, Buyantuyev and Wu (2010) demonstrated and quantified the link between land use land cover, surface temperature and socio-economic patterns. Martin (2001) found little differences between mesic and xeric outdoor water use, because residents with xeric landscapes do not adjust their water application to account for seasonal changes in ET. Our results suggest that in mesic neighborhoods, the population responds to climate variations by increasing irrigation during drought conditions in order to preserve a greener landscape. In contrast, during wet conditions, the same neighborhoods use less water for irrigation. This approach might be sustainable from an economic point of view where you save money during 'good' times in order to spend it during 'hardship'. However, such an approach might not be sustainable at the long term, especially under the assumption of increasing drought frequency and intensity. An increase in drought frequency and intensity can lead to a negative feedback chain reaction in which water supply is further decreased. For example – a persistent long drought with less precipitation will lead to less flow in the Verde and Salt basins, which in its turn lead to a drop in reservoirs levels. A more regional scale drought can lead, in addition to reduced runoff in the Verde and Salt basins, to a reduced flow in the Colorado River. As a result less water will be allocated to the Phoenix metropolitan areas via the CAP canal, forcing higher withdrawals from local resources such as ground water. Such feedback mechanism will have implications for the region's water security, and will face decision makers and residents with choices on changing life

style and landscape practices. With only local resources, the Phoenix metropolitan area is highly vulnerable to drought (Morehouse et al. 2002), and probably will not be able to sustain itself under existing water use characteristics and population trends.

5.6: Conclusions

Urbanization is one of the most obvious disturbances by human induced land transformations. In arid regions, in addition to changing land surface processes and characteristics, it also impacts the most important resource: water. As Phoenix metropolitan area population continues to grow, residential water use will increase especially outdoor usage to support vegetation. At the same time climate projections indicate an increase in drought frequency and intensity. Continuous development of the area depends on water availability and management, thus, a better understanding of urban LULC sensitivity to drought can promote a more sustainable urban development and mitigate effects of drought in a rapidly expanding city in an arid environment.

We have demonstrated how a detailed spatio-temporal mapping of actual ET and the implications of LULCC on the surface energy balance can be obtained by remote sensing techniques. Results indicate that the S-ReSET provides good estimations for outdoor water consumption, and that its applications can be extended to the urban environment. The model simplicity (use of only remote sensing and weather data) makes it suitable for estimating water usage in urban setting with similar characteristics as Phoenix (single family housing, wide streets etc.), This provides a cost effective method

for identifying hot spots, drought resilience and effective policy outcomes – all critical in environmental management and decision making.

The spatio-temporal variation of ET indicates that drought leads to higher variability within all land covers, especially in “unmanaged” landscapes. Results also indicate that undisturbed desert and xeric residential areas have lower daily and seasonal outdoor water usage, with high variability between drought and wet years. On the other hand, landscapes supported by constant irrigation (i.e., cultivated grass and mesic residential areas) to sustain their greenness and conditions show high water usage regardless of climate conditions. Considering the limited water availability of the region with the projected warmer and drier climate (based on IPCC high emissions A2 scenario), the irrigated landscapes are not sensitive to drought and may not be sustainable. As urbanization continues to intensify, this may have significant implications for future development plans and the region’s water security.

5.7: Acknowledgments

This material is based upon work supported by the National Science Foundation under Grant SES-0951366, Decision Center for a Desert City II: Urban Climate Adaptation and Grant and DEB-0423704, Central Arizona-Phoenix Long-Term Ecological Research (CAP LTER). Any opinions, findings, and conclusions or recommendations expressed in this material are those of the authors and do not necessarily reflect the views of the National Science Foundation.

5.8: References

Allen, R.G., M. Tasumi, A. Morse, and R. Trezza, 2007 Satellite-based energy balance for mapping evapotranspiration with internalized calibration (METRIC) – model. *Journal of Irrigation and Drainage Engineering*, 133, 380-394.

AZMET: The Arizona meteorological network (2012). <http://ag.arizona.edu/azmet/index.html>. (accessed 31 October 2012).

Baker, L.A., A.J. Brazel, N. Selover, C. Martin, N. McIntyre, F. Steiner, A. Nelson, and L. Musacchio, 2002. Urbanization and warming of Phoenix (Arizona, USA): impacts, feedbacks, and mitigation. *Urban Ecosystems*, 6, 183-203.

Balling, R.C.Jr. and P. Gober, 2007 Climate variability and residential water use in the city of Phoenix, Arizona. *Journal of Applied Meteorology and Climatology* 46, 1130-1137.

Balling, R.C.Jr., P. Gober, and N. Jones, 2007. Sensitivity of residential water consumption to variations in climate: An intraurban analysis of Phoenix, Arizona. *Water Resources Research*. doi: 10.1029/2007WR006722.

Balling, R.C.Jr., and C. Cubaque, 2009 Estimating future residential water consumption in Phoenix, Arizona based on simulated changes in climate. *Physical Geography*, 30, 308-323.

Bastiaanssen, W.G.M, M. Menenti, R.A. Feddes, and A.A.M. Holtslag, 1998. Remote sensing surface energy balance algorithm for land (SEBAL): 1. Formulation. *Journal of Hydrology*, 213, 198–212.

Bastiaanssen, W.G.M., 2000. SEBAL based sensible and latent heat fluxes in the irrigated Gedez Basin, Turkey. *Journal of Hydrology*, 229, 87–100.

Bonan, G.B., 2000. The microclimates of a suburban Colorado (USA) landscape and implications for planning and design. *Landscape and Urban Plan*, 49, 97-114

Buyantuyev, A. 2007, Land cover classification using Landsat Enhanced Thematic Mapper (ETM) data - year 2005. <http://caplter.asu.edu/data/?id=377> (accessed 26 Dec 2012).

Buyantuyev, A., and J. Wu, 2009. Urbanization alters spatiotemporal patterns of ecosystem primary production: a case study of the Phoenix metropolitan region, USA. *Journal of Arid Environments*, 73, 512-520.

Buyantuyev, A., and J. Wu, 2010. Urban heat islands and landscape heterogeneity: linking spatiotemporal variations in surface temperatures to land-cover and socioeconomic patterns. *Landscape Ecology*, 25, 17-33

Chavez, P.S.Jr., 1996. Image-based atmospheric corrections – revised and improved. *Photogrammetric Engineering and Remote Sensing*, 62, 1025-1036.

Elhaddad, A., and L.A. Gracia, 2008. Surface energy balance-based model for estimating evapotranspiration taking into account spatial variability in weather. *Journal of Irrigation and Drainage Engineering*, 134, 681-689.

Harlan, S, A.J. Brazel, L. Prashad, W.L. Stefanov, and L. Larsen, 2006. Neighborhood microclimates and vulnerability to heat stress. *Social Science and Medicine*, 63, 2847-2863

Hart, M.A., and D.J. Sailor, 2009. Quantifying the influence of land-use and surface characteristics on spatial variability in the urban heat island. *Theoretical and Applied Climatology*, 95, 397-406

Hankerson, B, J. Kjaersgaard, and C. Hay, 2012. Estimation of Evapotranspiration from Fields with and without cover crops using remote sensing and in situ methods. *Remote Sensing*, 4, 3796-3812.

Gober, P., A. Brazel, R. Quay, S. Myint, S. Grossman-Clarke, A. Miller, and S. Rossi, 2009. Using watered landscapes to manipulate urban heat island effects, how much water will it take to Cool Phoenix?, *Journal of the American Planning Association*, 76, 109-121.

Gober, P., 2010. Decision making under uncertainty: A new paradigm for water management and practice. In: Wang LK, Yang CT (ed) *Handbook of Water Engineering*, Vol. 15, Humana Press Inc, New York, 49 pp.

Gober, P., E.A. Wentz, T. Lant, M.K. Tschudi, and C.W. Kirkwood, 2011. WaterSim: a simulation model for urban water planning in Phoenix, Arizona, USA. *Environmental Planning Bulletin*, 38, 197-215.

Gober, P., A. Middel, A.J. Brazel, S.W. Myint, H. Chang, J-D. Duh, and L. House-Peters, 2012. Tradeoffs between water conservation and temperature amelioration in Phoenix and Portland: implications for urban sustainability. *Urban Geography*, 33:1030-1054.

Grimm, N.B., S.H. Faeth, N.E. Golubiewski, C.L. Redman, J. Wu, X. Bai, and J.M. Briggs, 2008. Global Change and the Ecology of Cities. *Science* 319, 756-760.

Grimmond, C.S.B., and T.R. Oke, 2002. Turbulent heat fluxes in urban areas: Observations and a Local-Scale Urban Meteorological Parameterization Scheme (LUMPS). *Journal of Applied Meteorology*, 41, 792-810.

Grimmond, C.S.B., 2007. Urbanization and global environmental change: Local effects of urban warming. *The Geographical Journal*, 173, 83-88

Idso, S.B., R.D. Jackson, and R.J. Reginato, 1975. Estimating evaporation: a technique adaptable to remote sensing. *Science* 189, 991-992.

Jenerette, D.A., S.L. Harlan, W.L. Stefanov, and C.A. Martin, 2011. Ecosystem services and urban heat riskcape moderation: water, green spaces and social inequality in Phoenix, USA. *Ecological Applications*, 21, 2637-2651.

Imhoff, M.L., C.J. Tucker, W.T. Lawrence, and D.C. Stutzer, 2000. The use of multisource satellite and geospatial data to study the effect of urbanization on primary productivity in the United States. *IEEE Transactions on Geoscience and Remote Sensing*, 38, 2549-2556.

IPCC, 2007. Climate Change 2007: The Physical Science Basis. *Contribution of Working Group I to the Fourth Assessment Report of the Intergovernmental Panel on Climate Change* [Solomon S, Qin D, Manning M, Chen Z, Marquis M, Averyt KB, Tignor M, Miller HL (eds.)]. Cambridge University Press, Cambridge, United Kingdom and New York, NY, USA, 996 pp.

Kaplan, S, and S. Myint, 2012. Estimating irrigated agricultural water use through Landsat TM and a simplified surface energy balance modeling in the semi-arid environments of Arizona. *Photogrammetric Engineering and Remote Sensing*, 78, 849-859.

Kunkel, K.E., L.E. Stevens, S.E. Stevens, L. Sun, E. Janssen, D. Wuebbles, K.T. Redmond, and J.G. Dobson, 2013. Regional Climate Trends and Scenarios for the U.S. National Climate Assessment. Part 5. Climate of the Southwest U.S., *NOAA Technical Report NESDIS 142-5*, 79 pp

Liu, W., Y. Hong, S.I. Khan, M. Huang, B. Voeix, S. Caliskan, and T. Grout, 2010. Actual evapotranspiration estimation for different land use and land cover in urban regions using Landsat 5 data. *Journal of Applied Remote Sensing*, DOI:10.1117/1.3525566.

Martin, C.A., 2001. Landscape water use in Phoenix, Arizona. *Desert Plants* 17, 26-31.

Middel, A., A.J. Brazel, P. Gober, S.M. Myint, H. Chang, and J. Duh, 2012. Land cover, climate, and the summer surface energy balance in Phoenix, AZ and Portland, OR. *International Journal of Climatology*. DOI: 10.1002/joc.2408

Mayer, P.M., and W.B. DeOreo, 1999. Residential end uses of water. *AWWA Research Foundation and American Water Works Association Rep.*, 310 pp.

Morehouse, B.J., R.H. Carter, and P. Tschankert, 2002. Sensitivity of urban water resources in Phoenix, Tucson, and Sierra Vista, Arizona, to severe drought. *Climate Research*, 21, 283-297.

Myint S.W., and G.S. Okin, 2009. Modeling land-cover types using multiple endmember spectral mixture analysis in a desert city. *International Journal of Remote Sensing*, 30, 2237 – 2257

Myint, S.W., P. Gober, A. Brazel, S. Grossman-Clarke, and Q. Weng, 2011. Per-pixel versus object-based classification of urban land cover extraction using high spatial resolution imagery, *Remote Sensing of Environment*, 115, 1145-1161.

Newman, B.D., B.P. Wilcox, S.R. Archer, D.D. Breshears, C.N. Dahm, C.J. Duffy, N.G. McDowell, F.M. Phillips, B.R. Scanlon, and E.R. Vivon, 2006. Ecohydrology of water-limited environments: A scientific vision. *Water Resources Research*, 42, w06302.

City of Phoenix - water services department: 2011 water resources plan. http://phoenix.gov/webcms/groups/internet/@inter/@dept/@wsd/documents/web_content/wsd2011wrp.pdf. (accessed Mar 7, 2013).

Pielke, R.A., 2001. Influence of the spatial distribution of vegetation and soils on the prediction of cumulus convective rainfall. *Review of Geophysics*, 32, 151-177.

Ruhoff, R.L., A.R. Paz, W. Collischonn, L.E.O.C. Aragao, H.R. Rocha , and Y.S. Malhi, 2012. A MODIS-based energy balance to estimate evapotranspiration for clear-sky days in Brazilian tropical savannas. *Remote Sensing*, 4, 703-725

Rundel P.W., and A.C. Gibson, 1996. *Ecological communities and processes in the Mojave Desert ecosystem: Rock Valley, Nevada*, pp. 55-83.

Sarrat C., A. Lemonsu, V. Masson, and D. Guedalia, 2006. Impact of urban heat island on regional atmospheric pollution. *Atmospheric Environment*, 40, 1743-1758

Sheppard P.R., A.C. Comrie, G.D. Packin, K. Angersbach, and M.K. Hughes, 1999. The Climate of the Southwest. *CLIMAS report series CL 1-99*. Institute for the Study of Planet Earth, The University of Arizona, Tucson, AZ.

Sun Z., Q. Wang, B. Matsushita, T. Fukushima, Z. Quyang, and M. Watanabe, 2009. Development of a simple remote sensing evapotranspiration model (Sim-ReSET): algorithm and model test. *Journal of Hydrology* 376, 476-485.

Teixeira A.H. de C., 2010. Determining regional actual evapotranspiration of irrigated crops and natural vegetation in the São Francisco River basin (Brazil) using remote sensing and Penman-Monteith equation. *Remote Sensing* 2, 1287-1319.

Wilhite D.A., 2000. Drought as a nature hazard: concepts and definitions. In: Wilhite DA (ed) *Drought - A Global Assessment*. Routledge London. pp 1-18.

CHAPTER 6: CONCLUSIONS

6.1: Summary of Dissertation Results

The overarching goal of this dissertation were to study LULC response to climate variability, specifically drought, and its implications for water security and sustainability in an arid climate. To address these goals, both natural and human controlled environments were considered.

Chapter 2 examined the spatio-temporal changes of functional types of vegetation in a natural desert environment. It introduced a new model coupling MESMA and phenological knowledge to delineate annuals, perennials and evergreen vegetation. I applied to Landsat 5 TM time series covering 1987-2010. Results show that the spatio-temporal variability of annuals follows short-term winter precipitation, with the highest annuals cover observed during years with high precipitation that followed drought years. No spatio-temporal difference was identified in the response of annuals to drought, and significant degradation was observed only at the local scale in specific locations. Spatially, perennials cover was highly variable, while temporally, perennials fractional cover appears to be consistent over a period of several years, following decadal variability and regime shift between wet and dry conditions. Evergreen vegetation has the highest and most spatially consistent fractional cover. Many areas show high fractional cover (>30%) even during drought years, suggesting evergreen growth is disconnected from short-term climate variability. Trend analysis showed both upwards- and downwards monotonic trends, suggesting different processes are dominant at the local scale. Regionally, the dominant trend for evergreens was positive, while perennials and annuals show a negative trend for most areas. Although for most areas the changes are

not significant, the existence of a monotonic trend may indicate the direction in which each functional type is changing (rehabilitation vs. degradation).

Chapter 3 applied remote sensing and a soil water balance model to study the difference in phenology and response to summer water inputs between the urban environment and its surroundings desert ecosystem. Results show that the urban environment has a year—round, high productivity with high rain-use efficiency (RUE) variability. The desert has lower productivity and responds strongly to summer water input. During drought conditions the desert ecosystem converge toward a maximum aridity index ($H=1$), and $RUE \sim 133 \text{ MJ/m}^2 \cdot \text{hour mm}^{-1}$. The urban area shows consistently lower H and higher RUE regardless of climate conditions. Based on above-ground net primary productivity and RUE calculations, 295 mm of water input are necessary to sustain the urban tree biomass.

Chapter 4 examined the impact of drought on agricultural water use in semi-arid environment. I developed an energy balance model and applied it to estimate actual evapotranspiration (crop water use - ET) from Landsat images and meteorological data. Results show reasonable accuracy across different irrigation districts, indicating the model can effectively quantify the spatio-temporal distribution of actual ET. Desert landscape was characterized by daily ET $< 5.4 \text{ mm/day}$, with high variability between wet and dry years. Active agriculture averaged $8.8 (+/-3.9) \text{ mm/day}$ during drought and $9.9 (+/- 3.6) \text{ mm/day}$ during the wet year, with alfalfa crop showing the highest ET with up to 17 mm/day . Seasonally, active agricultural fields had high, consistent ET regardless of climatic conditions because the crops' water requirements were met by adequate irrigation. The desert and urban land cover experienced lower ET during drought. Water

usage of the entire agricultural sector did not differ statistically between drought and wet conditions, and the total precipitation equivalent water addition was 438 mm and 494 mm during dry and wet conditions, respectively.

Chapter 5 applied the model developed in Chapter 4 to estimate ET over the urban landscape of the Central Arizona Phoenix Long-Term Ecological Research area (CAP-LTER) as a proxy for outdoor water consumption of different LULC types. It then compared the spatio-temporal variation of water consumption between drought and wet years. Within the urban locales of CAP-LTER, xeric neighborhoods show significant differences from year to year, while mesic neighborhoods retain their ET values (400-500 mm) during drought, reinforcing the results from Chapter 3 that considerable use of irrigation helps sustain greenness. Spatially, ET coefficient of variance indicated that drought leads to higher variability within all land covers, especially in “unmanaged” landscapes. Considering the potentially limiting future water availability of this region due to both large population increases and the threat of a warming and drying climate, maintaining large-scale irrigated landscapes will come in conflict with sustainable water conservation and the desire to provide amenities in this desert area for enhancing quality of life.

6.2: Contribution to academic knowledge

Each dissertation chapter has provided new contributions to existing LULC response to drought knowledge, as well as towards remote sensing methodology. First, this dissertation contributed two new models in the form of the coupled MESMA-phenology model to delineate functional types and the S-ReSET model to spatially and temporally

monitor water consumption without the need for crop classification. The S-ReSET was also applied to the urban environment and demonstrated how remote sensing can be used to monitor outdoor water consumption over a settled environment area.

Second, the long-term analysis at the functional-type level showed how the natural desert environment vegetation has changed over the last three decades in conjunction with the moisture regime, and the geographic and temporal trend of these changes. The analysis suggests processes and drivers at the micro and local scales are involved, and influence different functional types in different ways. The pattern of water availability affects both the spatial and temporal variability of ecosystem processes. Furthermore, the method and approach developed here allows us to look simultaneously at both local and regional scales, and provide insight into the relationship between different functional types. These findings could be a useful guide to inform ongoing and future scientific investigation and management efforts related to conservation, vulnerability, and recoverability of the natural desert environment.

Third, comparing the irrigated urban landscape with the natural desert enabled us to estimate the amount of water needed to preserve current greenness and revealed new insights into the buffer irrigation provides against climate variability. Additionally, the analysis implied that different land-cover types have a detectable signal and that the urban environment is decoupled from the climate. Identifying these signals and how they change over time and space can help us understand the role of vegetation in the hydrological partitioning across different land cover types, especially those controlled by man.

Fourth, in natural undisturbed desert environments drought promotes spatial homogeneity of vegetation cover. In contrast, human—controlled landscapes vary more during drought. It is important to quantify this variation in order to better understand the impact of drought on different LULC types, and its implication for future ecological and societal sustainability in arid regions. The insensitivity of agriculture and mesic landscapes to drought threatens regional water security because of the implied need for increased irrigation. Increasing irrigation to sustain human activities has significant implications and tradeoffs that must be considered for long term sustainability.

REFERENCES

- Allen, R. G., M. Tasumi, A. Morse, and R. Trezza, 2005. A Landsat based energy balance and evapotranspiration model in western U.S. water rights regulation and planning. *Irrigation and Drainage Systems*, 19, 251–268.
- Allen, R. G., M. Tasumi, A. Morse, and R. Trezza, , 2007. Satellite-based energy balance for mapping evapotranspiration with internalized calibration (METRIC) – model, *Journal of Irrigation and Drainage Engineering*, 133, 380-394.
- Allen T.G., 2008. Why do we care about ET? *Southwest Hydrology*, 7, 18-19.
- ADWR, 2010. Available at: <http://www.azwater.gov> (accessed: 12 October 2011).
- Archer, S.R. and K.I. Predick, 2008. Climate Change and Ecosystems of the Southwestern United States. *Rangelands*, 30, 23-28.
- AZMET: The Arizona meteorological network (2012). <http://ag.arizona.edu/azmet/index.html>. (accessed 31 October 2012).
- Baker, L.A., A.J. Brazel, N. Selover, C. Martin, N. McIntyre, F. Steiner, A. Nelson, and L. Musacchio., 2002. Urbanization and warming of Phoenix (Arizona, USA): impacts, feedbacks, and mitigation, *Urban Ecosystems*, 6, 183-203.
- Baldwin, M. P., L. J. Gray, T. J. Dunkerton, K. Hamilton, P. H. Haynes, W. J. Randel, J. R. Holton, M. J. Alexander, I. Hirota, T. Horinouchi, D. B. A. Jones, J. S. Kinnersley, C. Marquardt, K. Sato, and M. Takahashi, 2001. The quasi-biennial oscillation. *Reviews of Geophysics*, 39, 179-229.
- Balling, R.C.Jr. and P. Gober, 2007 Climate variability and residential water use in the city of Phoenix, Arizona. *Journal of Applied Meteorology and Climatology* 46, 1130-1137.
- Balling, R.C.Jr., P. Gober, and N. Jones, 2007. Sensitivity of residential water consumption to variations in climate: An intraurban analysis of Phoenix, Arizona. *Water Resources Research*. doi: 10.1029/2007WR006722.
- Balling, R.C.Jr., and C. Cubaque, 2009 Estimating future residential water consumption in Phoenix, Arizona based on simulated changes in climate. *Physical Geography*, 30, 308-323.
- Bastiaanssen, W.G.M., T. Van der Wal, T.N.M. Visser, 1996. Diagnosis of regional evaporation by remote sensing to support irrigation performance assessments, *Irrigation and Drainage Systems*, 10, 1-23.

Bastiaanssen, W. G. M., H. Pelgrum, J. Wang, Y. Ma, J.F. Moreno, G.J. Roerink, and T. Van der val, 1998a. Remote sensing surface energy balance algorithm for land (SEBAL): 2. Validation. *Journal of Hydrology*, 212, 213–229.

Bastiaanssen, W. G. M., M. Menenti, R.A. Feddes, and A.A.M Holtslag, 1998b. Remote sensing surface energy balance algorithm for land (SEBAL): 1. Formulation. *Journal of Hydrology*, 213, 198–212.

Bastiaanssen, W.G.M., 2000. SEBAL based sensible and latent heat fluxes in the irrigated Gedez Basin, Turkey, *Journal of Hydrology*, 229, 87–100.

Bastiaanssen, W.G.M., R.A.L Brito, M.G., Bos, R. Souza, E.B. Cavalcanti, and M.M Bakker, 2001. Low cost satellite data applied to monthly irrigation performance monitoring; benchmarks of Nilo Coelho, Brazil, *Irrigation and Drainage Systems*, 15, 53-79.

Beatley J.C. 1974. Phenological events and their environmental triggers in Mojave-Desert. *Ecosystem Ecology*, 55, 856–863.

Beatley, J.C., 1979, Shrub and tree data for plant associations across the Mojave/Great Basin desert transition of the Nevada Test Site, 1963-1975, Springfield, VA, National Technical Information Service, DOE/EV/2307-15 U-48, 52 p.

Bellone, T., P. Boccoardo, and F. Perez, 2009. Investigation of vegetation dynamics using long term Normalized Difference Vegetation Index time series. *American Journal of Environmental Sciences*, 5, 460-466.

Bonan, G.B., 2000. The microclimates of a suburban Colorado (USA) landscape and implications for planning and design. *Landscape and Urban Plan*, 49, 97-114.

Bonan, G.B., 2002. Ecological climatology – concepts and applications. Cambridge university press, United Kingdom, pp 678.

Brown, P.W., 2005. Standardized reference evapotranspiration: a new procedure for estimating reference evapotranspiration in Arizona. [rfwww:Cals.arizona.edu/pubs/water/az1324.pdf](http://www.cals.arizona.edu/pubs/water/az1324.pdf).

Buyantuyev, A. 2007, Land cover classification using Landsat Enhanced Thematic Mapper (ETM) data - year 2005. <http://caplter.asu.edu/data/?id=377> (accessed 26 Dec 2012).

Buyantuyev, A. and J. Wu, 2009. Urbanization alters spatiotemporal patterns of ecosystem primary production, a case study of the Phoenix metropolitan region, USA. *Journal of Arid Environment* 73, 512-520.

Buyantuyev, A. and J. Wu, 2010. Urban heat island and landscape heterogeneity: linking spatiotemporal variations in surface temperature to land-cover and socioeconomic patterns. *Landscape Ecology*, 25, 17-33.

Casady, G.M., W.J. van Leeuwen, and B.C. Reed, 2013. Estimating winter annual biomass in the Sonoran and Mojave Deserts with satellite- and Ground-Based observations. *Remote Sensing*, 5, 909-926; doi:10.3390/rs5020909.

Chapin, F.S., P.A. Matson, and H.A. Mooney, Principles of Terrestrial Ecosystem Ecology, 2002. Springer-Verlag Press, NY.

Chavez, P.S. Jr., 1996 Image-based atmospheric corrections – revised and improved. *Photogrammetric Engineering and Remote Sensing*, 62, 1025-1036.

City of Phoenix - water services department: 2011 water resources plan. http://phoenix.gov/webcms/groups/internet/@inter/@dept/@wsd/documents/web_content/wsd2011wrp.pdf. (accessed Mar 7, 2013).

CLIMAS: Climate Assessment for the Southwest. 2012. Available at: <http://www.climas.arizona.edu> (accessed Jan. 18, 2013).

Colaizzi, P.D., S.R. Evett, T.A. Howell, and J.A. Tolck, 2006. Comparison of five models to scale daily evapotranspiration from one-time-of-day measurements, *Trans. ASABE*, 49, 1409-1417.

Congalton, R.G. and K. Green, 1999. *Assessing the Accuracy of Remotely Sensed Data: Principles and Practices*, Lewis Publishers, Boca Raton, Florida, 137 p.

Congalton, R.G. 1991. A review of assessing the accuracy of classifications of remotely sensed data. *Remote Sensing of Environment*, 37, 35-46.

Conrad, C., S.W. Dech, M. Hafeez, J. Lamers, C. Martins, and G. Strunz, 2007. Mapping and assessing water use in a Central Asian irrigation system by utilizing MODIS remote sensing products. *Irrigation and Drainage Systems*, 21, 197-218.

Daniel, W.W. 1990. *Applied nonparametric statistics*. Duxbury, Pacific Grove, California, USA.

Dennison, P. E. and D.A. Roberts, 2003. Endmember Selection for Multiple Endmember Spectral Mixture Analysis using Endmember Average RSME, *Remote Sensing of Environment*, 87,123-135.

Ehleringer, J.R. 1985. Annuals and perennials of warm deserts. pp.162-180. In Chabot B.F. and Mooney, H.A. (eds.) *Physiological ecology of North American Plant Communities*. Chapman and Hall, New-York.

Elhaddad , A and L.A. Gracia, 2008. Surface energy balance-based model for estimating evapotranspiration taking into account spatial variability in weather, *Journal of Irrigation and Drainage Engineering*, 134, 681-689.

Elhaddad A., L.A. Gracia, and J.L. Chaves, 2011. Using a surface energy balance-based model to calculate distributed actual evapotranspiration, *Journal of Irrigation and Drainage Engineering*, 137, 17-26.

Elmore, A.J., J.F. Mustard, S.J. Manning, and D.B. Lobell, 2000. Quantifying vegetation change in semiarid environments: precision and accuracy of spectral mixture analysis and the normalized difference vegetation index. *Remote Sensing of Environment*, 73, 87-102.

Elvidge, C.D., 1990. Visible and infrared reflectance characteristics of dry plant materials. *International Journal of Remote Sensing*, 12, 1775–1795.

Folhes, M.T., C.D. Renno, and J.V. Soares, 2009. Remote sensing for irrigation management in the semi-arid northeast of Brazil, *Agricultural Water Management*, 96, 1398-1408.

Gober, P., A. Brazel, R. Quay, S. Myint, S. Grossman-Clarke, A. Miller, and S. Rossi, 2009. Using watered landscapes to manipulate urban heat island effects, how much water will it take to Cool Phoenix?, *Journal of the American Planning Association*, 76, 109-121.

Gober, P., 2010. Decision making under uncertainty: A new paradigm for water management and practice. In: Wang LK, Yang CT (ed) *Handbook of Water Engineering*, Vol. 15, Humana Press Inc, New York, 49 pp.

Gober, P., E.A. Wentz, T. Lant, M.K. Tschudi, and C.W. Kirkwood, 2011. WaterSim: a simulation model for urban water planning in Phoenix, Arizona, USA. *Environmental Planning Bulletin*, 38, 197-215.

Gober, P., A. Middel, A.J. Brazel, S.W. Myint, H. Chang, J-D. Duh, and L. House-Peters, 2012. Tradeoffs between water conservation and temperature amelioration in Phoenix and Portland: implications for urban sustainability. *Urban Geography*, 33:1030-1054.

Grimm, N. B., S.H. Faeth, N.E. Golubiewski, C.L. Redman, J. Wu, X. Bai, and J.M. Briggs, 2008. Global Change and the Ecology of Cities. *Science*, 319, 756-760.

Grimmond, C.S.B., and T.R. Oke, 2002. Turbulent heat fluxes in urban areas: Observations and a Local-Scale Urban Meteorological Parameterization Scheme (LUMPS). *Journal of Applied Meteorology*, 41, 792-810.

Grimmond, C.S.B., 2007. Urbanization and global environmental change: Local effects of urban warming. *The Geographical Journal*, 173, 83-88

Gowda, P.H., J.L. Chavez, T.A. Howell, T.H. Marek, and L.L. New, 2008. Surface energy balance based evapotranspiration mapping in the Texas high plains. *Sensors*, 8, 5186-5201.

Guida, R.J., S.R. Abella, W.J. Smith jr., H. Stephen, and C.L. Roberts, 2013. Climatic change and desert vegetation distribution: assessing thirty years of change in southern Nevada's Mojave Desert. *The Professional Geographer*. doi: 10.1080/00330124.2013.787007.

Hankerson, B, J. Kjaersgaard, and C. Hay, 2012. Estimation of Evapotranspiration from Fields with and without cover crops using remote sensing and in situ methods. *Remote Sensing*, 4, 3796-3812.

Harlan, S, A.J. Brazel, L. Prashad, W.L. Stefanov, and L. Larsen, 2006. Neighborhood microclimates and vulnerability to heat stress. *Social Science and Medicine*, 63, 2847-2863.

Hart, M.A., and D.J. Sailor, 2009. Quantifying the influence of land-use and surface characteristics on spatial variability in the urban heat island. *Theoretical and Applied Climatology*, 95, 397-406.

Hereford, R., R.H. Webb, and C.I. Longpre, 2006. Precipitation history and ecosystem response to multidecadal precipitation variability in the Mojave Desert region, 1983-2001. *Journal of Arid Environments* 67, 13-34.

Hostert, P., A. Roder, and J. Hill, 2003. Coupling spectral unmixing and trend analysis for monitoring of long-term vegetation dynamics in Mediterranean rangelands. *Remote Sensing of Environment*, 87, 183-197.

Huxman, T. E., M.O. Smith, P.A. Fay, A.K. Knapp, M.R. Shaw, M.E. Loik, S.D. Smith, D.T. Tissue, J.C. Zak, J.F. Weltzin, W.T. Pockman, O.E. Sala, B.M. Haddad, J. Harte, G.W. Koch, Su. Schwinning, E.E. Small, and D.G. Williams, 2004. Convergence across biomes to a common rain-use efficiency. *Nature*, 429, 651-654.

Idso, S.B., R.D Jackson, and R.J. Reginato, 1975. Estimating evaporation: a technique adaptable to remote sensing. *Science*, 189, 991-992.

Imhoff, M. L., C.J. Tucker, W.T. Lawrence, and D.C. Stutzer, 2000. The use of multisource satellite and geospatial data to study the effect of urbanization on primary productivity in the United States. *IEEE Transactions on Geoscience and Remote Sensing*, 38, 2549-2556.

IPCC (Intergovernmental Panel on Climate Change), 2007. Summary for policymakers. In: *Climate Change 2007: The Physical Science Basis*. Contribution of Working Group I to the Fourth Assessment Report of the Intergovernmental Panel on Climate Change [Solomon, S., D. Qin, M. Manning, Z. Chen, M. Marquis, K.B. Averyt, M. Tignor, and H.L. Miller (Eds.)]. Cambridge University Press, Cambridge, UK, and New York, pp. 1-18.

Jenerette, D.A., S.L. Harlan, W.L. Stefanov, and C.A. Martin, 2011. Ecosystem services and urban heat riskcape moderation: water, green spaces and social inequality in Phoenix, USA. *Ecological Applications*, 21, 2637-2651.

Jensen, J.R. 2005. *Introductory Digital Image Processing: A Remote Sensing Perspective*, 3rd Edition, Upper Saddle River: Prentice-Hall, 526 p.

Kaplan, S, and S. Myint, 2012. Estimating irrigated agricultural water use through Landsat TM and a simplified surface energy balance modeling in the semi-arid environments of Arizona. *Photogrammetric Engineering and Remote Sensing*, 78, 849-859.

Kunkel, K.E., L.E. Stevens, S.E. Stevens, L. Sun, E. Janssen, D. Wuebbles, K.T. Redmond, and J.G. Dobson, 2013. Regional Climate Trends and Scenarios for the U.S. National Climate Assessment. Part 5. Climate of the Southwest U.S., *NOAA Technical Report NESDIS 142-5*, 79 pp

Kustas, W.P., and J.M. Norman, 1996. Use of remote sensing for evapotranspiration monitoring over land surfaces, *Hydrological Sciences Journal*, 41, 495-516.

Laio, F., A. Porporato, L. Ridolfi, and I. Rodriguez-Iturbe, 2001. Plants in water controlled ecosystems: active role in hydrologic processes and response to water stress II. Probabilistic soil moisture dynamics. *Advances in Water Resources*, 24, 707-723.

Lillesand, M. R.W. Kiefer and J.W. Chipman, 2008. *Remote sensing and image interpretation*, John Wiley & Sons, Inc., New York.

Liu, S., Hu, G., Lu, L. and Mao, D, 2007. Estimation of regional evapotranspiration by TM/ETM+ data over heterogeneous surfaces. *Photogrammetric Engineering & Remote Sensing*, 73, 1169-1178.

Liu, D. and F. Xia, 2010. Assessing object-based classification: advantages and limitations. *Remote Sensing Letters*, 1, 187-194.

Liu, W., Y. Hong, S.I. Khan, M. Huang, B. Voeix, S. Caliskan, and T. Grout, 2010. Actual evapotranspiration estimation for different land use and land cover in urban regions using Landsat 5 data. *Journal of Applied Remote Sensing*, DOI:10.117/1.3525566.

- Loik M.E., D.D. Breshears, W.K. Lauenroth, and J. Belnap, 2004. A multi-scale perspective of water pulses in dryland ecosystems: climatology and ecohydrology of the western USA. *Oecologia*, 141, 269–281.
- Ludwig, J.A., B.P. Wilcox, D.D. Breshears, D.J. Tongway, and A.C. Imeson, 2005. Vegetation patches and runoff erosion as interacting ecohydrological processes in semiarid landscapes. *Ecology*, 86, 308-319.
- Mariotto, I., V.P. Gutschick, and D.L. Clason, 2011. Mapping evapotranspiration from ASTER data through GIS spatial integration of vegetation and terrain features. *Photogrammetric Engineering & Remote Sensing*, 77(5), 483-493.
- Markham, B. L. and J.L. Barker, 1986. Landsat MSS and TM Post-Calibration Dynamic Ranges, Exoatmospheric Reflectances and At-Satellite Temperatures, EOSAT Landsat Technical Notes, No. 1, August 1986.
- Martin, C.A., 2001. Landscape water use in Phoenix, Arizona. *Desert Plants* 17, 26-31.
- Masoner, J.R., C.S. Mladinich, A.M. Konduris and S.J. Smith, 2003. Comparison of irrigation water use estimates calculated from remotely sensed irrigated acres and state reported irrigated acres in the Lake Altus drainage basin, Oklahoma and Texas, 2000 growing season. *Water-Resources Investigations Report 03-4155*. USGS. (url: <http://pubs.usgs.gov/wri/wri034155/pdf/wri034155.pdf>).
- Mayer, P.M., and W.B. DeOreo, 1999. Residential end uses of water. *AWWA Research Foundation and American Water Works Association Rep.*, 310 pp.
- McAuliffe, J.R. and E.P. Hamerlynck, 2010. Perennial plant mortality in the Sonoran and Mojave deserts in response to severe, multi-year drought. *Journal of Arid Environments*, 74, 885-896.
- Middel, A., A.J. Brazel, P. Gober, S.M. Myint, H. Chang, and J. Duh, 2012. Land cover, climate, and the summer surface energy balance in Phoenix, AZ and Portland, OR. *International Journal of Climatology*. DOI: 10.1002/joc.2408.
- Miriti, M.N., S. Rodriguez-Buritica, S.J. Wright, and H.F. Howe, 2007. Episodic death across species of desert shrubs. *Ecology*, 88, 32-36.
- Mojave National Preserve, 2002. General Management Plan. Available at: <http://www.nps.gov/moja/parkmgmt/gmp.html> (accessed Nov. 19, 2013).
- Morehouse, B.J., R.H. Carter, and P. Tschankert, 2002. Sensitivity of urban water resources in Phoenix, Tucson, and Sierra Vista, Arizona, to severe drought. *Climate Research*, 21, 283-297.

- Myint, S.W., and G.S. Okin, 2009. Modeling land-cover types using multiple endmember spectral mixture analysis in a desert city, *International Journal of Remote Sensing*, 30, 2237–2257.
- Myint, S.W., P. Gober, A. Brazel, S. Grossman-Clarke, and Q. Weng, 2011. Per-pixel versus object-based classification of urban land cover extraction using high spatial resolution imagery, *Remote Sensing of Environment*, 115, 1145-1161.
- NASS, 2009. 2008 Arizona Cropland Data Layer, USDA, Washington, D.C.
- Neil, K. L., L. Landrum, and J. Wu, 2010. Effects of urbanization on flowering phenology in the metropolitan phoenix region of USA: Findings from herbarium records. *Journal of Arid Environment*, 74, 440-444.
- Newman, B. D., B.P. Wilcox, S.R. Archer, D.D. Breshears, C.N. Dahm, C.J. Duffy, N.G. McDowell, F.M. Phillips, B.R. Scanlon, and E.R. Vivoni, 2006: Ecohydrology of water-limited environments: A scientific vision. *Water Resources Research*, 42, w06302.
- Nimmo, J.R., K.S. Perkins, K.M. Schmidt, D.M. Miller, J.D. Stock, and K. Singha, 2009. Hydrologic characterization of desert soils with varying degrees of pedogenesis: 1. Field experiments evaluating plant-relevant soil water behavior. *Vadose Zone Journal*, 8, 480-495.
- Norman, J., W. Kustas, and K. Humes, 1995. A two-source approach for estimating soil and vegetation energy fluxes from observations of directional radiometric surface temperature. *Agricultural and Forest Meteorology*, 77, 263–293.
- Ogle, K., and J.F. Reynolds, 2004. Plant response to precipitation in desert ecosystems: integrating functional types, pulses, thresholds and delays. *Oecologia* 141, 282-294.
- Pelgrum, H. and W.G.M. Bastiaanssen, 1996. An intercomparison of techniques to determine the area-averaged latent heat flux from individual in-situ observations: A remote sensing approach using the European Field Experiment in a Desertification-Threatened Area data, *Water Resources Research*, 32, 2775-2786.
- Pennington, D., & S. Collins, 2007: Response of an aridland ecosystem to interannual climate variability and prolonged drought. *Landscape Ecology*, 22, 897-910.
- Pielke, R.A., 2001. Influence of the spatial distribution of vegetation and soils on the prediction of cumulus convective rainfall. *Review of Geophysics*, 32, 151-177.
- Reynolds, J.F., P.R. Kemp, K. Ogle, and R.J. Fernandez, 2004. Modifying the ‘pulse-reserve paradigm for deserts of North America: precipitation pulses, soil water, and plant responses. *Oecologia*, 141, 194-210.

Roderick, M.L., I.R. Nobel and S.W. Cridland, 1999. Estimating woody and herbaceous vegetation cover from time series satellite observations. *Global Ecology and Biogeography*, 8, 501-508.

Roerink, G.J., W.G.M. Bastiaanssen, J. Chambouleyron, and M. Menenti, 1997. Relating crop water consumption to irrigation supply by remote sensing, *Water Resources Management*, 11, 445-465.

Roerink, G.J., Z. Su, and M. Menenti, 2000. S-SEBI: a simple remote sensing algorithm to estimate the surface energy balance, *Phys. Chem. Earth (B)*, 25, 147-157.

Rosenberg, N.J., 1974. *Microclimate: the biological environment*, John Wiley and Sons, New-York, 315 p.

Rundel P.W. and A.C. Gibson, 1996. *Ecological communities and processes in a Mojave desert ecosystem: Rock Valley*, Nevada. Cambridge University press.

Ruhoff, R.L., A.R. Paz, W. Collischonn, L.E.O.C. Aragao, H.R. Rocha , and Y.S. Malhi, 2012. A MODIS-based energy valance to estimate evapotranspiration for clear-sky days in Brazilian tropical savannas. *Remote Sensing*, 4, 703-725

Sarrat C., A. Lemonsu, V. Masson, and D. Guedalia, 2006. Impact of urban heat island on regional atmospheric pollution. *Atmospheric Environment*, 40, 1743-1758

Senay, G.B., M. Budde, J.P. Verdin, and A.M. Melesse, 2007. A Coupled Remote Sensing and Simplified Surface Energy Balance Approach to Estimate Actual Evapotranspiration from Irrigated Fields, *Sensors*, 7, 979-1000.

Sheppard P.R., A.C. Comrie, G.D. Packin, K. Angersbach, and M.K. Hughes, 1999. The Climate of the Southwest. *CLIMAS report series CL 1-99*. Institute for the Study of Planet Earth, The University of Arizona, Tucson, AZ.

Shepherd, J. M., 2006. Evidence of urban-induced precipitation variability in arid climate regimes. *Journal of Arid Environment*, 67, 607-628

Shoshany, M. and T. Svoray, 2002. Multidate adaptive unmixing and its application to analysis of ecosystem transitions along a climatic gradient. *Remote Sensing of Environments* 82, 5-20.

Smith, S.D., C.A. Herr, K.L. Leary, and J.M. Piorkowski, 1995. Soil-plant water relations in a Mojave Desert mixed shrub community: a comparison of three geomorphic surfaces. *Journal of Arid Environments*, 29, 339-351.

Sonnenschein, R., T. Kuemmerle, T. Udelhoven, M. Stellmes, and P. Hostert, 2011. Differences in Landsat based trend analyses in drylands due to the choice of vegetation estimate. *Remote Sensing of Environment*, 115, 1408-1420.

Story, M., and R.G. Congalton, 1986. Accuracy Assessment: A User's Perspective, *Photogrammetric Engineering and Remote Sensing*, 52, 397-399.

Sun, Z., Q. Wang, B. Matsushita, T. Fukushima, Z. Quyang, and M. Watanabe, 2009. Development of a simple remote sensing evapotranspiration model (Sim-ReSET): algorithm and model test, *Journal of Hydrology*, 376, 476-485.

Teixeria, A.H., 2010. Determining regional actual evapotranspiration of irrigated crops and natural vegetation in the Sao Francisco River basin (Brazil) using remote sensing and Penman-Monteith equation. *Remote Sensing*, 2, 1287-1319.

Thenkabail, T.S., 2010. Global croplands and their importance for water and food security in the twenty-first century: towards an ever green revolution that combines a second green revolution with a blue revolution. *Remote Sensing*, 2, 2305-2312.

Troch, P. A., G.F. Martinez, V.R.N. Pauwels, M. Durcik, M. Sivapalan, C. Harman, P.D. Brooks, H. Gupta, and T. Huxman, 2009. Climate and vegetation water use efficiency at catchment scales. *Hydrological Processes*, 23, 2409-2414.

USDA, May 1982. Consumption use of water by major crops in the Southwestern United States. *ARS Conservation Research Report 29*.

Ustin, S.L. and J.A. Gamon, 2010. Remote sensing of plant functional types. *New Phytologist*, 186, 795-816.

Vitousek, P. M. and H.A. Mooney, 1997. Human domination of Earth's ecosystems. *Science*, 277, 494-499.

Wallace, S.A., and K.A. Thomas, 2008. An annual plant growth proxy in the Mojave Desert using MODIS-EVI data. *Sensors* 8, 7792-7808.

Wallace, S.A., R.H. Webb, and K.A. Thomas, 2008. Estimation of perennial vegetation cover distribution in the Mojave Desert using MODIS-EVI. *GIScience & Remote Sensing* 45, 167-187.

Webb, W., S. Szarek, W. Lauenroth, R. Kinerson, , and M. Smith, 1978. Primary productivity and water use in native forest, grassland, and desert ecosystems. *Ecology*, 59, 1239-1247.

Wilhite, D. A. 2000. Drought as a nature hazard. *Drought. A Global Assessment*. London, Routledge. 1, 1-18.

Zhao-Liang, L., T. Ronglin, W. Zhengming, B. Yuyun, Z. Chenghu, T. Bohui, Y. Guangjian, and Z. Xiaoyu, 2009. A Review of current methodologies for regional evapotranspiration estimation from remotely sensed data, *Sensors*, 9, 3801-3853.

Zwart, S.J. and L.M.C. Leclert, , 2010. A remote sensing based irrigation performance assessment: a case study of the Office du Niger in Mali, *Irrigation Science*, 28, 371-385.

APPENDIX A
STATEMENT OF PERMISSION

I declare that I have obtained explicit permission from my co-authors for including two peer-reviewed scientific journal manuscripts as chapters in this dissertation. They are:

- Soe W. Myint (Chapters 4 and 5);
- Anthony J. Brazel (Chapter 5);
- Chao Fan (Chapter 5).

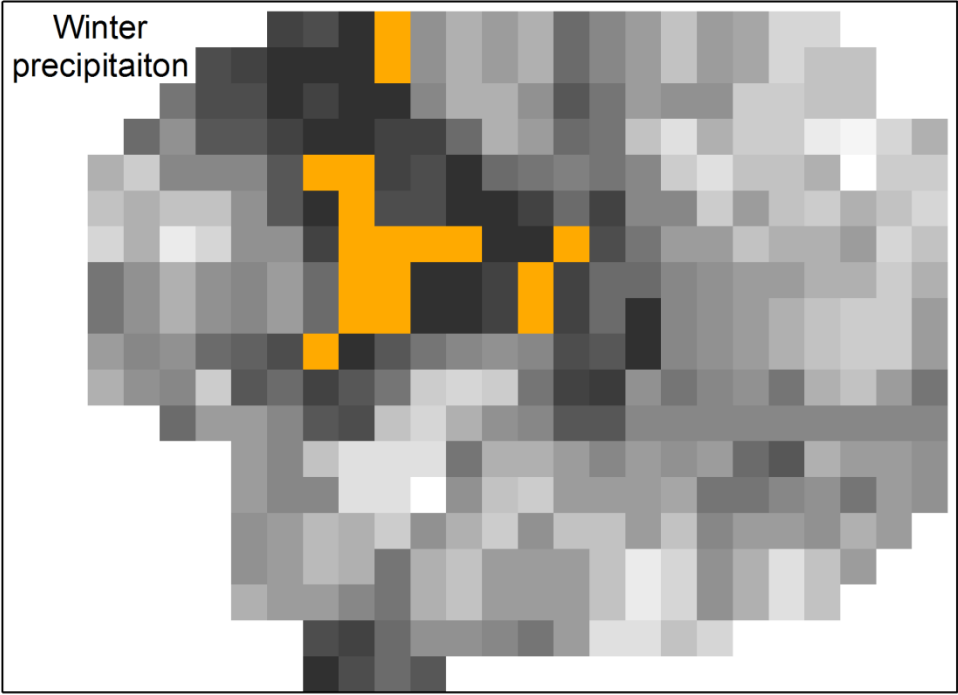
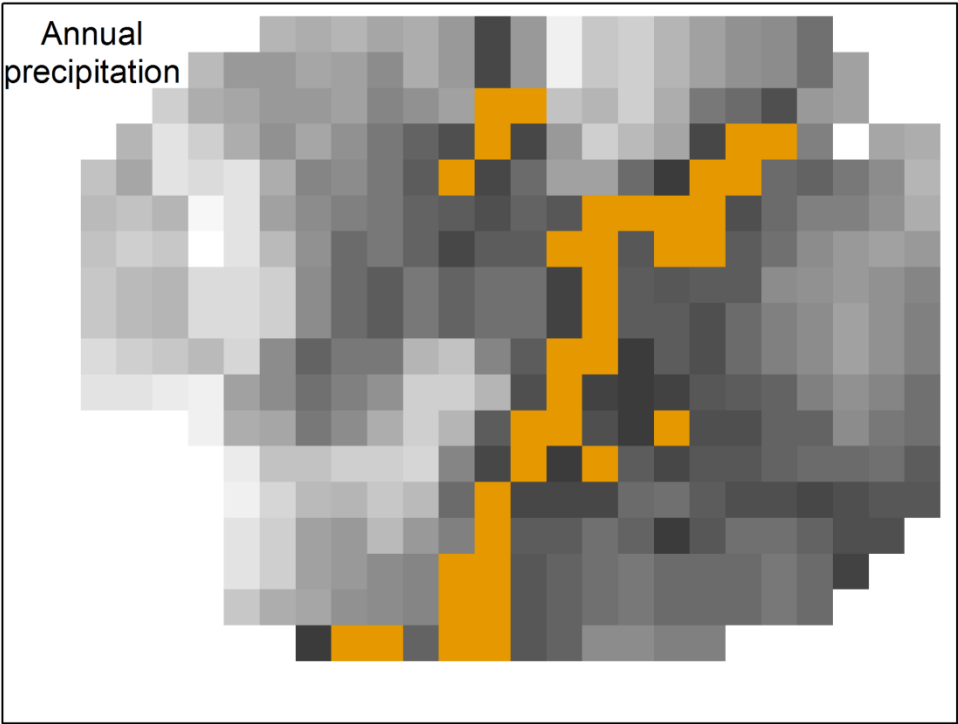
Shai Kaplan


December 4th 2013.

APPENDIX B

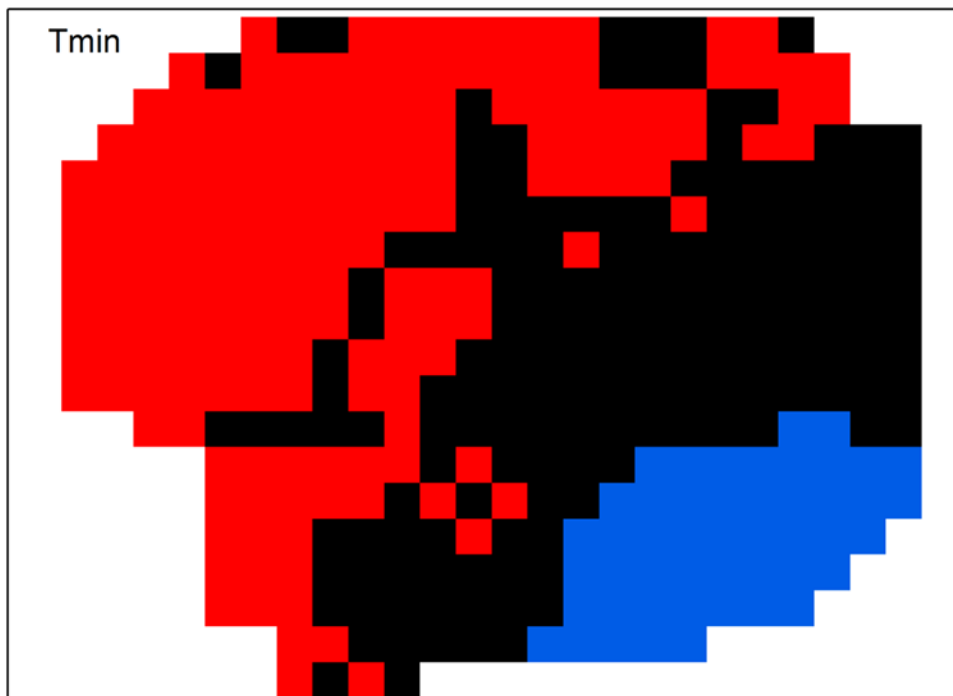
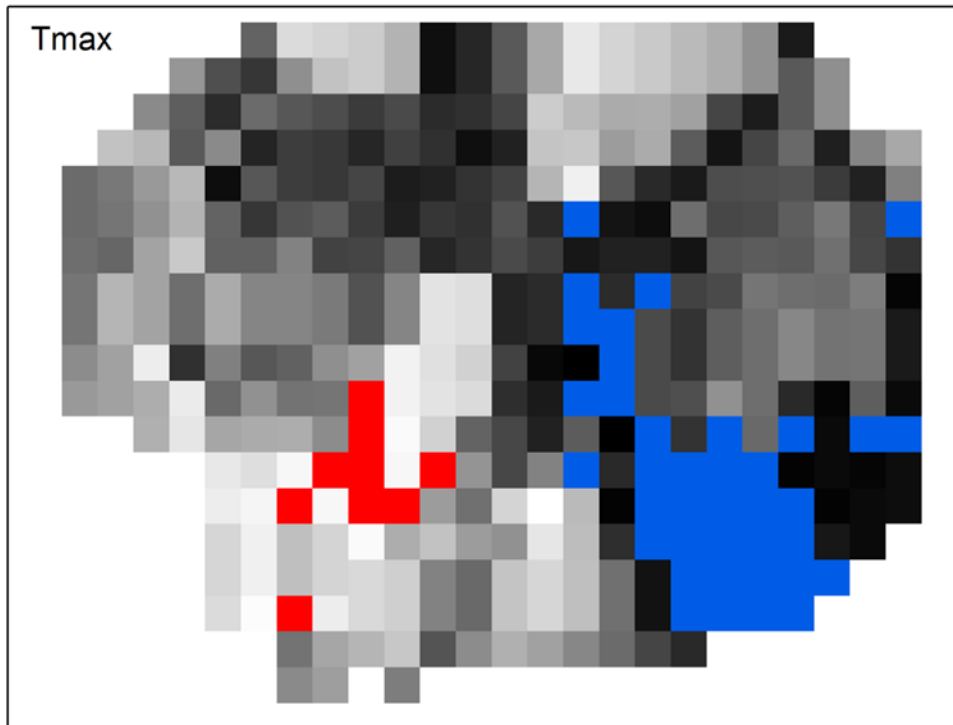
PRECIPITATION AND TEMPERATURE TREND MAPS



Areas of statistically significant trend in precipitation ($p < 0.1$)



 Downward trend

Areas of statistically significant trend in temperatures ($p < 0.05$)



 Downward trend  Upward trend

